Study the Effect of Interface Friction on the Behaviour of Fiber-Reinforced Polymer Piles under Axial Loads

by

Ahmad Almallah

Submitted in partial fulfilment of the requirements
for the degree of Master of Applied Sciences

at

Dalhousie University
Halifax, Nova Scotia
April 2019

I dedicate this thesis to my father Zouher, and my mother Rana who literally would do anything for me anytime and every time.

TABLE OF CONTENTS

LIST OF TABLES

LIST OF FIGURES

ABSTRACT

Fiber-reinforced polymer (FRP) composites provide potential alternatives for overcoming interface problems between conventional piling materials (wood, concrete, and steel) and soil. FRP composites are corrosion resistant, and more durable than conventional materials. More research is required to adapt these new materials to geotechnical practises. This study examines the enhancement of interface friction between glass FRP (GFRP) piles and sandy soils. The research comprises two phases. Phase I is an experimental study using direct shear test on the interface between sandy soils and sand coated GFRP composites. Phase II presents testing 5 small scale sand coated GFRP piles under axial loading in a soil tank. Phase I results indicate that GFRP surface roughness has a significant effect on GFRP-sand interface friction. Phase II results show that coating GFRP piles with silica sand significantly increases pile friction resistance in sand under axial loads with optimum sand coating ratio 1500 g/m^2.

LIST OF SYMBOLS

τ	Interface / Shear Stress
σ	Applied Normal Stress
Φ	Internal Friction Angle of Soil
δ	Interface Friction Angle between Soil and Material
c	Cohesion of Soil
C_a	Adhesion between Pile Material and Soil
q_s	Friction Resistance along Pile Shaft
$P_{friction}$	Pile Friction Capacity
L	Pile Length
q_t	Bearing Resistance at Pile Toe
A_t	Pile Area at the Toe
A_s	Pile Surface Area
σ_v	Effective Stresses
σ_{0avg}	Average Effective Stresses Along Pile Shaft
K_s	Lateral Earth Pressure Coefficient for Displacement Piles
K_o	Lateral Earth Pressure Coefficient
N_q	Bearing Capacity Factor
β	Pile Friction Resistance Factor
Q_s	Shaft Capacity of Piles
Q_t	End Bearing Capacity of Piles
Q_{ult}	Ultimate Bearing Capacity of Piles
W_p	Pile Weight

S_u Undrained Shear Strength of Soil

α Pile Friction Resistance Factor

N_γ Bearing Capacity Factor

Υ Unit Weight of Soil

σ'_t Effective Stresses at Pile Toe

D Pile Diameter

h Soil Depth

N_c Bearing Capacity Factor

ACKNOWLEDGMENTS

I would like to thank my co-supervisors Dr. Hany El Naggar, and Dr. Pedram Sadeghian for their endless support, motivation, encouragement, and help all the way in my masters' journey. I wish to extend my appreciation to my committee members, Dr. Zoheir Farhat and Dr. Fadi Oudah for their helpful comments on my thesis. Also, I would like to thank my colleagues (Ahmed Mahgoub, Hun Choi, Mostafa Jafarian Abyaneh, Ali Iranikhah, Mohammad Ashari Ghomi, Ahmed Moussa, Badir Alsaeed and Koosha Khorramian) and the technical staff (Brian Kennedy, Jordan Maerz, Jesse Keane, and Blair Nickerson) at the Department of Civil and Resource Engineering at Dalhousie University, Canada, for their support and help. I would like to appreciate and thank my friends Obbay Tuffaha, and Georges Sarkis for their support and help. Finally, I would like to thank my parents for their motivation, support, and care throughout my educational journey.

CHAPTER 1 INTRODUCTION

1.1 GENERAL

Two types of foundations are important in foundation engineering. The first type is shallow foundations, which are used when the soil underneath the foundation is firm and suitable for construction. The second type of foundations are deep foundations (piles). Piles are used when the soil underneath the structure is weak, and when the strong soil or stratum are so deep under the ground. A foundation element can be described as a pile if its depth is at least three times greater than its breadth (Atkinson, 2007). There are two main types of piles. The first type is an end bearing pile, where the end of the pile transfers loads from the structure to the soil. The second type is a friction pile, where loads from the structure are transferred to the soil via the interface friction between the pile material and the soil. The soil-structure interface friction is an important factor in the design of friction pile foundations. Piles have conventionally been fabricated by using the conventional materials; concrete, steel, and wood. However, these construction materials have been found to exhibit serious soil-substructure problems over time, especially in terms of durability, deterioration, and corrosion (Iskander et al. 2002).

Fiber-reinforced polymer (FRP) composites provide potential alternatives for overcoming these interface problems. FRP composites are lighter, stronger, more corrosion resistant, and more durable than conventional materials. Fiber types include carbon, glass, and aramid fibers, of which glass FRP (GFRP) is cost-effective compared to other types of FRP (Saafan, 2006). However, engineers still require more research and data to adapt FRP composites to the design of foundation piles. Due to a lack of data concerning FRP interface

behaviour in sandy soils, this study was designed to obtain a better friction performance of FRP piles in sand under axial loads.

1.2 Research Objectives

The objectives of this research are:

- To enhance the interface friction behaviour of GFRP against sandy soils.
- To increase the friction resistance and the capacity of GFRP piles in sand under axial loads.

1.3 Thesis Structure

This thesis contains the following five chapters:

- **Chapter 1** introduces the research.
- **Chapter 2** provides a literature review and background concerning different pile types, focusing on the structural performance of FRP piles and the friction behaviour of the soil-pile interface.
- **Chapter 3** presents phase I of the research, which focuses on the enhancement of the interface friction behaviour of flat GFRP specimens in sandy soils.
- **Chapter 4** presents phase II of the research, which deals with the behaviour of GFRP friction piles in sand under axial loads.
- **Chapter 5** summarizes the results and presents recommendations for future research.

REFERENCES

Atkinson, J. (2007). The mechanics of soils and foundations. CRC Press, Florida, USA.

Iskander, M., Mohamed, A., Hassan, M. et al. (2002). Durability of recycled fiber-reinforced polymer piling in aggressive environments. *Transportation research record*, **1808**(1), 153-161.

Saafan, M. A. A. (2006). Shear strengthening of reinforced concrete beams using GFRP wraps. *Acta Polytechnica*, **46**(1).

CHAPTER 2 LITERATURE REVIEW

2.1 INTRODUCTION

Pile foundations are used when the rock or stratum is deep under the ground, or when the soil underneath the structure is not strong enough to carry the loads. Pile foundations transfer loads from the structure to the soil via tip resistance in the case of end bearing piles, and via shaft resistance due to the interaction between the pile shaft and the soil in the case of friction piles.

Piles can also be classified based on the method of installation; driven and bored. A driven pile is installed in the soil by striking the pile head and pushing the pile into the soil by penetrating the soil. In contrast, a bored pile is installed by excavating a space in the soil large enough for placing the pile.

In addition, a pile can be classified based on its length and on the construction material. The convention pile materials including reinforced concrete, steel, and timber more likely to have serious durability problems, such as corrosion of steel rebars and deterioration (Iskander et al. 2002) due to the soil-structure interaction. For this reason, researchers are searching for alternative materials to be used for piles, particularly in harsh environments and in marine construction. Due to their higher strength in tension, light weight, low density, corrosion resistance and lower cost of maintenance, FRP composites have the potential to be widely used as pile materials in the future.

2.2 TYPES OF PILES

This section presents and discusses various pile types based on their load carrying mechanism, function, method of installation, materials used for manufacture and length.

2.2.1 Load Carrying Mechanism

2.2.1.1 End Bearing Piles

End bearing piles in deep foundations transfer loads through the end tip to a strong layer of soil or rock. Most of the pile end bearing capacity is derived from the resistance of the pile tip (Aashto, 2002). It is necessary for the end (tip) of the pile to sit on a strong bearing stratum. In this way an end bearing pile acts as a column and safely transmits the load to a strong layer of soil. End bearing piles are used when a strong bearing stratum is located at a suitable depth under the ground.

2.2.1.2 Friction Piles

A friction or floating pile is a pile installed in deep strata of limited bearing capacity or in a soft soil where the soil strength increases with depth. Friction piles in deep foundations transfer loads via the entire pile surface by adhesion with the soil or by interface friction with the soil. Friction piles are used when there is no strong layer of soil located at a depth that can be reached economically. Most of the friction pile bearing capacity is derived from soil resistance mobilized along the sides of the pile (Aashto, 2002). Thus, a friction pile develops most of its bearing capacity by shear stress along pile shaft.

A combined friction and end bearing pile transmits loads into the soil via interface friction between the pile shaft and the surrounding soil, as well as via the end toe which sits on a strong bearing stratum. Figure 2.1 illustrates the difference between end bearing piles and friction piles.

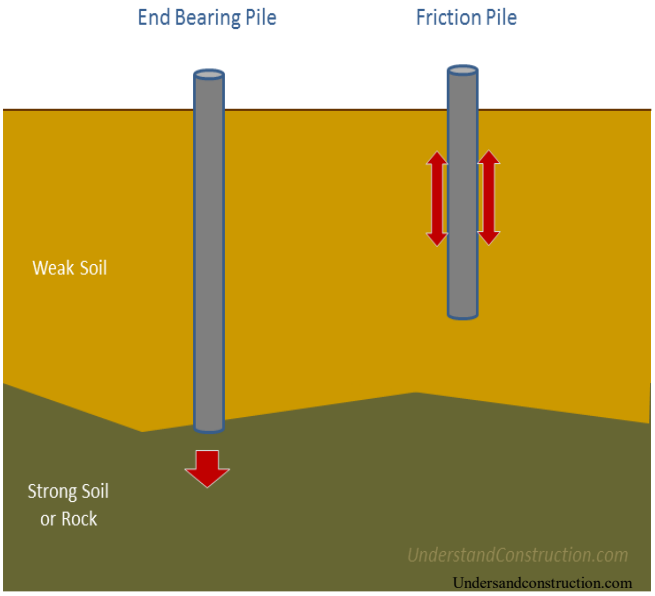

Figure 2. 1 The Difference Between End Bearing Pile and Friction Pile (Understanding construction website)

2.2.2 Pile Function

2.2.2.1 Tension Piles

Tension piles are uplift piles used to anchor structures subjected to uplift forces. These uplift forces can extract the structure from the ground due to hydrostatic pressure or seismic activity.

2.2.2.2 Compaction Piles

These piles are used to compact loose granular soil to increase its bearing capacity. Compaction piles can be made of relatively weak materials. For example, sand piles can be used as compaction piles.

2.2.2.3 Anchor Piles

These piles are used to provide anchorage against horizontal pull associated with sheet piling as shown in Figure 2.2. They resist lateral loads and they come with or without bracing. They are used in critical applications that is why they are designed with high strength in its characteristics.

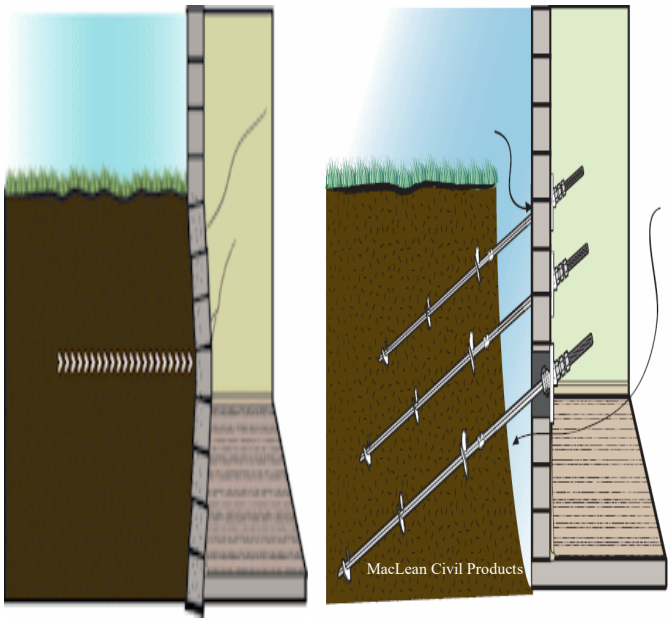

Figure 2. 2 Anchor Piles (MacLean civil website)

2.2.2.4 Fender Piles and Dolphins

Fender piles and dolphins are used to protect marine or waterfront structures from the impact of any floating object and secure vessels or boats during loading and unloading as presented in Figure 2.3. The Dolphins normally consist of a group of driven piles connected above the water level.

Figure 2. 3 Fender Piles (I am civil engineer website)

2.2.3 Method of Installation

2.2.3.1 Driven Piles

Driven or displacement piles are deep foundations installed in the ground by using impact or vibration hammers, so that the piles penetrate the soil to the desired level. A driven pile transfers loads from the structure to a strong layer of soil underneath it. Driven piles displace the soil as they penetrate it, causing an increase of lateral stresses. Piles with a smaller cross-sectional area cause less displacement of the soil. Driven piles can be manufactured based on the specifications required for the particular application. A major disadvantage is the noise generated as the piles are driven into the soil, since heavy materials and installation equipment are used. Figure 2.4 shows an example of driving several piles vertically into the soil.

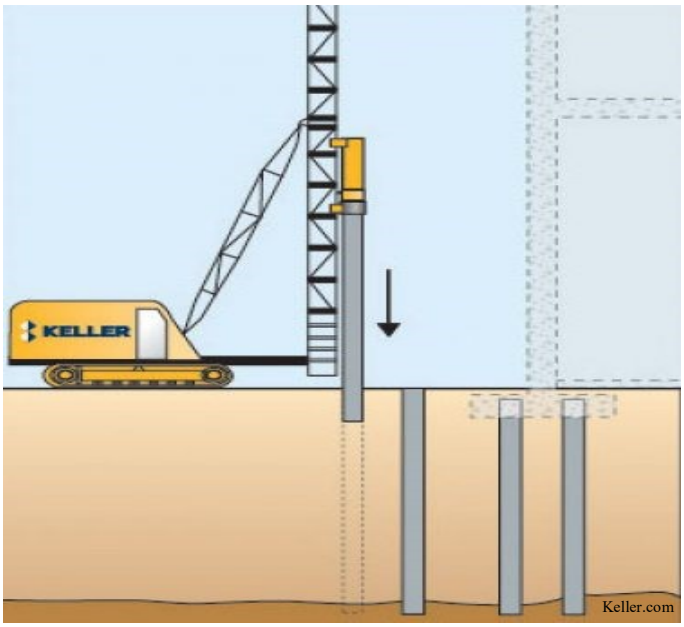

Figure 2. 4 Driven Piles (Keller website)

2.2.3.2 Bored Piles

Bored or replacement piles are deep foundations installed in the ground by removing the required amount of soil and then installing the pile in the cavity created. Bored piles can also be installed by drilling the soil, inserting a reinforcement in the resulting cavity, and then pouring concrete and removing the casing. In comparison to pile driving, boring results in reduced lateral soil stress. In urban areas, bored piles are often preferred to driven piles, since less noise is generated during the installation. Bored piles can transfer loads to a layer of soil that has adequate settlement characterises. Figure 2.5 illustrates a method used of excavating the soil and installing bored piles into it.

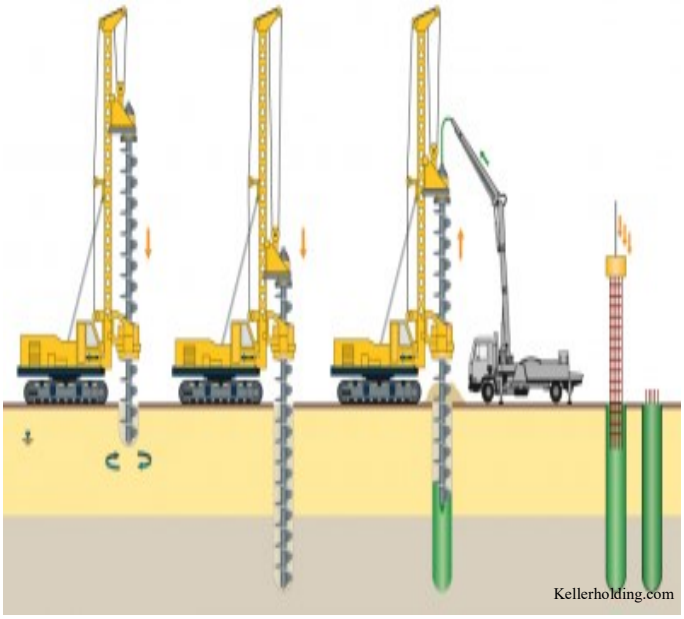

Figure 2. 5 Bored Piles (Keller holding website)

2.2.4 Material Used in Manufacturing

2.2.4.1 Concrete Piles

Concrete is widely used as a pile material in geotechnical applications, due to its relatively high bearing capacity and cost-effectiveness (Coduto, 2001). Concrete is often preferable to steel for such applications because steel can corrode easily, especially in marine and offshore construction. Concrete can also be used as a composite material, when steel reinforcements, fiber bars, or plastics are added. Concrete piles can be employed to support caissons and bridge piers, and large pile groups can be used for extensive, heavy structures. Either precast concrete, or concrete cast in-situ can be used. Precast concrete piles employ members that are prestressed or reinforced at the site of manufacture and then transported and placed at the construction site as shown in Figure 2.6. Precast concrete piles involve some difficulties in transportation, handling, driving, and cutting. Cast in-situ concrete piles

use concrete that is poured into a mould in the soil after reinforcement and other required elements are installed.

Concrete piles are widely accepted for use in the construction industry because they can be manufactured to meet the specifications of the particular application. However, concrete piles have the disadvantage of being subject to damage by organic soils, harsh environments, corrosion of the steel reinforcement due to concrete cracks, and loss of concrete section at sea-bed level due to abrasion from water-borne sediments (Mays, 2002). Sodium chlorides and calcium chlorides have been found to be the most harmful agents in the corrosion of concrete piles (Iskander, 2002). Cracking also occurs in concrete piles because of tensile internal stress formed by corrosion along the steel surface. Also, freeze-thaw cycles can reduce the service life of the piles. Nevertheless, concrete piles are still commonly used in construction due to their reliability and overall good performance.

Figure 2. 6 Driven Precast Concrete Piles (The constructer website)

2.2.4.2 Steel Piles

Steel piles have gained their popularity since the 1890s for building construction. Steel piles have high strength in both tension and compression, and high resistance to damage during driving into the soil. They can also be spliced conveniently to meet any desired specification, thus permitting increased bearing capacity with greater pile lengths. Steel pipes are strong, easy to handle, and can carry heavy loads. They can be driven into the soil either open-ended or close-ended.

The ability of steel piles to carry heavy loads and to reduce settlement of the structure makes them suitable for engineering applications. The reliability and wide range of ductility offered by steel enables steel piles to be driven into dense soil. Figure 2.7 presents a group of drilled steel piles driven into soil.

Steel piles can be made in different shapes depending upon the desired application. The most common types of steel pile are H-piles, pipe piles, and monotube piles. H-piles are H-shaped steel sections. They are very suitable for hard driving conditions, especially to bedrock, enabling them to act as end bearing piles. H-piles have high strength and cause less disturbance to the soil during driving than is the case with pipe piles (Allen & Iano 2013). Steel pipe piles consist of pipe sections with diameters typically ranging from 200 to 1000 mm, or even up to 3000 mm. Pipe piles can be open-ended or close-ended. The load bearing capacity of pipe piles could exceed that of H-piles based on the method and way of pile design (Coduto, 2001), but the driving of pipe piles leads to a greater disturbance of the soil. Steel monotube piles have longitudinal flutes, with a tapered surface (Horvath et al., 2004).

However, despite their advantages, steel piles have major shortcomings in terms of durability and cost. The high initial cost and the likelihood of corrosion associated with steel piles has led to a search for more cost-effective pile materials than steel. Especially for marine construction, since the corrosion reduces the lifespan of the piles. In neutral soils (with pH 7) steel is estimated to corrode up to 1.2 mm/year in off-shore construction (Iskander, 2002). Although the corrosion can be minimized via coatings containing specific metals, these coatings are not environmentally friendly. Despite these considerations, steel continues to be used as a pile material due to its various advantages and high load bearing capacity.

Figure 2. 7 Driven Drilled Steel Piles (Sky line steel website)

2.2.4.3 Timber Piles

Timber is an inexpensive material that has been used for foundation piles for thousands of years. Whether hardwood or softwood, timber has a high strength to weight ratio. Its

availability and low cost have favoured its use like some cases in northern Canada and Europe. Timber is available in nature, and is easy to transport, handle, and cut to the desired dimensions. The diameter of timber piles varies from 250 to 500 mm (Aysen, 2005), with larger diameters providing greater load bearing capacity. Timber piles can be driven into the soil. They have a natural taper and can be trimmed and cut to the desired shape. However, the design size of timber piles is limited to the natural state of wood, and the design capacity is typically less than 500 kN. due to the relatively small pile diameter and poor drivability (Elson et al., 2008). However, in some cases, there is a possibility of having higher capacity than 500 KN for end bearing.

In addition to their cost-effectiveness, timber piles have a long service life when continually submerged (Chellis, 1961). Their durability can be improved by protection against rotting via advanced techniques. Timber is widely used for fendering applications. However, timber piles have many disadvantages due to its limited structural length and capacity. When placed in harsh environments, timber can degrade through natural decay, and marine borer attacks can also reduce its lifespan (Iskander, 2002).

The drivability of timber is also a serious problem, due to its limited end bearing capacity (Coduto, 2001). As well, in offshore construction, some typical treatments of timber piles can lead to harmful effects on marine life. Despite these drawbacks, timber piles remain suitable for waterfront construction as shown in Figure 2.8, and structures with limited load bearing requirements.

Figure 2. 8 Timber Piles (American pole and timber website)

2.2.4.4 FRP Piles

In the past few decades, the use of fiber-reinforced polymers (FRP) has been increasing in geotechnical applications and the design of foundations (Hollaway, 2009). FRP is a composite material which combines two or more phases to create a new material that has improved performance and properties. In FRP, one phase is called the reinforcing phase, and the other phase is referred to as the matrix. The reinforcement fibers can be arranged as unidirectional continuous fibre composites, where all fibers are parallel to one another. Reinforcing fibers can also be a cross ply or woven fabric of continuous fiber composites, where fibers are oriented at right angles to one another. When the fibers are oriented in several directions, the composite is referred to as a multi-directional continuous fiber composite. Polymer matrix composites often include polyester, vinylester, epoxy, phenolic elements, and thermoplastic. Resins can be reinforced with glass (GFRP), carbon (CFRP), or aramid (AFRP) (Kaw, 2006). Adding carbon nanofibers to resin improves the resin

mechanical properties (Soltannia and Taheri, 2015). The matrix and fibers are joined together to form a composite unit referred to as a lamina. The properties of FRP composite materials depend upon the geometrical properties, the distribution of the phases, and the constituents of the composite. One of the most important parameters of FRP composites is the fibre volume ratio, or the volume (or weight) fraction of reinforcement.

FRP composites are potential alternatives to traditional pile materials, due to their advantageous characteristics. They are strong, light, durable and corrosion resistant, with a long lifespan and low maintenance costs in-terms of rehabilitation of the material (Nishizaki et al., 2006). Research has been done on FRP composite piles to check its performance, drivability, bearing capacity, and the interface characteristics with the soil.

FRP composites consist of a combination of fiber material and epoxy resin. The latter acts as a glue to hold the composite together as a single fabric. Different kinds of fiber can be employed to manufacture composites. The most commonly used types are carbon fiber, aramid fiber, and glass fiber, which is the most cost-effective. Since 1987, piles have been made with various types of composite. These include fiberglass-reinforced polymer piles (GFRP), FRP hollow piles, concrete-filled FRP piles, FRP sheet piles, reinforced plastic piles, steel core piles, and fiberglass pultruded piles. Composites can be manufactured via pultrusion, filament winding, or moulding processes (Guades et al., 2012). FRP piles can also be manufactured from a recycled plastic matrix or high-density polyethylene (HDPE) reinforced with fiberglass. FRP can be used in rehabilitating the conventional piling material as shown in Figure 2.9, where timber piles are strengthened with GFRP.

The use of FRP in pile applications also has certain disadvantages, such as a relatively high initial cost, low stiffness, and a lack of data and proven design guidelines, which limit its

acceptance in the geotechnical industry. However, due to their durability and long lifespan, FRP composites could be an effective alternative to conventional pile materials which exhibit serious soil-structure interface problems, especially in marine construction.

Figure 2. 9 Timber Piles Strengthened with GFRP (Five-star products website)

2.2.4.4.1 Glass Fibre Reinforced Polymer (GFRP)

One of the most commonly used type of fiber as a piling material is Glass fibre reinforced polymer (GFRP). Glass fiber is also the type of fiber most commonly used for composite reinforcement. Figure 2.10 shows a sample of unidirectional fiber glass. It is a processed form of glass, composed mostly of silica oxide mixed with raw materials such as limestone, boric acid, clay, and fluorspar. GFRP is manufactured by drawing melted oxides into filaments ranging in diameter from 3 μm to 24 μm. In comparison to other types of fiber, GFRP is more cost-effective (Saafan, 2006).

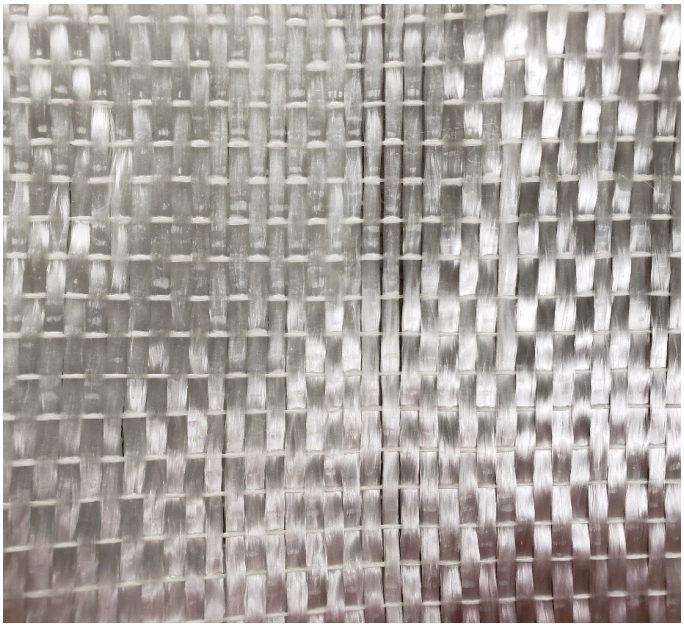

Figure 2. 10 Unidirectional Fiber Glass

2.2.4.4.2 Advantages of FRP Piles

Many problems occur as a result of using the traditional concrete, steel, and wood as a piling material. These problems are due to the pile-soil and pile-water interface, and include the corrosion of steel, deterioration of wood, and degradation of reinforced concrete, especially in the case of construction in harsh environments. When the pile material deteriorates or degrades, the cross-section of the pile is reduced, which decreases the pile carrying capacity. The advantages of FRP materials make them a potential alternative for replacing conventional materials in pile construction, to overcome these interface problems. Because FRP composites are corrosion resistant, chemical resistant, and degradation resistant, they have a long service life without the need for rehabilitation. This makes them cost-effective for use in construction (Zobel et al., 2005). Many geotechnical structures are now reaching their design service life and need to be rehabilitated, repaired, or replaced. The fact that FRP composites are more durable than conventional pile materials

opens up the possibility that they could be used to replace traditional materials in geotechnical applications and the design of pile foundations.

2.2.4.4.3 Reinforced Plastic Piles (RPP)

These piles are composed of an extruded recycled plastic matrix reinforced with fibreglass rebars or steel rods. The plastic matrix is chemically treated with ultraviolet inhibitors and antioxidants to retard the effects of UV light on the plastic (Taylor, 1995). RPP piles are typically reinforced with 6 to16 fiberglass reinforcing bars, which range in diameter from 25 to 30 mm (Guades et al., 2011). The piles themselves are available mostly in diameters of 250 to 400 mm. The size, type, and number of reinforcing elements selected depend upon the structural requirements of the specific pile application. Figure 2.11(a) presents a group of steel reinforced plastic piles, and Figure 2.11(b) shows concrete-filled FRP pile.

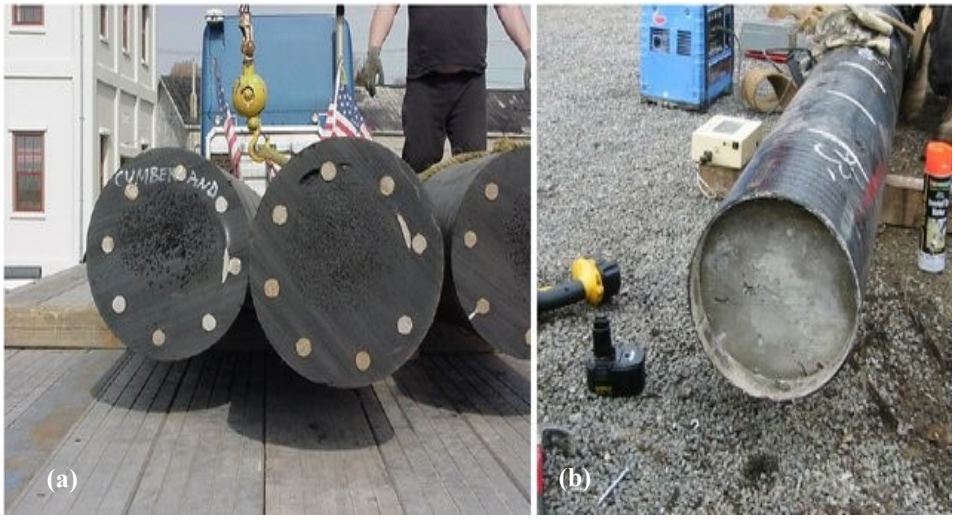

Figure 2. 11 (a) Steel reinforced plastic pile (Plastic Pilings, Inc.); and (b) Concrete-filled FRP pipe pile (Lancaster Composite), (Baxter et al. 2005)

2.2.4.4.4 Fibreglass Pultruded Piles

To provide greater structural strength, fibreglass pultruded piles are composed of an outer fibreglass sheet fitted with a fibreglass grid. The grid inserts are sometimes filled with high

density polyethylene (HDPE), plastic lumber, or polyethylene foam fills. The grid consists of two sets of orthogonal plates joined at four intersecting points. The shell and inserts are used to help absorb vessel impact and to connect fender fittings for fender pile applications (Guades et al., 2011).

2.2.4.4.5 Concrete-Filled FRP Tube Piles

Concrete can be used to fill FRP piles, where FRP forms the pile shell and concrete is the filling material which is poured into the pile. Filling FRP piles with concrete reduces buckling of the FRP tube and increases its stiffness (Yuan and Mirmiran 2001), while the FRP shell confines the filling material, providing greater strength. FRP shells forming the outer surface of piles provide a suitable interface with soil, since FRP is more durable than conventional pile materials and its corrosion resistance increases the pile lifespan. It has been found that the performance under axial load of piles composed of FRP shells with concrete filling is comparable to the performance of reinforced concrete structural members (Mirmiran et al., 2000). Fam and Rizkalla (2001) found that the ductility and the strength of concrete-filled circular GFRP tubes were improved due to the confinement which GFRP provides. Concrete-filled FRP tube piles have also been found to perform well in the rehabilitation of bridges and their structural components (Pando et al., 2003).

2.2.5 Pile Length

A pile can be classified as long or short, based on its length to diameter ratio (L/D). Piles are considered long if their length to diameter ratio is greater than or equal to 20 and are considered short if the L/D ratio is less than 20.

2.3 PILE-SOIL INTERFACE

The soil-structure interface refers to the structural material in immediate contact with the soil zone where the shearing mechanism takes place. The pile capacity has a significant dependence on the soil-pile interface, especially when pile resistance is mobilized through shaft friction. Friction or shear parameters of the interface between the pile material and the soil, such as the interface friction angle and the adhesion between the pile material and the soil, are important for estimating the shaft friction resistance of piles. Soil-pile interface friction parameters are important for foundation design and geotechnical applications. By using a simple shear apparatus, research has been done on different pile materials with different types of soil to characterize these interface parameters.

The use of direct shear test apparatus provides an effective test to characterize soil-structure interface parameters. The interface or shear strength parameters are defined by Coulomb's equation, as follows:

$$\tau = \sigma \, tan(\Phi) + C \tag{2.1}$$

or:

$$\tau = \sigma \, tan(\delta) + C_a \tag{2.2}$$

where

τ is the interface or shear stress

σ is the applied normal stress

Φ is the internal friction angle of the soil

δ is the interface friction angle between the soil and material

c is the cohesion of the soil, and

C_a is the adhesion between the pile material and soil.

Potyondy (1961) studied the characteristics of interface friction between conventional materials (i.e., concrete, steel, and wood) and different types of soil. By using a direct shear test, it has found that the factors affecting the soil-pile interaction are the magnitude of normal loading, the moisture content of the soil, the surface roughness of the pile material, and the soil composition.

The following sections discuss the interface friction behaviour of steel, concrete, and FRP against different types of soils

2.3.1 Pile-Clay Interface

In the study of the shear strength of cohesive soils under undrained conditions, three different failure modes can be identified: Turbulent, sliding, and transitional.

When the clay microstructure is disturbed, the failure mode is classified as turbulent. When there is a lack of interlocking between particles of the soil sample, the failure mode is classified as sliding failure. An intermediate state between these two failure modes is classified as transitional failure (Lupini et al., 1981).

The interface friction behaviour of the clay-structure interaction depends on the clay fraction, the soil mineral type, and the surface roughness of the structural material. Taha (2010) studied the friction behaviour of the interface between pile materials and marine clay. He found that the controlling parameters affecting the pile-marine clay interaction were the surface roughness of the pile material, the density of the soil, the degree of saturation of the soil, and the salt content of the clay.

In a study of the interface friction behaviour with London clays and sandstone, Rouaiguia (2012) found that the controlling parameter was surface roughness. Greater surface roughness plays an important role in the interface interaction due to the increase in friction

between the soil particles and the pile material. Chu and Yin (2006) studied soil-grout interface friction behaviour and found that the angle of interface friction increased as the interface waviness angle and the applied normal stresses increased.

In a study of the interface between soil and concrete, Goh and Donald (1984) found that the factors affecting the interface parameters were the concrete surface texture and the clay content of the soil. Velez (2013) confirmed that the controlling parameter affecting the clay-pile interface is the pile surface roughness. All these studies emphasize the important role played by surface roughness in the interface behaviour of the clay-structure interaction.

2.3.2 Pile-Sand Interface

In pile-sand interface interaction studies, the surface roughness of the pile material and the angularity of the sand particles have been found to be the controlling parameters. Uesugi and Kishida (1986) found that the interface friction between steel and sand depends upon steel surface roughness and is less influenced by normal stresses in the soil. O'Rourke et al. (1990) studied the interface friction behaviour of sand and geosynthetic material and found that the interface friction increased with increasing soil density. In a study of the characteristics of pile-sand interfaces, Pando et al. (2002) found that pile capacity can be increased by increasing the interface friction between the pile material and sand, resulting in greater friction and higher shaft resistance.

All of these studies confirm that for the sand-pile interface, the sand composition and the pile material surface play a major role in determining the friction behaviour, increasing or decreasing the interface shear strength.

2.3.3 FRP-Soil Interface

Due to its durability, long service life, corrosion resistance, and high strength, in recent decades FRP has been used more widely in the design of pile foundations and marine construction (Guades et al., 2010). FRP piles have been found to have lower maintenance costs and a better interface with the soil in offshore construction than is the case with conventional pile materials (Iskander and Hassan, 1998). Sakr et al. (2004) found that the durability of piles can be increased by using FRP as a pile material.

Frost and Han (1999) studied the interface friction behaviour of FRP and sand by using a direct shear apparatus and compared the results to a soil-steel interface. The results showed that the surface roughness of the material affected the interface strength parameters more than the method of soil sample preparation or the test procedure.

Pando et al. (2002) studied the sand-FRP interface interaction and found that reduced surface hardness of the FRP material resulted in increased interface friction resistance with the soil. Pando (2003) evaluated the FRP pile-soil interface and compared the results with those for conventional piles. His study showed that relative asperity was the controlling parameter. Shaia (2013) found that the surface roughness of the material, the mean particle size, and the type of granular soil were the parameters controlling the peak interface friction coefficient for FRP and sand.

Giraldo and Rayhani (2013) compared the interface friction behaviour of FRP piles in clay with that of a steel reference pile. The results showed that the FRP piles performed better than the steel reference pile in terms of the interface friction resistance.

Aksoy et al. (2016) studied the interface friction angle of FRP composites in soil and compared the results with those of conventional pile materials (steel and wood). It was found that the bearing capacities of FRP and wood piles are higher than those of steel piles. All these studies show that FRP-soil interface friction depends on the surface roughness of FRP and the particle angularity of the soil composition. More research and investigations concerning FRP piles are required for them to gain wider acceptance in geotechnical applications. Due to a lack of research, data, and design guidelines, the present study has been designed to investigate the interface friction behaviour of FRP piles in sand, and to examine the enhancement of friction resistance by using a shaft with a roughened skin.

2.4 Structural Performance of FRP Piles

FRP has been introduced in the last few decades as a pile material. More research and data are necessary to obtain an in-depth understanding of the structural behaviour of FRP piles. The following sections provide an overview of the drivability of FRP piles and their performance under axial loads.

2.4.1 Drivability of FRP Piles

The driving of FRP piles in various types of soil presents difficulties when they are used as hollow piles. Because FRP has low stiffness, density, and pile impedance, driving FRP piles is challenging in terms of pile buckling, surface cracks, and increased stresses around the pile shafts. These characterises of FRP piles result in considerable pile dumping (Gaudes et al., 2012).

Hollow FRP piles require more research and investigation to adapt them to geotechnical applications in the pile industry. Ashford and Jakrapiyanun (2001) studied the driving performance of hollow FRP piles and compared the results to those for concrete-filled FRP

piles, steel piles, and concrete piles. Due to the lower impedance of FRP piles, the results showed an ultimate bearing capacity at driving refusal equal to 65% to 75% of that of steel and concrete piles.

Mirmiran et al. (2000) performed a dynamic driving analysis for hollow and concrete-filled FRP piles. It was found that concrete in-fill FRP piles performed similarly to prestressed concrete piles in terms of ultimate bearing capacity and driving stresses. Concrete in-fill FRP piles exhibited a better performance in preventing pile buckling. Iskander et al. (2001) investigated the influence of different parameters on pile driving by using wave equation analysis (WEAP) software. The results showed that FRP piles have a good capacity as load bearing piles. Sakr et al. (2004) introduced a driving technique (toe-driving) for FRP piles to improve the axial capacity and reduce pile damage while driving.

The drivability of FRP piles with no filling materials is one of the concerns addressed in this thesis, where improvement in the structural performance of FRP piles is studied by using glass FRP, in order to obtain a better understanding of its behaviour in sand.

2.4.2 FRP Piles Performance under Axial Loads

The use of axial tests for small and large scale FRP piles is important in order to adapt FRP for use as a pile material and to understand its characteristics under different conditions.

Few studies related to the response of FRP piles to axial loads are available in the literature. Frost and Han (1999) studied buckling loads of FRP piles during driving. The results showed that the critical buckling of FRP piles depends upon the shear effect coefficient, the critical length of the pile, the lateral soil resistance, the embedment ratio, and the overall boundary condition.

Pando et al. (2000) performed a full-scale pile load test on FRP tubes with confined concrete and compared the results with those for prestressed piles. They performed Statnamic axial load tests on these samples. The results indicated that the axial geotechnical capacities of the piles tested were higher for prestressed concrete piles than for FRP piles.

In the year 2001, Fam and Rizkalla (2001) investigated the compressive behaviour of concrete-filled FRP tubes with different degrees of filling. The results showed that FRP provided confinement for the concrete, which increased the tube axial capacity. Failure of these FRP tubes occurred in the brittle state as a rupture of the FRP shell.

Fam and Rizkalla (2002) studied the flexural behaviour of hollow and concrete-filled FRP piles and found that the flexural strength of filled FRP piles is higher than that of hollow piles. It is also showed that due to horizontal shearing, sections with fewer hoop-oriented fibers failed. On the other hand, it was found that compressive failure occurred in sections with more axially oriented fibers.

The following year, Fam et al. (2003) established a full-scale field test for two pile types (concrete-filled FRP composite and prestressed concrete piles). Two strain gauges were placed near the opposite faces of the pile at each level. The results showed that concrete-filled FRP composite piles and prestressed concrete piles performed similarly during driving.

Pando (2003) studied the behaviour of concrete-filled FRP piles and compared the results to those for prestressed concrete piles. It was found that the two pile types exhibited a similar performance in the material capacity.

Mirmiran and Shahawy (2003) used pile field tests to evaluate the drivability of an FRP tube filled with concrete, and prestressed concrete. The results indicate that during driving

of the FRP tube filled with concrete, there was no pile head damage, and no separation between the FRP tube and the concrete core was observed.

The following year, Sakr et al. (2004) found that FRP piles under axial loads exhibited a performance comparable to that of steel piles. Shaia (2013) found that carbon FRP tubes have a higher strength than glass FRP tubes due to the high modulus in the axial direction and high tensile strength. Velez (2013) found that the capacity of FRP piles was greater than or equal to that of steel piles. Sadeghian et al. (2010) examined a new moment connection of concrete filled FRP tubes to footings under monotonic and cyclic loadings. The findings of this research Showed that a smaller tube embedment length (X) over tube diameter ratio (X/D) leads to bond failure at lower capacity than that of the critical ratio. The controlling parameters for the tube embedment over tube diameter critical ratio were the FRP tube, and concrete filling geometry, and the mechanical properties of both. Sadeghian and Fam (2010) did a closed form model and parametric study on connection of concrete-filled FRP tubes (CFFTs) to concrete footings by direct embedment. The results showed that increasing the diameter, and; or the embedment length of CFFTs outside the footing reduces the embedment length over diameter critical ratio. Also, they found that increasing the axial compression load or reducing the eccentricity reduces the critical embedment depth of the tube.

More research and data are needed to understand the axial capacity and performance of hollow FRP piles. For this reason, the behaviour of hollow FRP piles under axial loads is a major focus of this thesis, in order to characterise the performance of FRP piles in sandy soils, and to increase their capacity under different loading conditions.

2.5 PILE CAPACITY

To determine the critical failure load of piles, several loading tests can be done to characterise the pile capacity and to find the maximum load the pile can withstand before failure.

In this thesis, the axial load capacity of several GFRP and control piles was examined. The following sections provide an overview of axial pile capacity.

2.5.1 Axial Pile Capacity

The axial pile capacity can be determined from the shaft capacity of the pile (the interface friction between the pile material and the soil), and the toe resistance at the end of the pile. The ultimate pile bearing capacity, Q_{ult}, can be calculated as the sum of the pile shaft resistance, Q_s, and the pile end bearing capacity, Q_t, while subtracting the weight of the pile, W_p, as follows:

$$Q_{ult} = Q_s + Q_t - W_p \tag{2.3}$$

The pile shaft capacity can be expressed as:

$$Q_s = A_s \, q_s \tag{2.4}$$

where

A_s is the pile surface

q_s is the friction resistance along the pile shaft, and

The pile end bearing capacity can be determined as:

$$Q_t = q_t \, A_t \tag{2.5}$$

where

q_t is the bearing resistance at the pile toe, and

A_t is the pile area at the toe

There are various methods of calculating the pile friction capacity and the end bearing capacity. These methods are discussed in the following sections.

2.5.1.1 Pile Friction Resistance

The pile friction resistance depends on the interface friction angle between the pile material and the soil, δ, the lateral earth pressure along pile shaft given that the coefficient of lateral earth pressure is K_s, and the effective stresses along pile shaft, σ'_v. Thus, the pile friction resistance, q_s, can be calculated as follows:

$$q_s = \sigma'_v \, K_s \, tan(\delta) \tag{2.6}$$

The coefficient of lateral earth pressure, K_s, can be determined as proposed by Vesic (1977), based on the bearing capacity factor, N_q, for driven piles in sand of loose to medium density, as follows:

$$K_s = \frac{N_q}{50} \tag{2.7}$$

Meyerhof (1976) suggested a factor, β, for both interface friction and confining pressures, to find the pile friction resistance. This factor can be determined as follows:

$$\beta = K_s \, tan(\delta) \tag{2.8}$$

This factor suggested by Meyerhof can be substituted in equation 2.6 to determine the pile friction resistance, q_s.

For driven piles, the value of K_s is a function of K_o, as for driven displacement-type piles K_s is normally assumed to be twice the value of K_o, where:

$$K_o = 1 - sin(\Phi) \tag{2.9}$$

For cohesive soils, the friction resistance of piles can be calculated through a total stress approach. This approach depends upon the undrained shear strength of the soil, S_u, and the

adhesion coefficient, α. Based on this approach, the pile friction resistance, q_s, can be calculated for cohesive soils as follows:

$$q_s = \alpha S_u \tag{2.10}$$

Many studies have been conducted to estimate the values of α and β to characterize the pile friction resistance for various types of pile, and different kinds of soil.

2.5.1.2 Pile End Bearing Resistance

The pile end bearing resistance can be estimated from the following formula:

$$q_t = N_q \sigma'_t + 0.5 \Upsilon D N_\Upsilon \tag{2.11}$$

where

N_q and N_γ are the bearing capacity factors

Υ is the unit weight of the soil

σ'_t represents the effective stresses at the pile toe, and

D is the diameter of the pile toe

For cohesionless soils, the pile end bearing resistance is typically calculated as:

$$q_t = N_q \sigma'_t \tag{2.12}$$

whereas for cohesive soils, the pile end bearing capacity is calculated as:

$$q_t = N_c S_u \tag{2.13}$$

where

N_c is the bearing capacity factor, and

S_u is the undrained shear strength of the soil

Based on Meyerhof (1976), the value of N_q for end bearing resistance depends on the internal friction angle of soil, while according to CFEM (2006), N_q depends on the type of soil and type of pile (bored or driven).

The values for these equations can be obtained via pile load tests on conventional pile materials (i.e., wood, steel, and concrete). However, for FRP piles, additional data are necessary to determine the bearing coefficients for the pile toe resistance.

2.6 Axial Pile Load Test

For pile-soil resistance design, empirical and analytical methods can be used to estimate the pile bearing capacity. Several factors influence the choice of pile testing method, such as the soil characteristics, scope of the project, and pile specifications. In the industry, the two pile testing methods most commonly used to estimate the pile axial capacity are the static pile load test and the dynamic pile load test.

Axial static pile load tests can be implemented for both compression and tension forces on the pile until failure settlement in the soil is reached. The test is done through a reaction frame connected on both sides to a reaction pile. The reaction beam carries a hydraulic jack which applies incremental loads until the pile fails. The loads can be measured by using a load cell, and the displacement of the pile can be measured through string pots, dial gauges, or a linear variable differential transformer (LVDT). All of these measurement instruments must be calibrated to ensure accuracy of the result. The load displacement criteria can be varied based on reference proposed by various researchers. Static pile load testing is typically carried out according to ASTM D1143/D114M (2007).

The dynamic pile load test, which estimates the pile resistance during driving and after driving, involves determining the elastic response of piles to the force applied while driving. The forces required to drive the pile create compressive waves around the pile shaft. These waves are recorded by strain transducers.

Novak and Grigg (1976) performed dynamic experiments on small individual and group piles in field and it was found that a theory of predicting the experimental results proposed by Novak was applicable as it predicted the general characteristics of the pile response well. A comprehensive approach to model a pile driving system was proposed by Smith (1960). This approach considers the pile-soil interaction, and the effect of time on the compressive strain waves during driving. The standard typically used for dynamic pile load testing is ASTM D4945 (2012). For FRP pile load tests, many data are still required to provide a better understanding of the behaviour of FRP piles under axial loads and new methods are needed to improve the pile-soil interaction to increase FRP pile capacities. In this thesis, several driving tests and pile load tests were carried out on one control steel pile and 5 GFRP piles with different surface roughness to gain a better understanding of the behaviour of GFRP piles in sand under axial loads. Four of the five GFRP piles were coated with silica sand with different sand coating ratios per unit of surface area (1000, 1500, 2000, and 2500 g/m^2) to enhance the friction resistance of the GFRP piles and to increase their ultimate bearing capacity.

2.7 Surface Roughness of Friction Piles

As the surface roughness of friction piles is a controlling parameter in enhancing the interface friction between pile foundation and soil, various researchers have been working on studying the effect of pile roughness to enhance the axial capacity of pile foundations.

Reddy et al. (2000) examined the interface friction between smooth and rough friction piles against sand and found that increasing the surface roughness of friction piles results in enhancing its friction resistance. This confirms the findings of Potyondy (1961), Uesugi and Kishida (1986), Frost and Han (1999), with later findings, Pando et al. (2002) and Shaia, H. (2013). These results concluded that enhancing the interface behaviour of friction piles is applicable through increasing the surface roughness of pilling material. However, interface studies were conducted on regular FRP surfaces. This study introduces a new effective way of roughening GFRP friction piles through sand coating to increase its friction resistance and capacity under axial loads against sand.

2.8 SUMMARY

The use of conventional pile materials (i.e., wood, steel, and concrete) can lead to serious soil-pile interface problems such as corrosion and degradation, which affect the service life of the piles. FRP can provide a potential alternative to overcome these interface problems and increase pile service life. FRP is currently used for fendering applications due to its energy absorption properties and bearing capacity. In this chapter, pile types, pile axial capacity, and the soil-pile interface are discussed and different methods of pile testing and estimating pile resistance are presented.

Factors affecting the pile axial capacity in compression are described, including the soil type, pile type, pile material, and pile installation method. In addition, various methods of estimating pile shaft resistance and end bearing resistance based on drained and undrained soil conditions are presented.

The controlling parameters for the FRP-soil interface have been identified as the surface roughness of the pile material, the density of the soil, the soil type, and the particle angularity of the soil. Increased interlocking between the soil particles and the pile results in greater pile frictional resistance.

Three main aspects of full-scale FRP piles are being examined: Pile driving performance, pile structural behaviour, and pile axial capacity. The drivability of FRP piles has been studied by comparing concrete-filled FRP piles with conventional pile materials. In contrast, driven hollow FRP piles have been found to reach refusal at 50% of the driving stresses of traditional materials. Similar results have been found for the structural behaviour of FRP piles. Although concrete-filled FRP piles exhibit better performance in terms of buckling prevention and increased pile stiffness, more research and data on the structural behaviour of hollow FRP piles are required. A better understanding of FRP pile axial capacity is needed to adapt these new materials to geotechnical applications and to improve their friction resistance in sandy soils. A direct shear test is an effective mean of characterising the interface shear strength of pile materials and soil. However, interface tests alone are not enough to provide a complete understanding of the friction behaviour of FRP piles in sand. Small- and large-scale experiments are necessary to confirm the results of interface shear tests and to compare FRP behaviour with that of conventional pile materials. This thesis focuses on some of these knowledge gaps, with the aim of enhancing the interface friction behaviour of GFRP as a pile material through sand coating and increasing the friction resistance and capacity of GFRP piles in sand under axial loads. For that reason, 4 out of 5 GFRP piles were coated with silica sand with different sand coating ratios per surface area (1000, 1500, 2000, and 2500 g/m^2) and tested under axial loads in

soil tank. Chapters 3 and 4 present the results of two phases of experiments that address these concerns.

REFERENCES

AASHTO. (2002). Standard specifications for highway bridges. Transportation officials.

Allen, E., & Iano, J. (2013). Fundamentals of building construction: materials and methods. John Wiley & Sons.

Anchor Piles, reprinted from MacLean Civil Products, Retrieved on December 10, 2018, from https://www.macleandixie.com/products/item.asp?ITEM_ID=2481, Copyright by MacLean Civil Products.

Ashford, S. A., & Jakrapiyanun, W. (2001). Drivability of glass FRP composite piling. *Journal of Composites for Construction*, **5**(1), 58-60.

Aksoy, H. S., Gör, M., İnal, E. et al. (2016). A new design chart for estimating friction angle between soil and pile materials. *Geomechanics and Engineering*, **10**(3), 315-324.

ASTM. D1143/D1143M. (2007). Standard Test Methods for Deep Foundations Under Static Axial Compressive Load.

ASTM. D4945. (2012). Standard Test Method for High-Strain Dynamic Testing of Deep Foundations, West Conshohocken, PA, USA.

Aysen, A. (2005). Problem solving in soil mechanics. Taylor & Francis, USA.

Baxter, C. D., Marinucci, A., Bradshaw, A. S., Morgan, R. J. et al. (2005). Field study of composite piles in the marine environment.

Bored Piles, reprinted from Keller Website Worldwide, Retrieved on December 20, 2018, from http://www.kellerholding.com/bored-piles.html/, Copyright by Keller.

CFEM (2006). Canadian Foundation Engineering Manual.

Chellis, R. D. (1961). Pile Foundations, McGraw Hill, New York, USA.

Chu, L. M., & Yin, J. H. (2006). Study on soil–cement grout interface shear strength of soil nailing by direct shear box testing method. *J Geomechanics and Geoengineering*, **1**(4), 259-273.

Coduto, D. P. (2001). Foundation Design Principles and Practices. Upper Saddle River, New Jersey: Prentice-Hall, USA.

Driven Drilled Steel Piles, reprinted from skyline steel website, Retrieved on October 5, 2018, from http://skylinesteel.com/globalnav/applications/bearing-piles, Copyright 2018 by Skyline Steel.

Driven Piles, reprinted from Keller Website Australia, Retrieved on December 19, 2018, from http://www.keller.com.au/solutions/techniques/driven-piles/, Copyright by Keller.

Driven Precast Concrete Piles, reprinted from the constructor website, Retrieved on October 5, 2018, from https://theconstructor.org/geotechnical/driven-precast-concrete-piles/7092/, Copyright 2017 by The Constructor.

Elson, K., Fleming, K., Randolph, M., Weltman, A. et al. (2008). *Piling engineering*. Taylor & Francis.

Fam, A. Z., & RizKalla, S. H. (2001). Behavior of Axially Loaded Concrete-Filled Circular Fiber-Reinforced Polymer Tubes. *ACI Structural Journal*, **98**(3), 280-289.

Fam, A. Z., & Rizkalla, S. H. (2002). Flexural Behaviour of Concrete-Filled Fiber-Reinforced Polymer Circular Tubes. *Journal of Composites for Construction*, **6**(2), 123-132.

Fam, A. Z., Pando, M., Filz, G., Rizkalla, S. et al. (2003). Precast piles for Route 40 bridge in Virginia using concrete filled FRP tubes. *PCI journal*, **48**(3), 32-45.

Fender Piles, reprinted from I am Civil Engineer website, Retrieved December 9, 2018, from https://www.iamcivilengineer.com/what-are-fender-piles/, Copyright by I am Civil Engineer Website.

Frost, J. D., & Han, J. (1999). Behavior of interfaces between fiber-reinforced polymers and sands. *J Geotechnical and Geoenvironmental Eng*, **125**(8), 633-640.

Frost, J. D., & Han, J. (1999). Buckling of vertically loaded fiber-reinforced polymer piles. *Journal of reinforced plastics and composites*, **18**(4), 290-318.

Giraldo, J., & Rayhani, M. T. (2013). Influence of fiber-reinforced polymers on pile–soil interface strength in clays. *Advances in civil engineering materials*, **2**(1), 534-550.

Goh, A. T. C., & Donald, I. B. (1984). *Investigation of soil-concrete interface behaviour by simple shear apparatus*. Paper presented at transportation research board (TRP 1984), Washington, USA.

Guades, E. J., Aravinthan, T., and Islam, M. M. et al. (2010). *An overview on the application of FRP composites in piling system.* Paper presented at the southern region engineering conference (SREC 2010), Toowoomba, Australia, 65-70.

Guades, E. J., Aravinthan, T., and Islam, M. M. et al. (2011). *Driveability of composite piles*. Paper presented at the 1st international postgraduate conference on engineering, designing and developing the built environment for sustainable wellbeing (EDDBE 2011), Queensland University of Technology, Australia, 237-242.

Guades, E., Aravinthan, T., Islam, M., Manalo, A. et al. (2012). A review on the driving performance of FRP composite piles. *Composite Structures*, 94, 932-1942.

Horvath, J. S., Trochalides, T., Burns, A., Merjan, S. et al. (2004). Axial-compressive capacities of a new type of tapered steel pipe pile at the John F. Kennedy International Airport.

Hollaway, L. C. (2010). A review of the present and future utilisation of FRP composites in the civil infrastructure with reference to their important in-service properties. *Construction and Building Materials*, 24, 2419-2445.

Iskander, M. G., & Hassan, M. (1998). State of the practice review in FRP composite piling. *J Composites for Construction*, **2**(3), 116-120.

Iskander, M. G., Hanna, S., Stachula, A. et al. (2001). Driveability of FRP Composite Piling. *Journal of Geotechnical and Geoenvironmental Engineering*, 127, 169-176.

Iskander, M. G. (2002). Recent Developments in FRP Composite Piling Practice. Paper presented at Transportation Research Board Annual Meeting, Washington, USA, 02-3589.

Iskander, M., Mohamed, A., Hassan, M. et al. (2002). Durability of recycled fiber-reinforced polymer piling in aggressive environments. *Transportation research record*, **1808**(1), 153-161.

Kaw, A. K. (2005). Mechanics of composite materials. CRC press, USA.

Lupini, J. F., Skinner, A. E., Vaughan, P. R. et al. (1981). Drained Residual Strength of Cohesive Soils. *Geotechnique*, **31**(2), 181-213.

Mays, G. C. (Ed.). (2002). Durability of concrete structures: investigation, repair, protection. CRC Press.

Meyerhof, G. (1976). Bearing Capacity and Settlement of Pile Foundations. *Journal of Geotechnical Engineering* - The 11th Terzaghi Lecture, ASCE, 102, 195-228.

Mirmiran, A., Shahawy, M., El Khoury, C., Naguib, W. et al. (2000). Large Beam-Column Tests on Concrete-Filled Composite Tubes. *ACI Structural Journal*, 97, 268-276.

Mirmiran, A., & Shahawy, M. (2003). Composite pile: A successful drive. *Concrete international*, **25**(3), 89-94.

Nishizaki, I., Takeda, N., Ishizuka, Y., Shimomura, T. et al. (2006). A case study of life cycle cost based on a real FRP bridge. In *Third international conference on FRP composites in civil engineering (CICE 2006).* Miami, 99-102.

Novak, M., & F. Grigg, R. (1976). Dynamic experiments with small pile foundations. *Canadian Geotechnical Journal*, **13**(4), 372-385.

O'Rourke, T. D., Drusche, l. S. J., Netravali, A. N. et al. (1990). Shear Strength Characteristics of Sand-Polymer Interfaces. *Journal of Geotechnical Engineering*, **116**(3), 451-469.

Pando, M., Filz, G., Hoppe, E., Ealy, C., Muchard, M. et al. (2000). Performance of a composite pile in a full scale Statnamic load testing program. In *Proceedings, 53rd Canadian Geotechnical Conference*, 1, 909-916.

Pando, M. A., Filz, G. M., Dove, J. E., Hoppe, E. J. et al. (2002). Interface shear tests on FRP composite piles. *Geotechnique*, **4**(1), 52-56.

Pando, M. A. (2003). A laboratory and field study of composite piles for bridge substructures, Dissertation, Virginia Tech.

Potyondy, J. G. (1961). Skin friction between various soils and construction materials. *Geotechnique*, **11**(4), 339-353.

Reddy, E. S., Chapman, D. N., Sastry, V. V. R. N. et al. (2000). Direct shear interface test for shaft capacity of piles in sand. *Geotechnical Testing Journal*, **23**(2), 199-205.

Rouaiguia, A. (2010). Residual shear strength of clay-structure interfaces. Int *J Civil and Environmental Eng*, **10**(3), 6-18.

Saafan, M. A. A. (2006). Shear strengthening of reinforced concrete beams using GFRP wraps. *Acta Polytechnica*, **46**(1).

Sadeghian, P., Lai, Y. C., Fam, A. et al. (2010). Testing and modeling of a new moment connection of concrete-filled FRP tubes to footings under monotonic and cyclic loadings. *Journal of Composites for Construction*, **15**(4), 653-662.

Sadeghian, P., & Fam, A. (2010). Closed-form model and parametric study on connection of concrete-filled FRP tubes to concrete footings by direct embedment. *Journal of Engineering Mechanics*, **137**(5), 346-354.

Sakr, M., El Naggar, M. H. E., Nehdi, M. et al. (2004). Novel toe driving for thin-walled piles and performance of fiberglass-reinforced polymer (FRP) pile segments. *Canadian geotechnical J*, **41**(2), 313-325.

Shaia, H. (2013). Behaviour of Fibre Reinforced Polymer Composite Piles: Experimental and Numerical Study, Doctoral dissertation, The University of Manchester, Manchester, UK.

Smith, E. (1960). Pile Driving Analysis by the Wave Equation. *Journal for Soil Mechanics and Foundation Division*, ASCE, 86, 35-61.

Soltannia, B., & Taheri, F. (2015). Influence of nano-reinforcement on the mechanical behavior of adhesively bonded single-lap joints subjected to static, quasi-static, and impact loading. *Journal of adhesion Science and Technology*, **29**(5), 424-442.

Taha, A. M. (2010). Interface Shear Behaviour of Sensitive Marine Clay - Leda Clay. Master's Thesis dissertation, University of Ottawa, Ottawa, Ontario, Canada.

Taylor, R. B. (1995). New developments in marine fendering. *Dredging & Port Construction*, **22**(3), 4.

The Difference Between End Bearing Pile and Friction Pile, reprinted from understand construction website, Retrieved on October 1, 2018, from http://understandconstruction.com/pile-foundations.html, Copyright by understanding construction website.

Timber Piles, reprinted from American pole and timer website, Retrieved October 5, 2018, from https://www.americanpoleandtimber.com/wood-timber-products/dock-pier-materials/, Copyright 2018 by American Pole and Timber.

Timber Piles Strengthened with GFRP, reprinted from five-star products website, Retrieved on October 5, 2018, from https://www.fivestarproducts.com/pileform-f-jacket.html, Copyright 2018 by Five Star Products, Inc.

Uesugi, M., & Kishida, H. (1986). Influential factors of friction between steel and dry sands. *Soils and foundations*, **26**(2), 33-46.

Ulitskii, V. M. (1995). History of Pile Foundation Engineering. *Soil Mechanics and Foundation Engineering*, **32**(3), 110-114.

Velez, J. D. G. (2013). Experimental study of Hollow Fibre Reinforced Polymer Piles in soft clay, Master's Thesis dissertation, Carleton University, Ottawa, Canada.

Vesic, A. (1977). Design of Pile Foundations - Synthesis of Highway Practice No. 42. Presented at Transportation Research Board (TRB), National Cooperative Highway Research Program. Washington, USA.

Yuan, W., & Mirmiran, A. (2001). Buckling analysis of concrete-filled FRP tubes. *International Journal of structural stability and dynamics*, **1**(3), 367-383.

Zobel, H. et al. (2005). Kompozyty polimerowe w mostownistwie. *Materiały Budowlane*.

CHAPTER 3 INTERFACE SHEAR TESTS BETWEEN SAND COATED GFRP AND SANDY SOILS

ABSTRACT

Soil-pile interface friction is an important geotechnical engineering factor to be considered in achieving a safe, cost-effective design. Conventional construction materials such as concrete, steel, and wood exhibit serious long-term soil substructure problems, particularly with regard to durability, deterioration, and corrosion. Fiber-reinforced polymer (FRP) composites are potential alternatives for addressing these long-term problems. FRP composites are corrosion resistant, with a higher strength to weight ratio and greater durability than conventional materials. More research and data, especially in terms of the interface with soil, are necessary to adapt these new materials to friction pile applications. This paper describes the results of an experimental study of the interface friction between sandy soil and glass FRP (GFRP) sheets coated with different ratios of sand per unit of surface area. A direct shear test was used to study 18 different groups of flat GFRP specimens. The test parameters were the amount of silica sand coating and normal stresses in the direct shear tests. The GFRP specimens were sheared against three types of soil: sand, silty sand, and sandy lean clay, of which the first two were used in both dense and loose states. The experimental results showed that coating the GFRP sheets with silica sand was effective in enhancing the interface friction with sandy soils under different normal stresses. A pile implication analysis was also performed to compare the effect of sand coated GFRPs on the load capacity of friction piles with different length to diameter ratios.

3.1 INTRODUCTION

The behaviour of interface friction between substructure materials and soils plays a significant role in many soil-structure systems, including friction pile foundations. The direct shear test is an effective means of obtaining strength parameters of the interface between soils and interfacing structures. Potyondy (1961) studied the friction behaviour of the interface between some conventional construction materials (i.e., concrete, steel, and wood) and soil. It was found that the primary factors affecting the soil-structure interaction are surface roughness, moisture content, soil composition, and the magnitude of normal loading. To examine the pile-clay interface, Taha (2010) studied the shear behaviour of the interface between marine clay and concrete and steel piles. By using an automated direct shear machine, it was found that the interface strength increased with increasing relative roughness of the material, resulting in an increased over consolidation ratio (OCR) and clay density. In contrast, the interface shear strength decreased as the degree of soil saturation increased. Rouaiguia (2012) investigated the residual shear strength of a clay-structure interface by using a modified direct shear test. The results showed that the surface roughness was the primary controlling parameter. Paikowsky et al. (1995) found that grain shape and surface roughness were key parameters which control the interface shear strength.

Chu and Yin (2006) investigated the soil-cement grout interface shear strength of soil nailing by using a large direct shear test apparatus. They found that the angle of interface friction increased with increased interface surface waviness and applied normal stresses. Goh and Donald (1984) studied a soil-concrete interface by using a simple shear apparatus. They found that the interface shear strength depends on the concrete surface texture and on

the amount of clay in the soil. To investigate a pile-sand interface, Uesugi and Keshida (1986) studied the friction behaviour of the interface between steel and sand by using a simple shear apparatus. The results showed that the controlling parameters are normal stress and surface roughness. The following year, in a study of the interface of sand and high-density polyethene (HDPE), Uesugi (1987) found that the interface shear strength increased with increasing soil density. Lehan et al. (1993) also confirmed that the interface friction between the structural material and sand depends upon the density of the sand. This finding is consistent with the fact that the friction angle of dense sand is a greater than that of loose sand. Pando et al. (2002) found that particle angularity and surface roughness were the controlling parameters in the pile-sand interaction. The results presented that lower surface hardness results in greater shear strength.

Conventional materials such as wood, steel, and concrete have been used extensively in pile applications, however, they have been observed to deteriorate over time, especially in coastal regions. Researchers are therefore looking for alternative materials such as fiber-reinforced polymers (FRP) to address this problem. Iskandar and Hasan (1998) investigated the performance of FRP piles. In comparison to steel and concrete piles for marine structures, the FRP piles exhibited greater durability, were lighter in weight, required less maintenance, and were more resistant to corrosion. Sakr et al. (2005) found that inexpensive interface shear tests can be used to capture the skin friction characteristics of FRP piles installed in granular soils. Pando (2003) performed laboratory and field studies of FRP piles for bridge substructures. In an evaluation of the soil-pile interface behaviour of five composite piles and two conventional piles, he found that the interface friction angle for the FRP piles increased with increasing relative asperity height and decreasing relative

asperity spacing. It was found that soil particle size and angularity were the controlling parameters for the soil-pile interface behaviour. Sakr et al. (2004) determined that the lifetime of a deep foundation can be increased by using FRP piles made of self-consolidated concrete (FRP-SCC), by increasing the durability and corrosion resistance so as to reduce the life cycle cost. Frost and Han (1999) studied the friction behaviour of the interface between FRP and sand by using a direct shear test. They found relative roughness (surface roughness/particle mean size) to be a controlling parameter for interface friction, with little influence being exerted by specimen thickness, rate of shearing, or method of preparation. Recently, Toufigh et al. (2015) performed a laboratory study of the behaviour of the interface between carbon FRP (CFRP) and sand. It was found that the interface behaviour was determined primarily by surface roughness and normal stress, and to a lesser extent by the curing age and rate of shearing. The experimental results of the direct shear tests showed that as the normal stress on CFRP interfacing with sand increased, the interface friction angle increased. Vineetha and Ganesan (2014) studied the interface friction between glass FRP (GFRP) and gravel soil. By using a direct shear test, they found that the interface friction angle was greater when the fiber direction was perpendicular to the shearing load. Lavanya et al. (2014) found that the interface friction angle of CFRP was greater when sheared with well graded gravel than when sheared with poorly graded gravel. Giraldo and Rayhani (2013) studied interfaces of both CFRP and GFRP with clay. Their results showed that in terms of the interface friction angle, FRP equalled or surpassed the performance of traditional steel piling under both drained and undrained conditions.

In designing pile foundations, many engineers consider that δ, the interface friction angle, should be equal to 1/2 to 2/3 of φ, the internal friction angle of the soil, depending upon the

materials used. For example, in the case of concrete, it is commonly considered that δ should be 2/3 of φ. However, designers continue to use an approximate value for the friction angle of the interface between different pile materials and soil, because no precise value or ratio is available. Aksoy et al. (2016) indicate that a higher value of δ results in a more economical design and decreased project costs, due to its role in determining the number of piles needed for construction, and their length and diameter.

For this reason, this study was designed to investigate the effect of enhancing the surface roughness of GFRP specimens by using a newly proposed sand coating, with different sand ratios per unit area. The new GFRP surface can be used as a roughened skin for frictional piles to improve their frictional load bearing capacity. The study also provides an in-depth understanding of the frictional behaviour of the enhanced GFRP interface with different types of sandy soils. In addition, a parametric study was conducted to investigate the implications of the proposed interface on the load-bearing capacity of GFRP frictional piles, and to compare the results with the currently available alternatives of conventional GFRP, steel and concrete piles.

3.2 Materials and Methods

Several flat GFRP specimens were coated with sand and tested in contact with different types of soil in a direct shear test, to characterize the friction behaviour of the GFRP-soil interface. The following sections present the details of the experimental program.

3.2.1 Test Matrix

The test matrix is shown in table 3.3 a total of 27 groups of specimens (99.7 mm x 99.7 mm), of which 18 groups were GFRP specimens. In each group three identical specimens

were tested. Each GFRP specimen was fabricated from epoxy resin and two layers of unidirectional fiberglass fabric. Silica sand was added to the surface of 15 of the GFRP specimens. The test parameters were the amount of sand coating per unit area and the applied normal stress in the direct shear test. The ratios of sand added to the surface of the specimens were 0, 500, 1000, 1500, 2000, and 2500 g/m^2. To provide a basis of comparison for the performance of the sand coated sheets, nine groups of smooth GFRP, steel, and concrete specimens were sheared with dense sand. In the direct shear tests, the normal stresses applied to the specimens were 50, 100, and 200 kPa. The test specimens used for comparison purposes were identified by the specimen identification (ID): Smooth GFRP-NY, Steel-NY, and Concrete-NY, where N stands for normal stress, and Y is a numerical indication of the normal stress applied to each specimen in the direct shear test. The GFRP specimens were identified by the ID: GSX-NY, where G stands for GFRP specimen, S stands for sand, and X is a numerical indication of the amount of sand added per unit area (g/m^2). For example, the identification GS1000-N50 indicates a GFRP specimen which has a sand coating of 1000 g/m^2 and is tested under a normal stress of 50 kPa in the direct shear test.

Table 3. 1 Test Matrix for Interface Shear Test

Group #	Specimen ID	Ratio of Sand Coating (g/m^2)	Normal Stress (kPa)
1	GS0-N50	0	50
2	GS0-N100	0	100
3	GS0-N200	0	200
4	GS500-N50	500	50
5	GS500-N100	500	100
6	GS500-N200	500	200
7	GS1000-N50	1000	50
8	GS1000-N100	1000	100
9	GS1000-N200	1000	200
10	GS1500-N50	1500	50
11	GS1500-N100	1500	100
12	GS1500-N200	1500	200
13	GS2000-N50	2000	50
14	GS2000-N100	2000	100
15	GS2000-N200	2000	200
16	GS2500-N50	2500	50
17	GS2500-N100	2500	100
18	GS2500-N200	2500	200
19	Smooth GFRP-N50	0	50
20	Smooth GFRP-N100	0	100
21	Smooth GFRP-N200	0	200
22	Steel-N50	0	50
23	Steel-N100	0	100
24	Steel-N200	0	200
25	Concrete-N50	0	50
26	Concrete-N100	0	100
27	Concrete-N200	0	200

Note: For each group, three identical specimens were prepared and tested

3.2.2 Material Properties

3.2.2.1 GFRP

All specimens were prepared with the same unidirectional fiberglass fabric, with two layers on top of one another as a single laminate (468.3 g/m^2 per fabric layer). The laminate was bonded with an epoxy resin (West System 105) and a hardener (West System 206). The tensile strength of the fiberglass fabric (dry fiber) was 1500 MPa, with an areal fabric weight of 450 g/m^2, elongation of 2.8%, and E-modulus of 72 GPa, as reported by the manufacturer (Haining Anjie Composite Material Co., Zhejiang, China). The tensile strength and elastic modulus of the GFRP composite were determined to be 502 MPa and 32 GPa, respectively, based on tensile tests.

3.2.2.2 Coating Sand

In order to determine the properties of the silica sand sprinkled on the GFRP composite, sieve analysis testing was carried out in accordance with the American Society for Testing and Materials (ASTM) C136-14 (2014). The silica sand gradation curve is shown in Figure 3.1(a). From the curve obtained, the values of D_{10}, D_{30}, D_{50}, and D_{60} were 1.1, 1.4, 1.8, and 1.9, respectively. The uniformity coefficient, C_u, was found to be 1.7, and the coefficient of gradation, C_c, was 0.9. In the sieve analysis, the percentage of the soil retained in sieve no. 16 from the total silica sand sample was 96.3%. Based on the unified soil classification system (USCS), the silica sand used was classified as poorly graded sand. The silica sand used for sprinkling the surface of the GFRP sheets was that retained in sieves #16 and #8 only.

3.2.2.3 Soil

The soils used for investigating the GFRP interface friction were mainly sandy soils. Three types of sandy soil were used in this experimental study. The first type was sand. The engineering properties of the sand used were classified by sieve analysis testing in accordance with ASTM C136-14 (2014) to determine the gradation curve shown in Figure 3.1(a). From the curve obtained, the values of D_{10}, D_{30}, D_{50}, and D_{60} were 0.2, 0.4, 0.7, and 0.9 respectively. The uniformity coefficient, C_u, was 3.9, and the coefficient of gradation, C_c, was close to 1. Based on the USCS, the sand was classified as poorly graded sand. The maximum dry density of the sand and the optimum water content shown in Figure 3.1(b) were determined by the laboratory compaction characteristics of the soil, by using standard effort in accordance with ASTM D698-12 (2012). The maximum dry density of the sand was 1717 kg/m^3, and the optimum water content was 13%. The second type of soil used was silty sand, which contains 40% silt and 60% sand. The maximum dry density of the silty sand was 1883 kg/m^3 and the optimum water content was 12%. The coefficient of uniformity, C_u, for the silty sand was 6, and the coefficient of curvature, c_c, was 0.7. Two different densities of both sand and silty sand were examined, as follows: dense sand (DS), loose sand (LS), dense silty sand (DSS), and loose silty sand (LSS). In the direct shear box used for the shear test, dense soil was achieved by compacting it to the desired level, while loose soil was obtained by filling the shear box with soil with no compaction. The difference between the peak interface friction angles of the loose and dense states was measured. The third type of soil used in this investigation was sandy lean clay, with a liquid limit (LL) of 25.2%, a plastic limit (PL) of 15.9%, and a plasticity index (PI) of 9.3. The

sandy lean clay had a maximum dry density of 1840 kg/m^3, and an optimum water content of 14%.

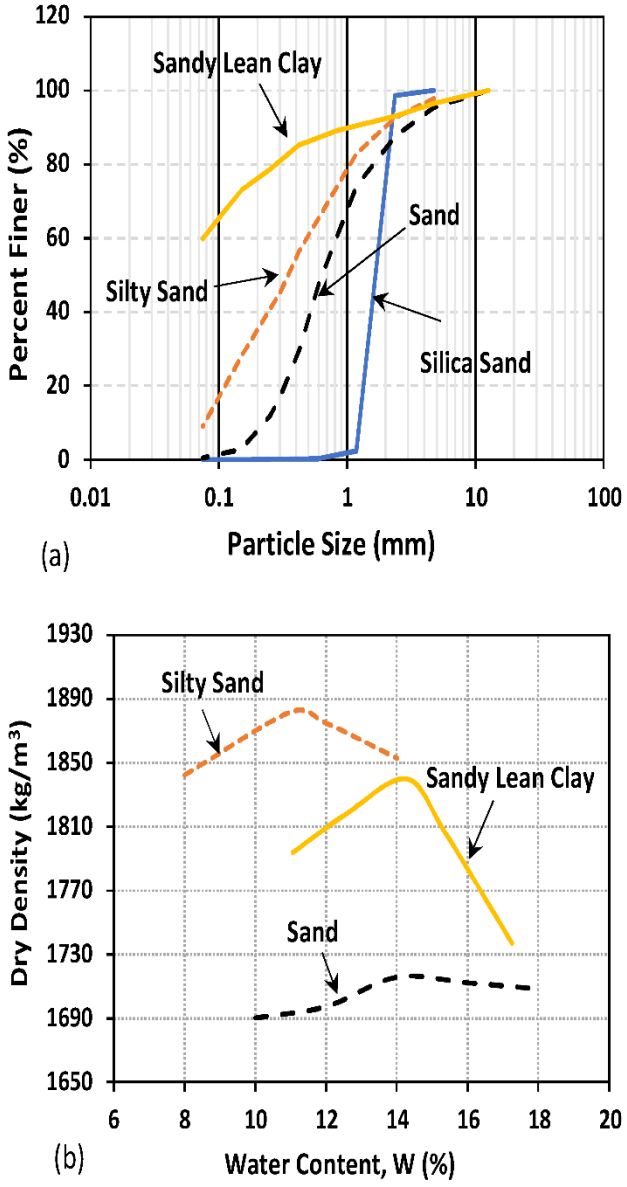

Figure 3. 1 Soil properties: (a) gradation curves, and (b) maximum dry density vs. optimum water content

3.2.3 Specimen Fabrication

A total of 6 GFRP sheets (406 mm x 406 mm) were fabricated initially. Each sheet consisted of two layers of glass fabric (936.7 g/m^2 dry fabric). 68.8 g of epoxy resin plus hardener was applied to the top and bottom surface of each glass fabric layer. Wax paper was used beneath each sheet, to prevent the resin from sticking to the workspace. Five of the six sheets were sprinkled with silica sand, as shown in Figure 3.2. For each of the five sheets, a different ratio of sand per surface area was used: 500, 1000, 1500, 2000, and 2500 g/m^2. After application of the sand coating, the weight of the composite sheets: GS0, GS500, GS1000, GS1500, GS2000, and GS2500 was 1902, 2557, 3179, 3617, 4035, and 4247 g/m^2, respectively. The sand was sprinkled uniformly on the surface of five of the sheets, while sheet GS0, which was used as a control specimen, had no sand coating on its surface.

All the sheets were cured at room temperature for a total of seven days from the date of fabrication. After curing was completed, the sheets were cut with a diamond blade saw into nine squares (99.7 mm x 99.7 mm), to be used as specimens for testing with the direct shear test. For each set of parameters, three identical specimens were tested. For comparison with the sand coated GFRP specimens, a smooth GFRP composite sheet was also prepared. The surface of this composite sheet was smoothed by using a roller over wax paper. Moreover, steel and concrete specimens were prepared as conventional materials to be tested in comparison with the GFRP specimens.

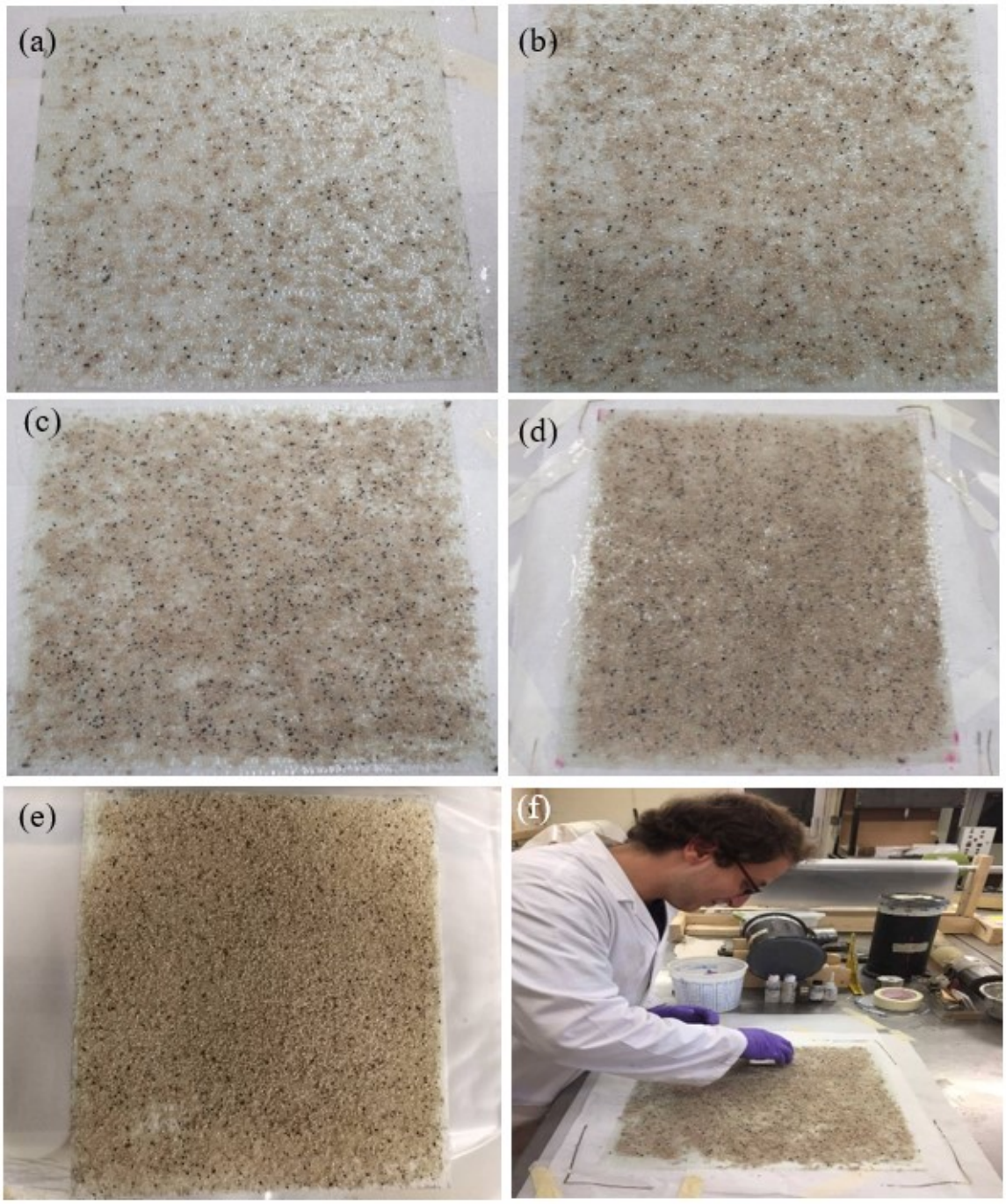

Figure 3. 2 Sand coated GFRP sheets: (a) GS500 specimen, (b) GS1000 specimen, (c) GS1500 specimen, (d) GS2000 specimen, (e) GS2500 specimen, and (f) manufacture of GFRP sheet coated with silica sand

3.2.4 Test Setup

A direct shear test (DST) was used to evaluate the internal friction angle of soil samples and the friction angle of the interface between the soil and GFRP as shown in Figure 3.3. A direct shear box with dimensions 99.7 mm x 99.7 mm and a depth of 29.6 mm was used in this study. In the lower half of the box was a steel plate. An epoxy resin was used to attach the GFRP specimen to the steel formwork. The top half of the box was filled with soil, and the GFRP specimen was sheared with the soil. The shear box was connected to dial gauges to measure the horizontal and vertical displacement of the specimen in the box, as shown in Figures 3.3 and 3.4. The direct shear test was carried out in accordance with ASTM D3080-11 (2011). Normal stress was applied through a steel bearing arm connected to the top section of the shear box. Three different normal pressures: 50, 100, and 200 kPa were applied to simulate typical lateral earth pressures along a pile shaft (interface friction) at a moderate driving depth. A horizontal shear force was applied to the sample, with a shearing rate of 0.24 mm/min.

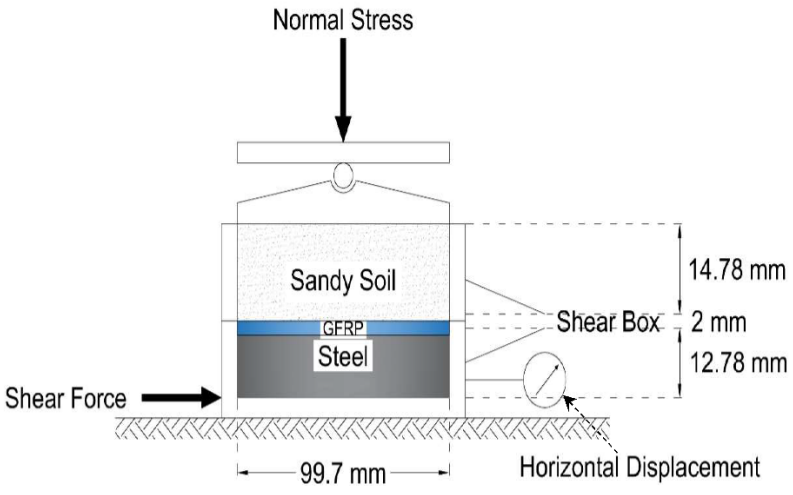

Figure 3. 3 Test set-up for interface friction measurement

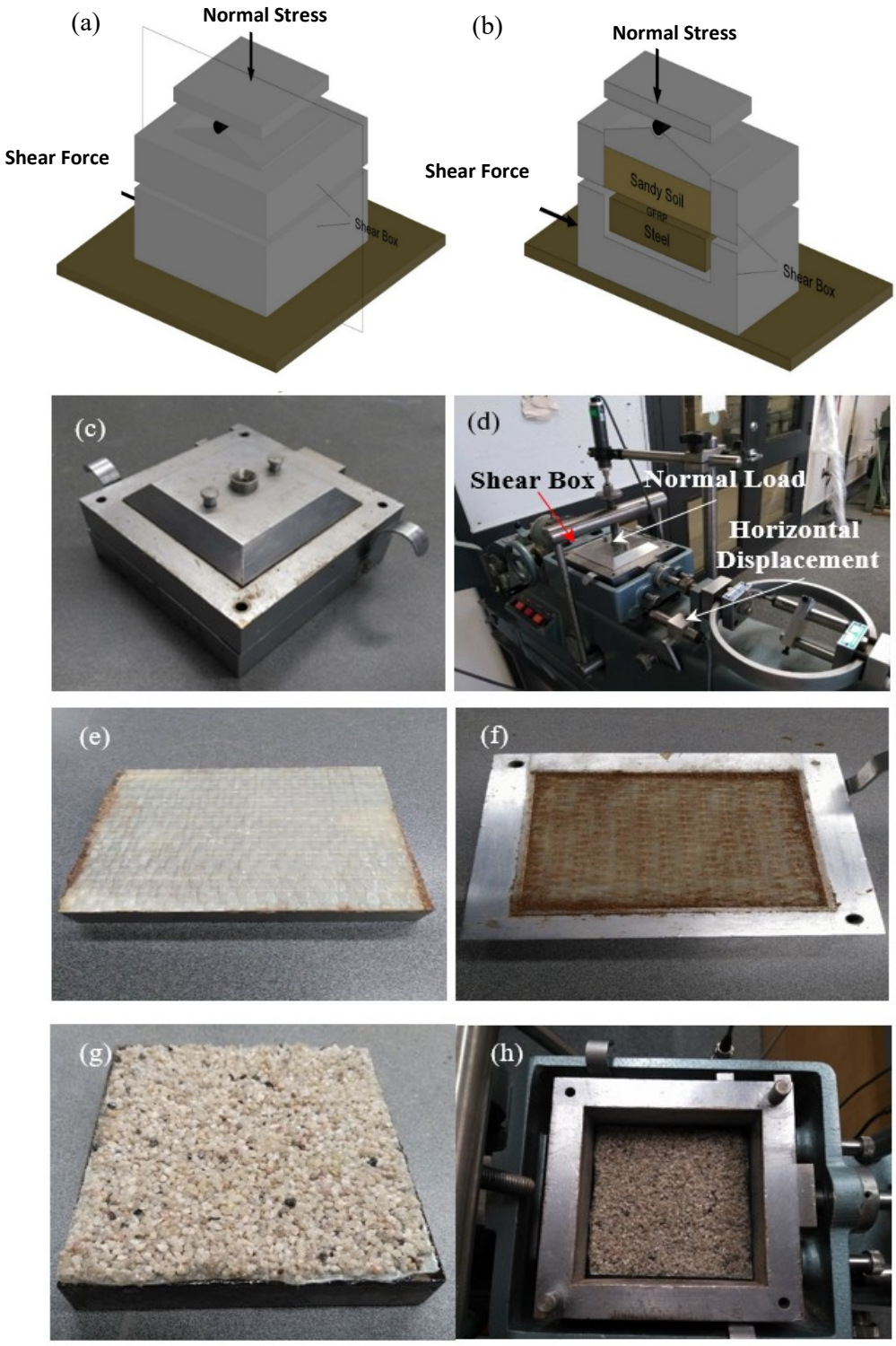

Figure 3. 4 Test set-up: (a) schematic diagram of direct shear box, (b) cross-section of direct shear box, (c) photograph of the direct shear box used, (d) illustration of the test set-up, (e) GFRP specimen on the steel formwork prior to the test, (f) GFRP specimen inside the shear box after the test, (g) GS2500 specimen before testing, and (h) GS2500 specimen inside the shear box

3.3 Results and Discussion

3.3.1 Effect of Soil Density

Three types of sand were used in this study: sand, silty sand, and sandy lean clay. Every soil used in this study was sheared with itself and against GFRP specimens as well in the direct shear box. The poorly graded sand and the silty sand were sheared in both dense and loose states. In order to characterize the shear strength parameters of the soil, the internal friction angle, φ, and the interface cohesion value, C, were determined from shear stress versus normal stress graphs for each type and state of soil. The objective was to determine the interface friction parameters: internal friction angle of the soil, cohesion of the soil, friction angle of the interface between the material and the soil, and adhesion between the material and the soil. For sand shear tests, the plotted lines of the shear stress versus the normal stress was intercepted to zero to eliminate the cohesion/adhesion.

As shown in Figure 3.5, the internal friction angle, φ, was 44.1° for sand in the dense state, and 34.7° for sand in the loose state. For silty sand in the dense state, the internal friction angle, φ, was 42.7° and the cohesion, C, was 19.0 kPa; while for silty sand in the loose state φ was 37.0° and the cohesion was 3.7 kPa, as shown in Figure 3.10. The silt added to the sand provided cohesion to the soil. As shown in Figure 3.15, for sandy lean clay, the internal friction angle was 22.5°, and the cohesion was 15.1 kPa.

3.3.2 Effect of Sand Coating

As reported by Uesugi and Keshida (1986), the interface friction angle depends upon the material surface roughness. In addition, Pando et al. (2002) indicated that particle angularity affects the behaviour of pile-soil interfaces. For this reason, silica sand with

angular to sub-angular particles was used to coat the surface of 15 GFRP specimens, with different sand ratios per unit of surface area. The GFRP/sand interface shear strength was investigated. The objective was to determine whether greater surface waviness of sand coating of the GFRP specimens contributes to higher shear strength values when the specimens are sheared with sandy soils, and to identify which GFRP surface provides the most optimal results.

3.3.2.1 Interface with Sand

The GFRP specimen GS0 without sand coating was sheared with both dense sand (DS) and loose sand (LS). The difference between the peak interface friction angle, δ, for GS0 with dense and loose sand was measured. As shown in Figures 3.6(a) and 3.6(b), the interface friction angle for GS0/DS is 38.7°, while the interface friction angle for GS0/LS is 36.3°. The effect of sand coating is shown in Figures3.6(c) and 3.6(d), where the interface friction angle, δ, increases to 40.3° for GS500/DS, and 38.2° for GS500/LS. For figure 3.6(d), the peak values of shear stresses for GS500/DS were taken close to the residual as neglecting a sudden jump occurred in Figure 3.6(c) following the same trend instead. The effect of sand coating can also be seen in Figures 3.7(a) and 3.7(b), where δ is 41.4° for GS1000 with dense sand, which is higher than the value for GS500/DS. In the GS1000 specimen, the sand particles are able to penetrate the voids in the silica sand coating, resulting in greater strength of the interface between the soil and the material. The interface friction angle, δ, for GS1000/LS is 38.2°.

Increasing the sand coating ratio above 1000 g/m^2 increased the interface friction angle with sand. As shown in Figures 3.7(c) and 3.7(d), for GS1500 with dense sand the interface friction angle is 42.0°. This specimen was found to have an optimum sand coating. Here the

increase in the sand coating ratio gives rise to more interlocking between the particles, resulting in greater interface friction. For GS1500/LS, the interface friction angle is 38.2°. Increasing the sand coating ratio to more than 1500 g/m^2 began to cause a decrease in the interface friction angle with sand. As shown in Figures 3.8(a) and 3.8(b), GS2000/DS has an interface friction angle of 39.9°, which is less than the value for GS1500/DS. In Figures 8(a) and 8(b) it can be seen that GS2000/LS has an interface friction angle of 36.8°.

A decrease in the interface friction angle is shown in Figures 3.8(c) and 3.8(d), where GS2500/DS has an interface friction angle of 39.5°, which is smaller than that of GS1500/DS and GS2000/DS. The reduced number of voids in the silica sand coating in GS2500 results in less interlocking with the soil, which decreases the friction angle with sand. For GS2500/LS, the interface friction angle is only 33.2°. Figure 3.9 presents a comparison of the interface parameters for different GFRP sheets, with dense and loose sand.

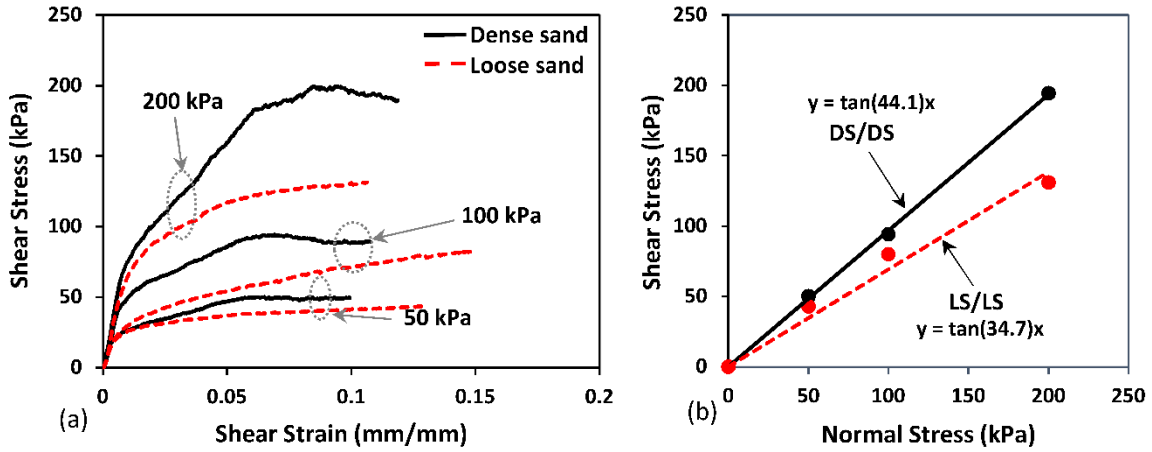

Figure 3. 5 Direct shear tests of loose sand (LS) and dense sand (DS): (a) shear stress vs. shear strain, and (b) shear stress vs. normal stress

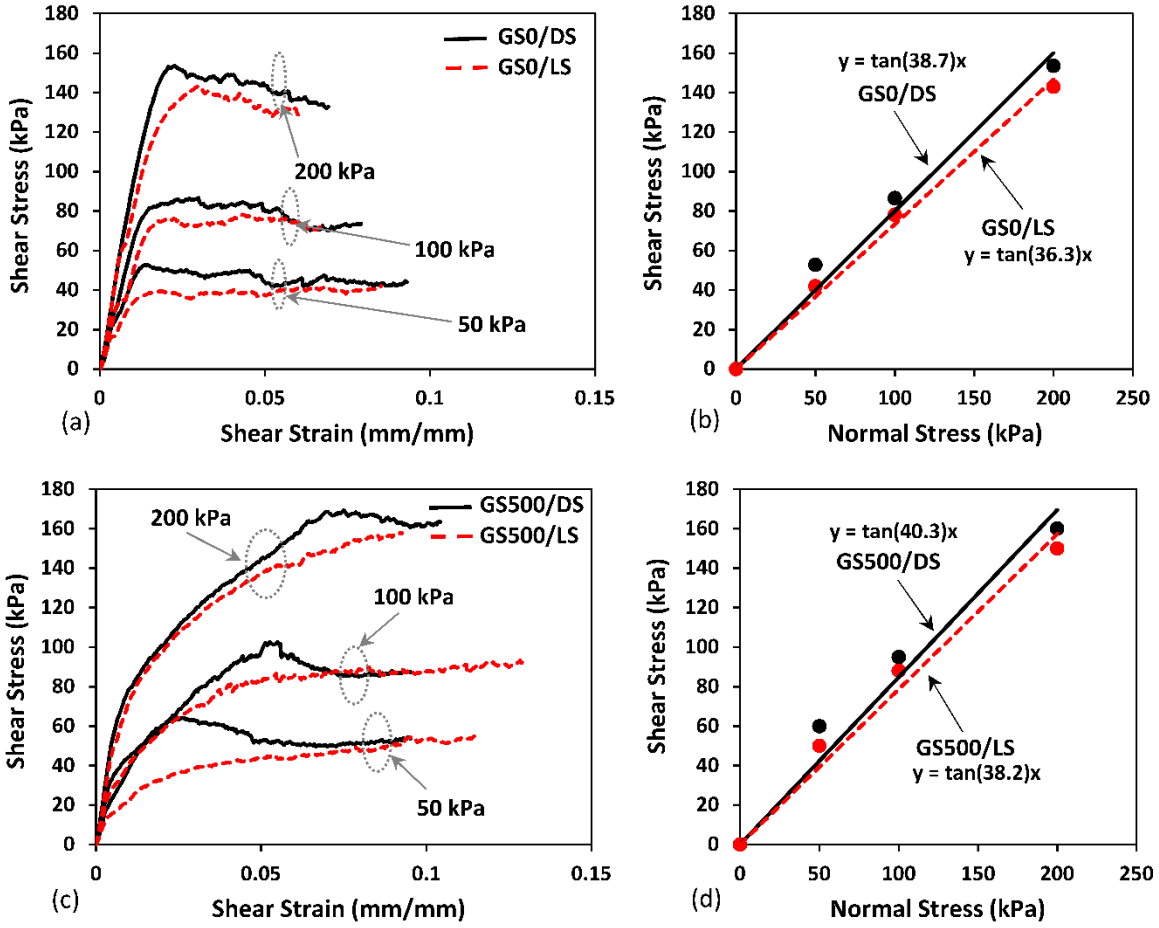

Figure 3. 6 Direct shear tests of loose sand (LS) and dense sand (DS), with GFRP without sand coating (GS0): (a) shear stress vs. shear strain, and (b) shear stress vs. normal stress; and with sand coated GFRP GS500: (c) shear stress vs. shear strain, and (d) shear stress vs. normal stress

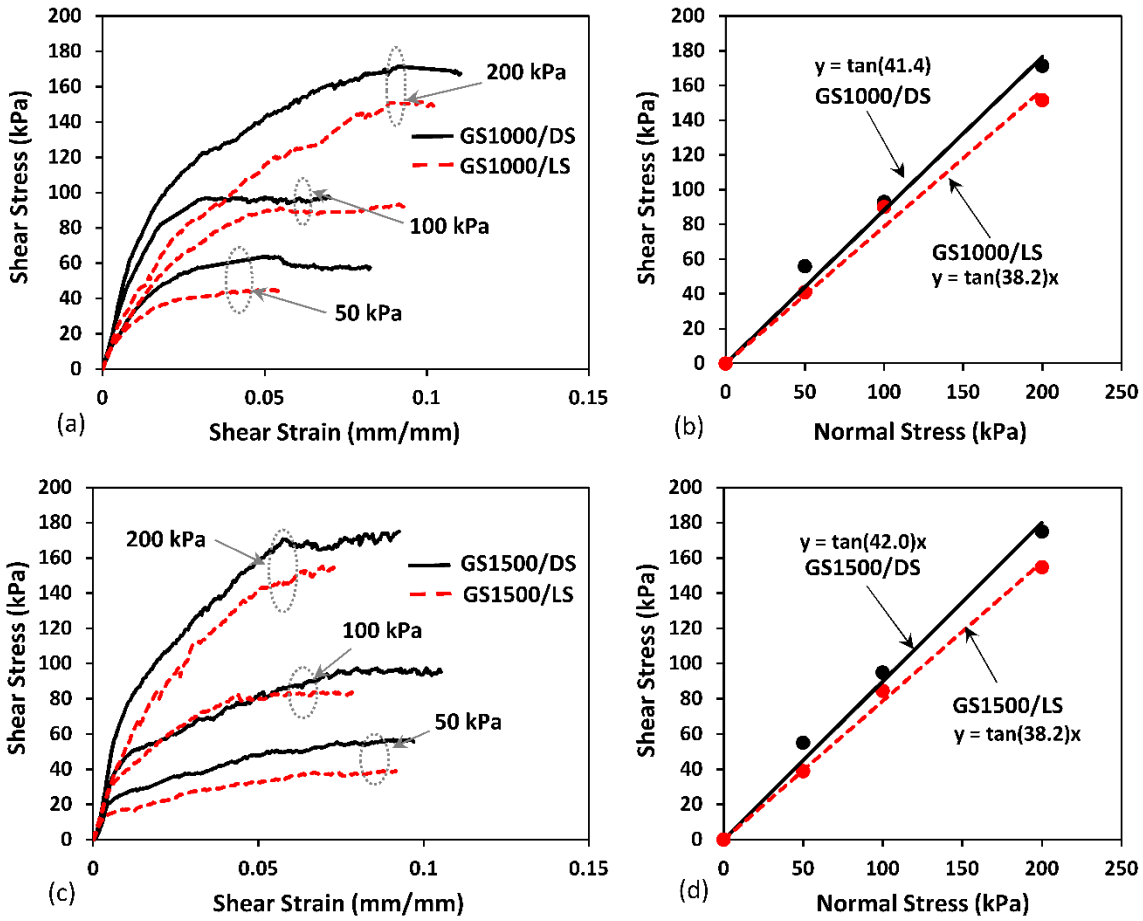

Figure 3. 7 Direct shear tests of loose sand (LS) and dense sand (DS), with sand coated GFRP GS1000: (a) shear stress vs. shear strain, and (b) shear stress vs. normal stress; and with sand coated GFRP GS1500: (c) shear stress vs. shear strain, and (d) shear stress vs. normal stress

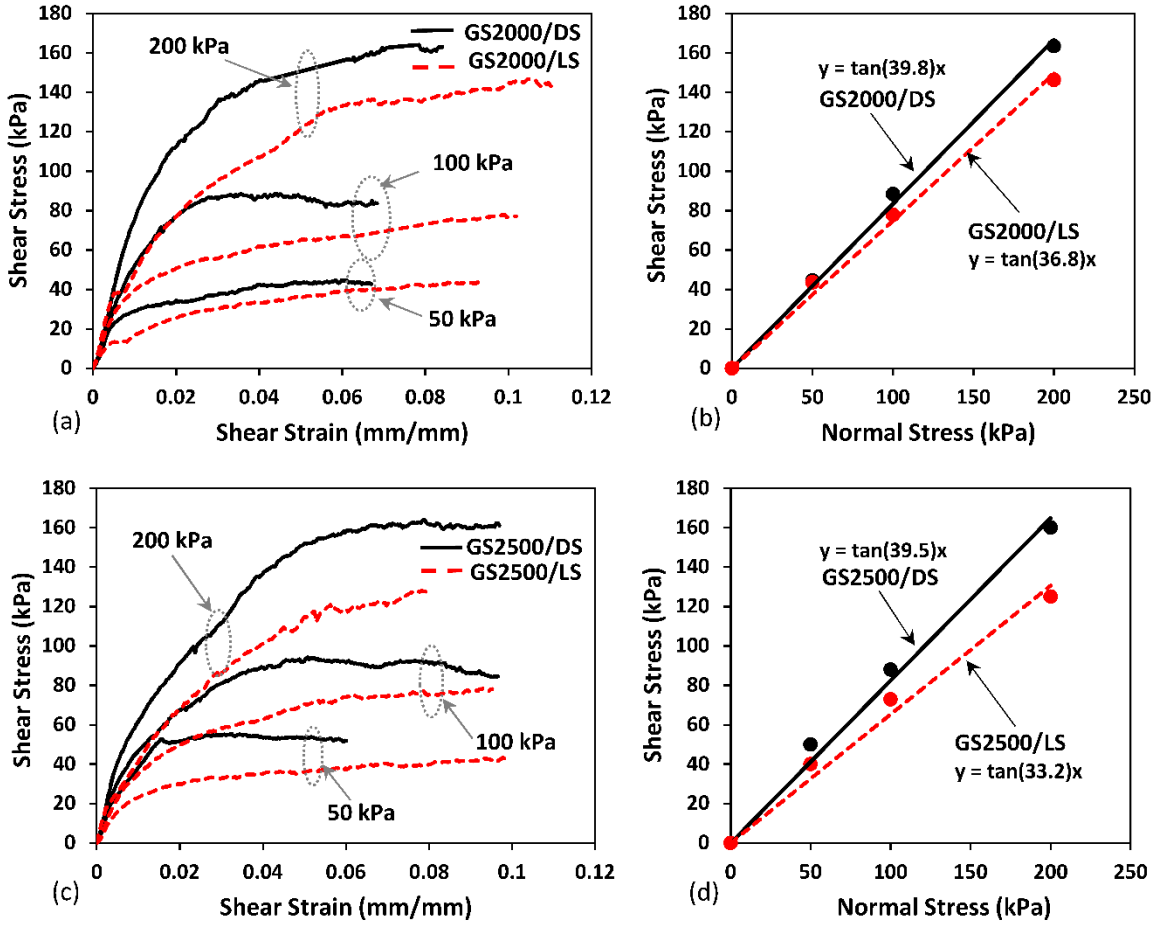

Figure 3. 8 Direct shear tests of loose sand (LS) and dense sand (DS), with sand coated GFRP GS2000: (a) shear stress vs. shear strain, and (b) shear stress vs. normal stress; and with sand coated GFRP GS2500: (c) shear stress vs. shear strain, and (d) shear stress vs. normal stress

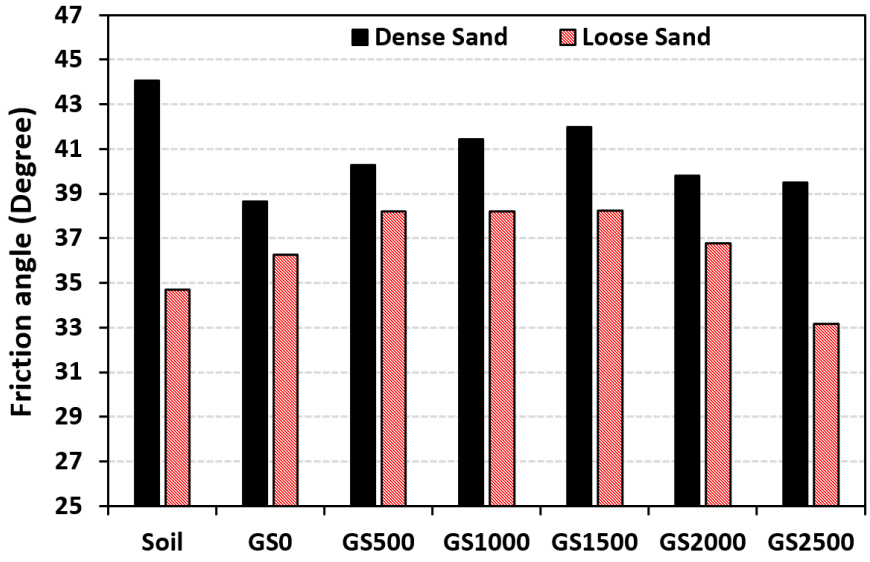

Figure 3. 9 Comparison of test results: friction angles with dense and loose sand

3.3.2.2 Interface with Silty Sand

As shown in Figures 3.11(a) and 3.11(b), for GS0 sheared with dense silty sand (GS0/DSS) and loose silty sand (GS0/LSS), the interface friction angles are 37.1° and 30.9°, respectively; and the adhesion values are 13.0 kPa and 4.0 kPa, respectively.

The effect of sand coating is shown in Figures 3.11(c) and 3.11(d), where the interface friction angle increases to 38.8° for GS500/DSS and the adhesion is 2 kPa. For GS500/LSS, δ is 34.6°, with an adhesion of 6.5 kPa. As shown in Figures 3.12(a) and 3.12(b), GS1000/DSS has an interface friction angle of 38.5° and an adhesion of 19.9 kPa; whereas GS1000/LSS has an interface friction angle of 34.1° and an adhesion of 3.0 kPa.

It can be seen in Figures 3.12(c) and 3.12(d) that the interface friction angle increases to 40.4° for GS1500/DSS, with an adhesion of 5.7 kPa. For GS1500/LSS, the interface friction angle is 34.6°, with an adhesion value close to zero. As shown in Figures 3.13(a) and 3.13(b), the interface friction angle for GS2000/DSS is higher than that for GS1500/DSS.

The small particles of soil are able to penetrate the voids in the silica sand coating of GS2000, forming a strong adhesion with the coating, with an optimum interface friction angle of 43.3° and an adhesion of 7.0 kPa. This was the highest interface friction found among all the GFRP specimens tested with sand. For GS2000/LSS the interface friction angle is 36.9°, with an adhesion of 4.0 kPa.

For GS2500/DSS, as shown in Figures 3.13(c) and 3.13(d), the interface friction angle, δ, decreases to 40.2°, with an adhesion value of 11.6 kPa. GS2500/LSS also has a decreased interface friction angle of 34.5°, with an adhesion value of 1.9 kPa. Increasing the sand coating ratio of the GFRP specimen to more than 2000 g/m^2 resulted in a decreased interface friction angle with silty sand, due to less interlocking with the material surface. Figure 3.14 shows a comparison of the interface parameters for different GFRP sheets, with dense and loose silty sand.

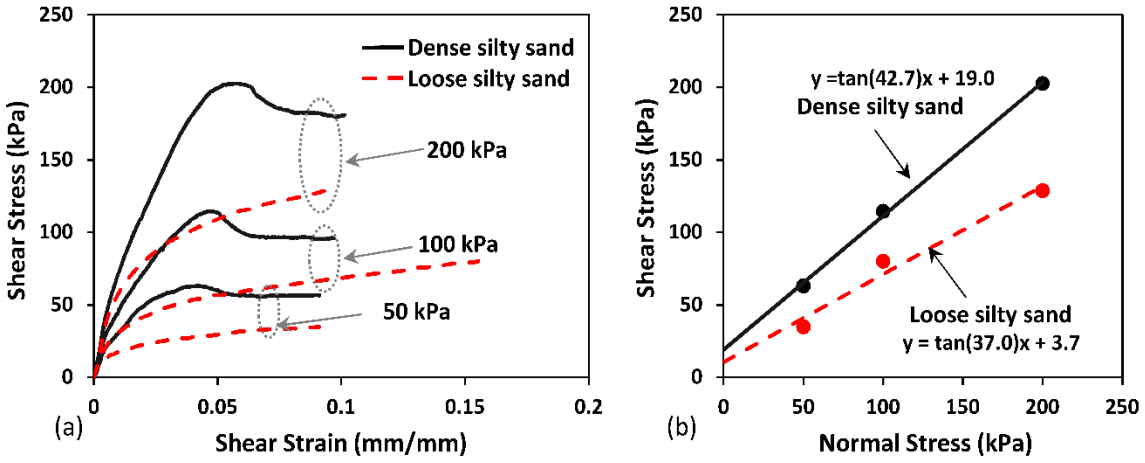

Figure 3. 10 Direct shear tests of loose silty sand (LSS) and dense silty sand (DSS): (a) shear stress vs. shear strain, and (b) shear stress vs. normal stress

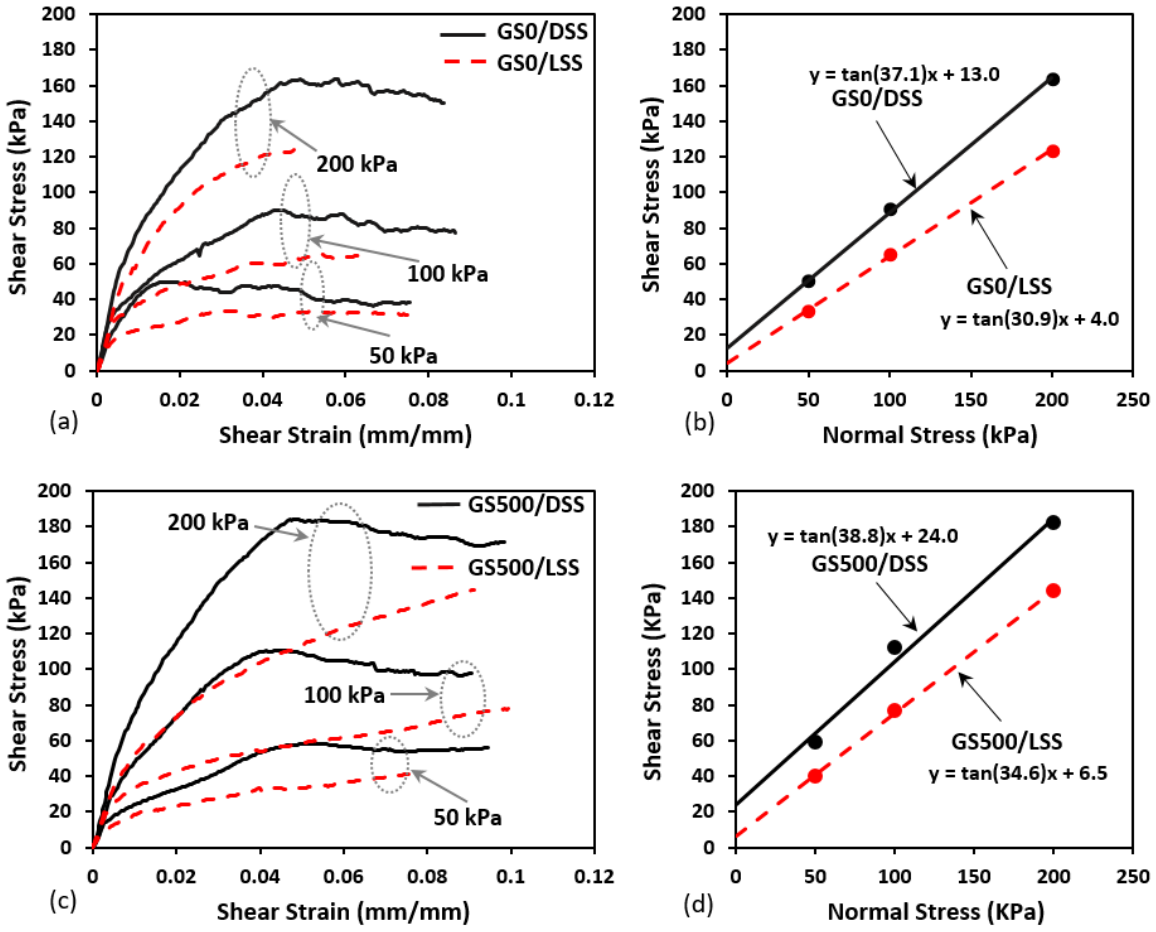

Figure 3. 11 Direct shear tests of loose silty sand (LSS) and dense silty sand (DSS), with GFRP without sand coating (GS0): (a) shear stress vs. shear strain, and (b) shear stress vs. normal stress; and with sand coated GFRP GS500: (c) shear stress vs. shear strain, and (d) shear stress vs. normal stress

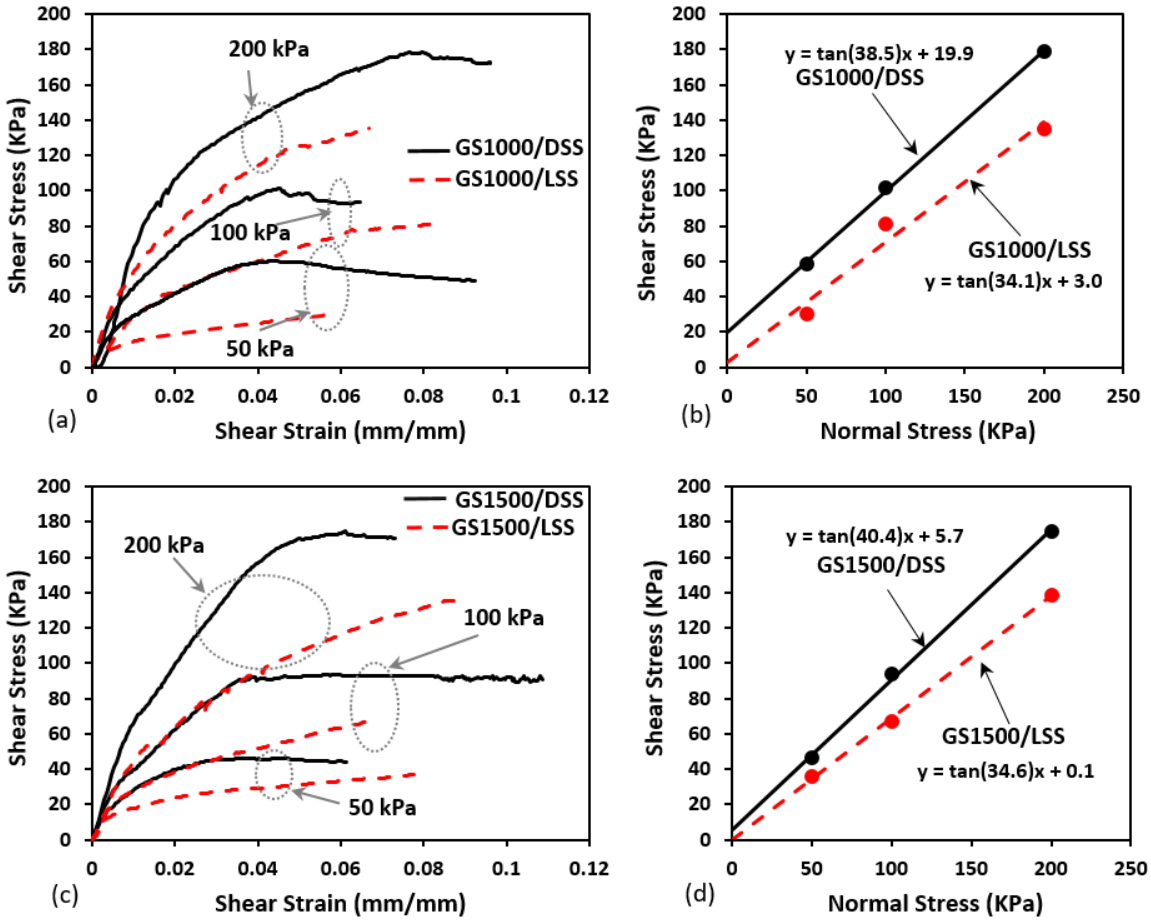

Figure 3. 12 Direct shear tests of loose silty sand (LSS) and dense silty sand (DSS), with sand coated GFRP GS1000: (a) shear stress vs. shear strain, and (b) shear stress vs. normal stress; and with sand coated GFRP GS1500: (c) shear stress vs. shear strain, and (d) shear stress vs. normal stress

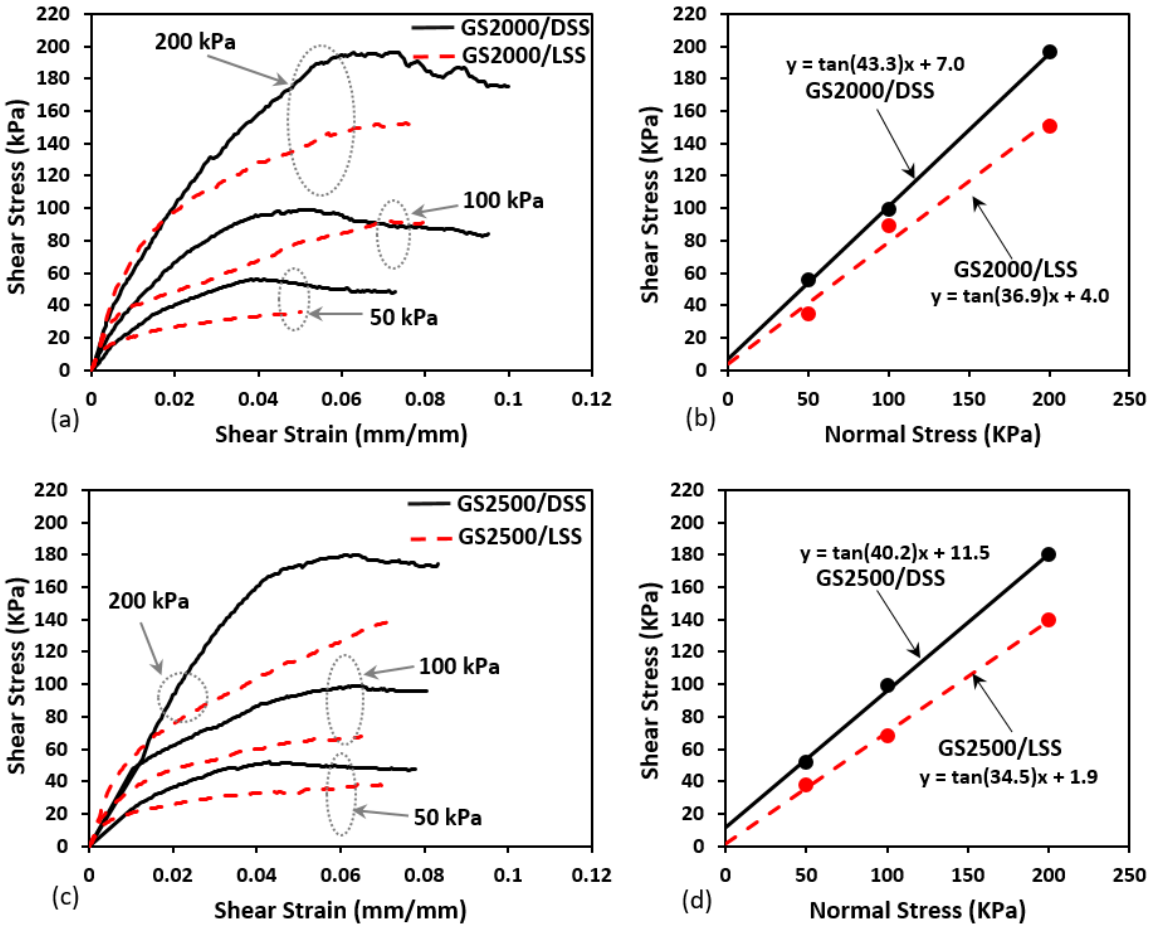

Figure 3. 13 Direct shear tests of loose silty sand (LSS) and dense silty sand (DSS), with sand coated GFRP GS2000: (a) shear stress vs. shear strain, and (b) shear stress vs. normal stress; and with sand coated GFRP GS2500: (c) shear stress vs. shear strain, and (d) shear stress vs. normal stress

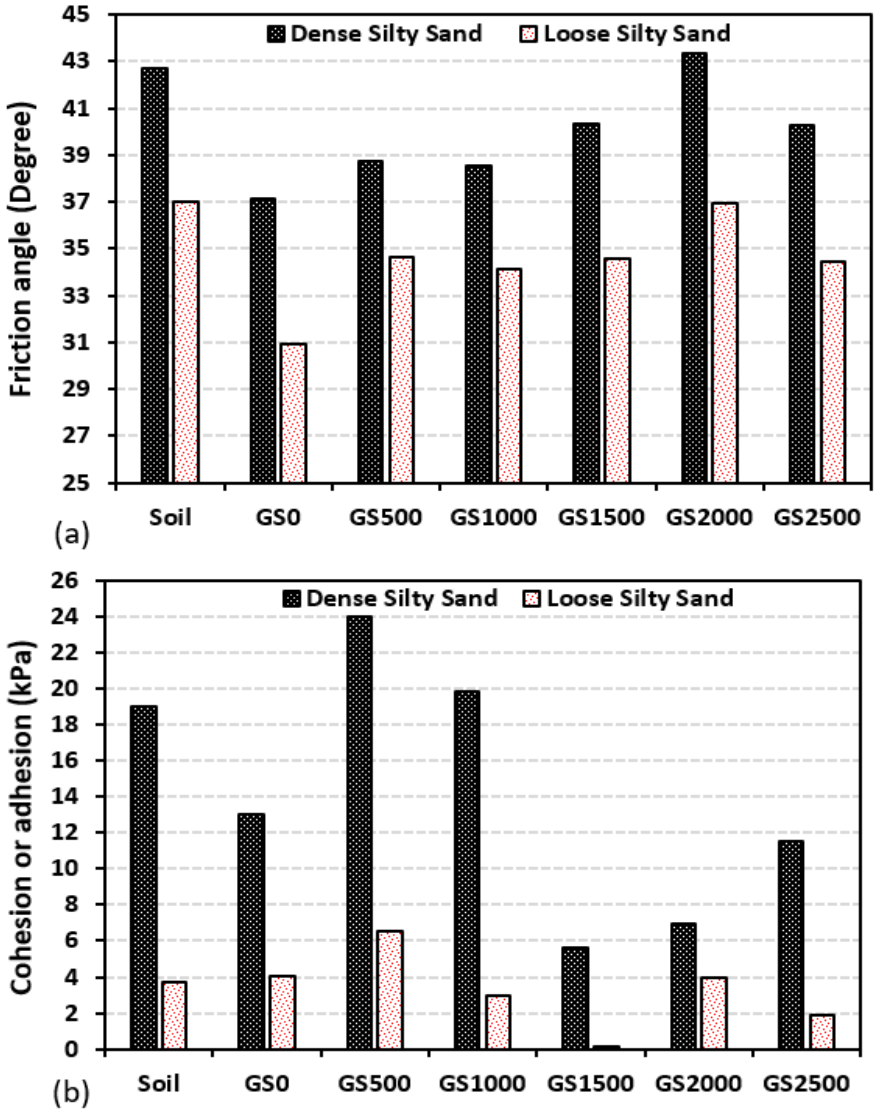

Figure 3. 14 Comparison of test results: (a) friction angles with dense and loose silty sand, and (b) cohesion or adhesion with dense and loose silty sand

3.3.2.3 Interface with Sandy Lean Clay

As shown in Figures 3.16(a) and 3.16(b), GS0 with sandy lean clay (GS0/SLC) has an interface friction angle of 15.7°, with an adhesion value of 22.2 kPa. The effect of sand coating can be seen in Figures 3.16(c) and 3.16(d), where GS500/SLC has an interface friction angle of 21.5°, which is greater than that of GS0/SLC. The rougher surface of the GS500 specimen provides more friction with the clay particles, resulting in greater interface strength and adhesion between the soil and the material, with an adhesion value of 23.1 kPa.

The effect of sand coating can also be seen in Figures 3.17(a) and 3.17(b), where the interface friction angle increases to 25.2° for GS1000/SLC, which is higher than the value for GS500/SLC. The rougher surface of the GS1000 specimen provides greater friction with the sand particles, resulting in the highest optimum adhesion, with a value of 64.0 kPa. As shown in Figures 3.17(c) and 3.17(d), for GS1500/SLC the adhesion is 46.2 kPa and the interface friction angle is 27.3°, which is greater than the value for GS1000/SLC. As can be seen in Figures 3.18(a) and 3.18(b), with a sand coating ratio of 2000 g/m^2, an optimum interface friction angle of 36.4° was found for GS2000/SLC, with an adhesion of 29.6 kPa. Increasing the sand coating ratio to 2500 g/m^2 resulted in a decreased interface friction angle of 30.6° for GS2500/SLC, with an adhesion value of 24.2 kPa, as shown in Figures 3.18(c) and 3.18(d). Increasing the sand coating ratio of the GFRP specimen to more than 2000 g/m^2 caused the interface friction angle with sandy lean clay to decrease, due to fewer voids in the particles of the material and less interlocking. Figure 3.19 presents a comparison of the interface parameters for different GFRP sheets with sandy lean clay.

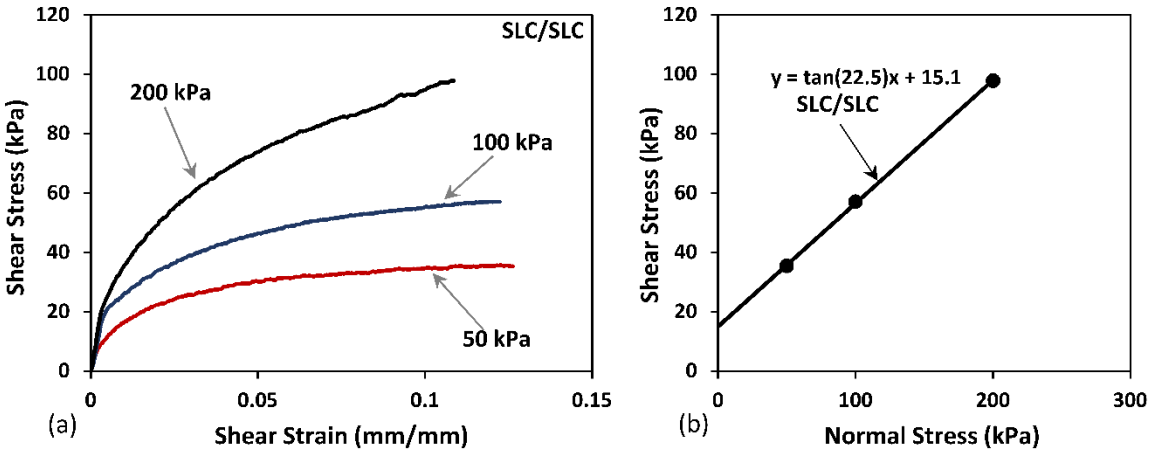

Figure 3. 15 Direct shear tests of sandy lean clay (SLC): (a) shear stress vs. shear strain, and (b) shear stress vs. normal stress

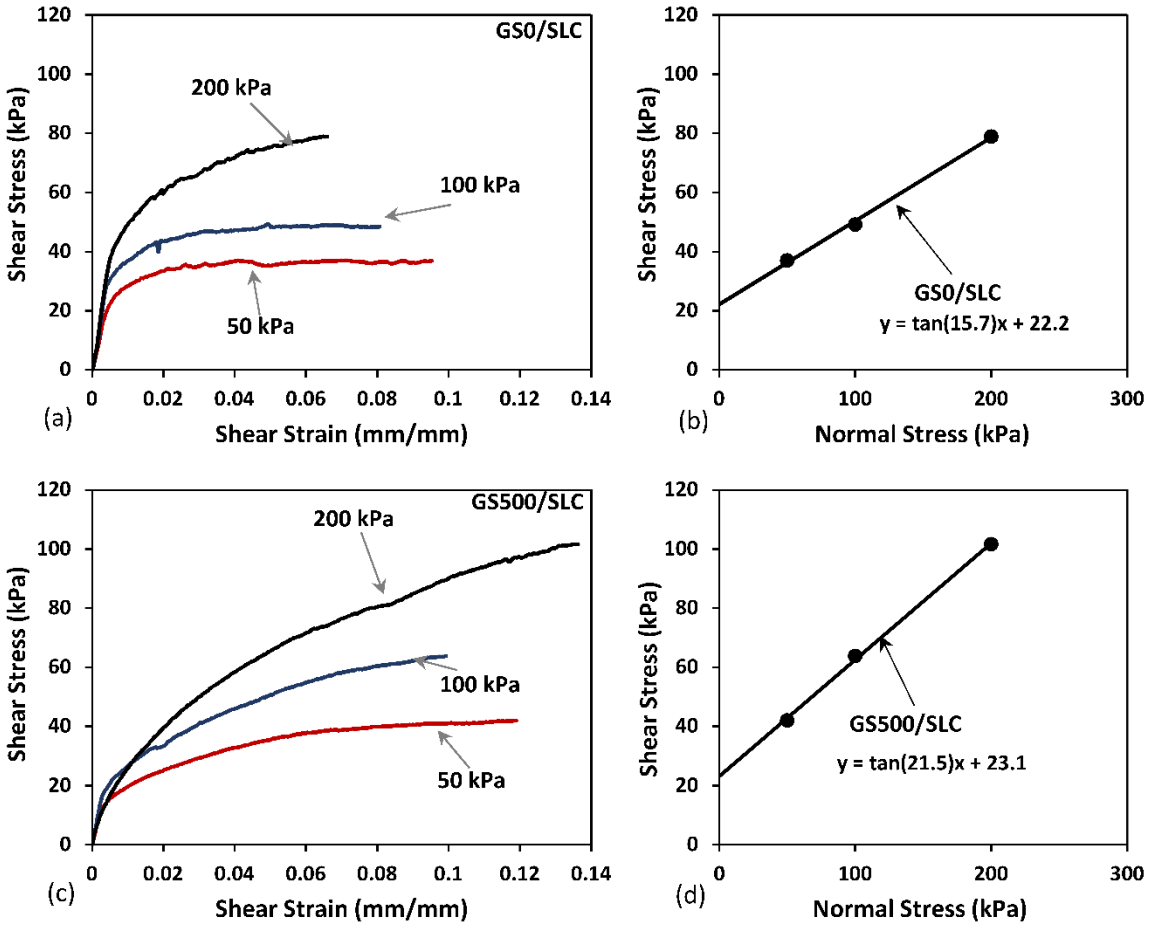

Figure 3. 16 Direct shear tests of sandy lean clay (SLC), with GFRP without sand coating (GS0): (a) shear stress vs. shear strain, and (b) shear stress vs. normal stress; and with sand coated GFRP GS500: (c) shear stress vs. shear strain, and (d) shear stress vs. normal stress

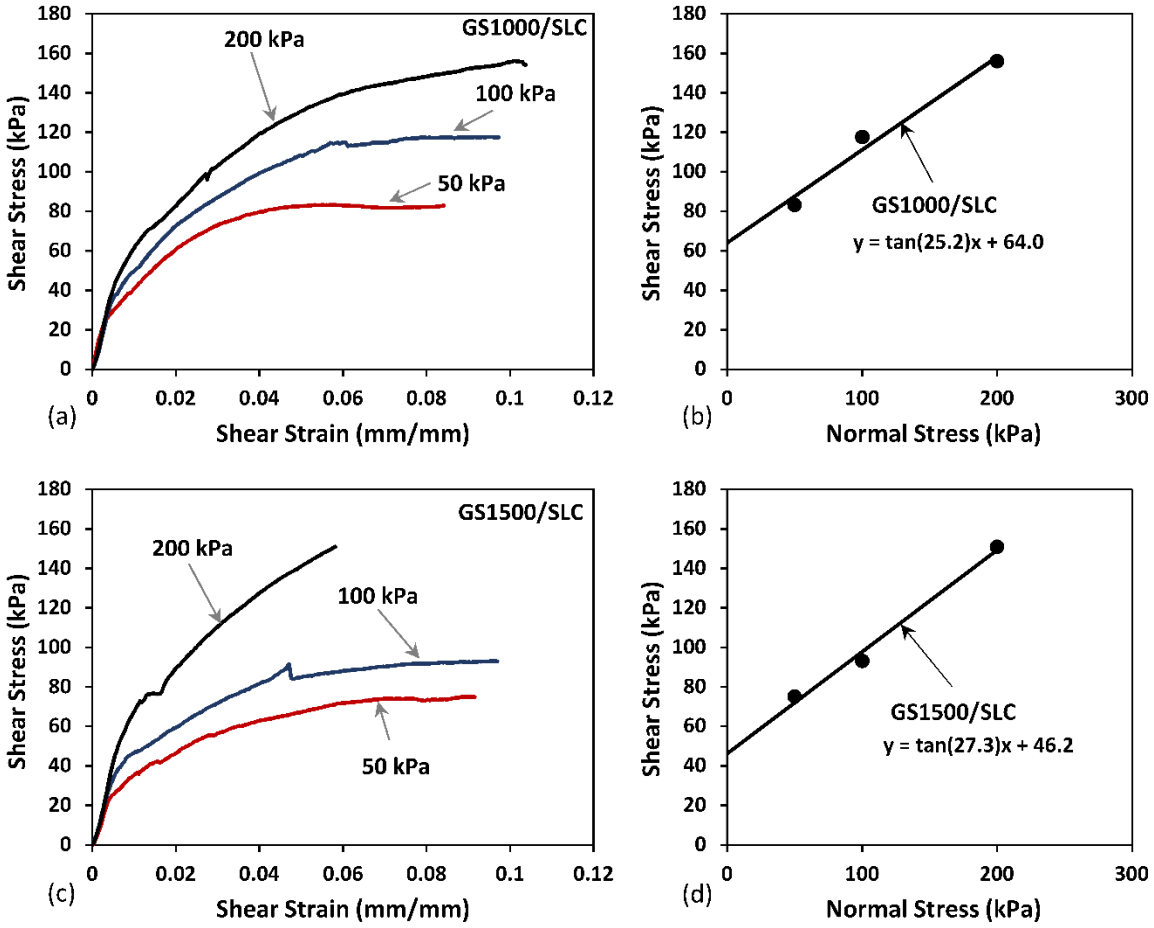

Figure 3. 17 Direct shear tests of sandy lean clay (SLC), with sand coated GFRP GS1000: (a) shear stress vs. shear strain, and (b) shear stress vs. normal stress; and with sand coated GFRP GS1500: (c) shear stress vs. shear strain, and (d) shear stress vs. normal stress

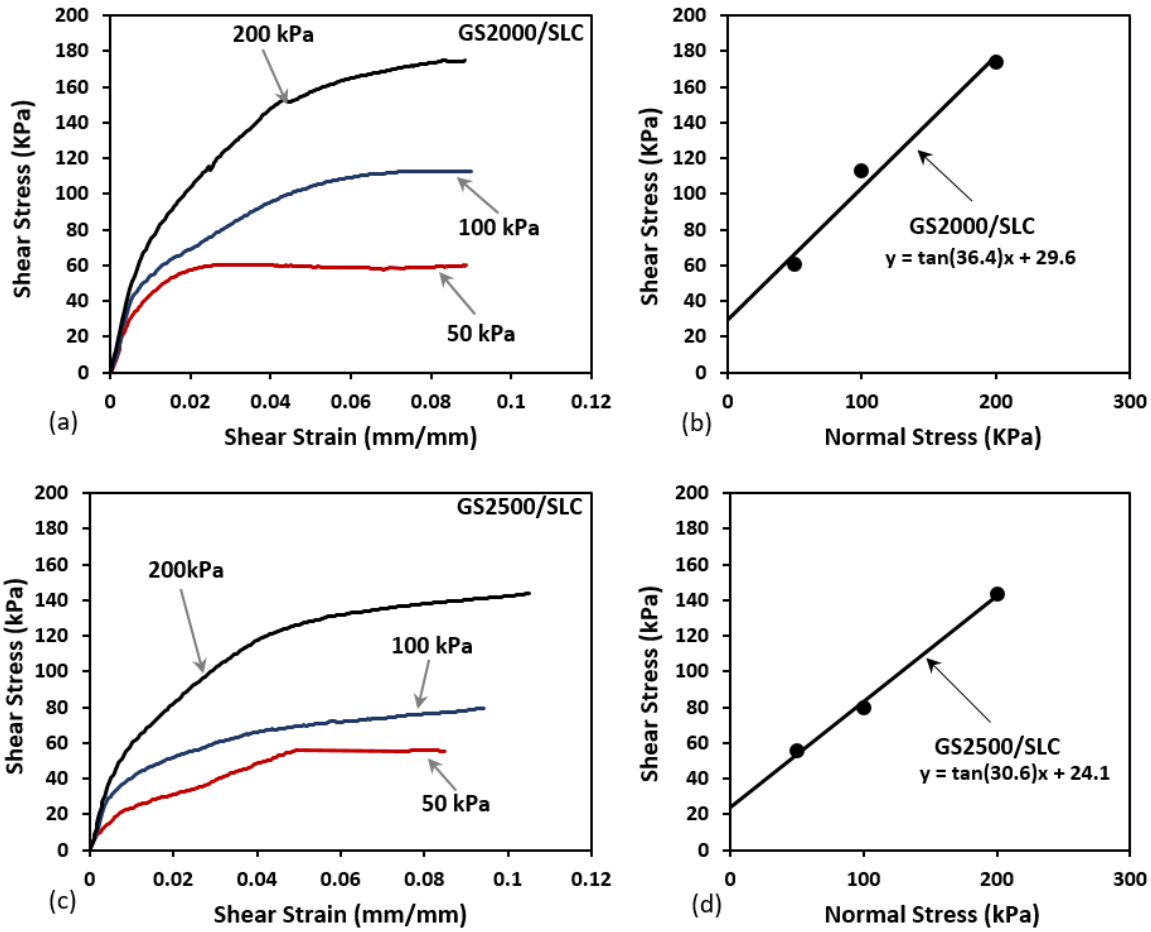

Figure 3. 18 Direct shear tests of sandy lean clay (SLC), with sand coated GFRP GS2000: (a) shear stress vs. shear strain, and (b) shear stress vs. normal stress; and with sand coated GFRP GS2500: (c) shear stress vs. shear strain, and (d) shear stress vs. normal stress

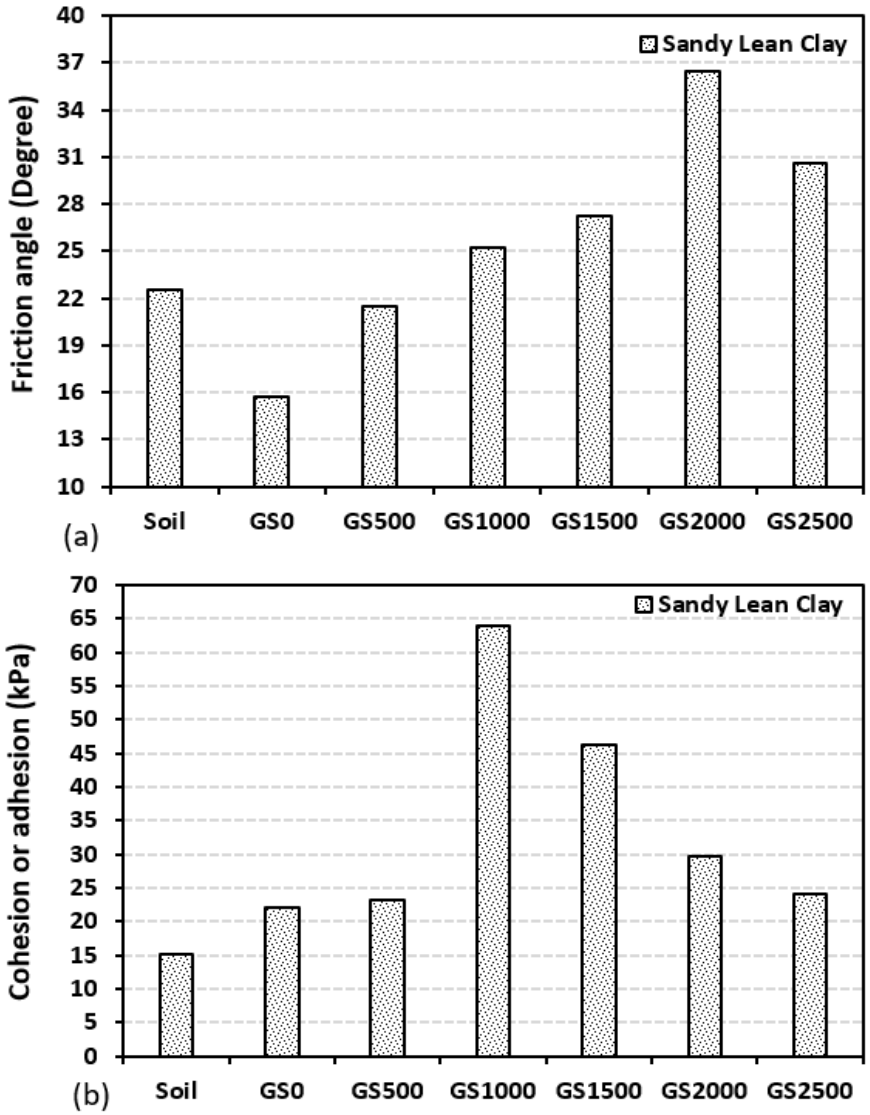

Figure 3. 19 Comparison of test results: (a) friction angles with sandy lean clay, and (b) cohesion or adhesion with sandy lean clay

3.3.3 Comparison with Conventional Pile Materials

For purposes of comparison with the experimental results for sand coated GFRP specimens, three different materials: smooth GFRP composite sheet (1852 g/m^2), steel, and concrete were sheared against dense sand under three different normal pressures: 50, 100, and 200 kPa. As shown in Figures 3.20(a) and 3.20(b), the smooth GFRP specimen sheared with

dense sand has an interface friction angle, δ, of 32.7°. The ratio of the interface friction angle to the internal friction angle of the soil (δ/φ) is 0.7, with a (tanδ/tanφ) ratio of 0.7. The δ/φ ratio for the optimum sand coated specimen GS1500 (the sand coated specimen which exhibited the greatest interface friction angle with sand) is close to 1, with a (tanδ/tanφ) ratio of 0.9. The percentage gain of the sand coated GFRP specimen GS1500 in comparison to the smooth GFRP specimen is 28.5%.

The second material used for comparison was steel. Steel has an ultimate tensile strength of 440 MPa, a yield tensile strength of 370 MPa, a modulus of elasticity (E) of 205 GPa, and a shear modulus of 80 GPa. As can be seen in Figures 3.20(c) and 3.20(d), the steel specimen sheared with dense sand has an interface friction angle of 28.6°. The ratio of the interface friction angle to the internal friction angle of the sand (δ/φ) is 0.7, with a (tanδ/tanφ) ratio of 0.6. The percentage gain of the sand coated GFRP specimen GS1500 in comparison to the steel specimen is 47.0%.

The third material used for comparison was concrete. As shown in Figures 3.21(a) and 3.21(b), the mould side surface of the concrete specimen sheered with dense sand has an interface friction angle of 38.8°. The ratio of the interface friction angle to the internal friction angle of the sand (δ/φ) is 0.9, with a (tanδ/tanφ) ratio of 0.8. The percentage gain of the sand coated GFRP specimen GS1500 in comparison to the concrete specimen is 8.1%. Figure 3.23 presents a comparison of the interface friction angles of smooth GFRP, steel, concrete, and the GS1500 specimen, with dense sand.

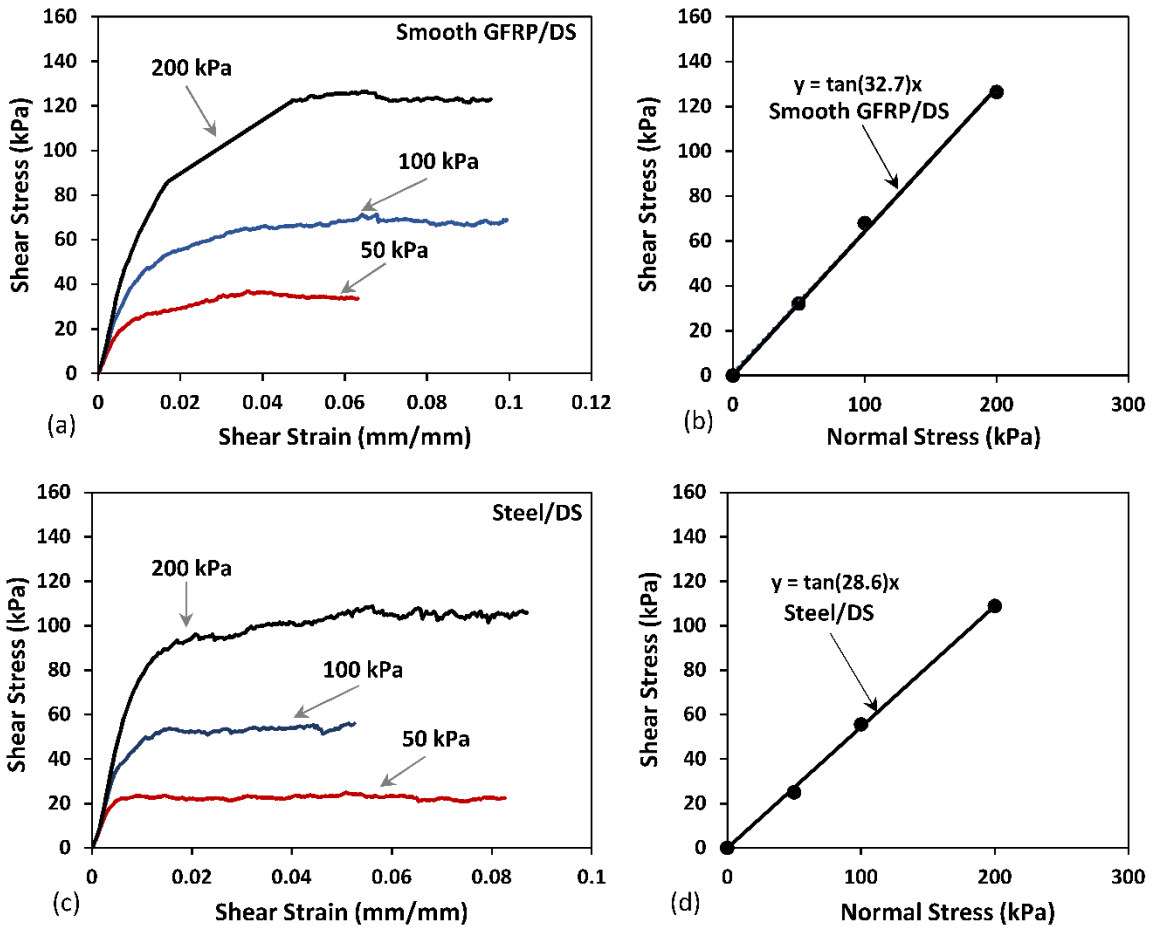

Figure 3. 20 Direct shear tests of dense sand (DS), with smooth GFRP: (a) shear stress vs. shear strain, and (b) shear stress vs. normal stress; and with steel: (c) shear stress vs. shear strain, and (d) shear stress vs. normal stress

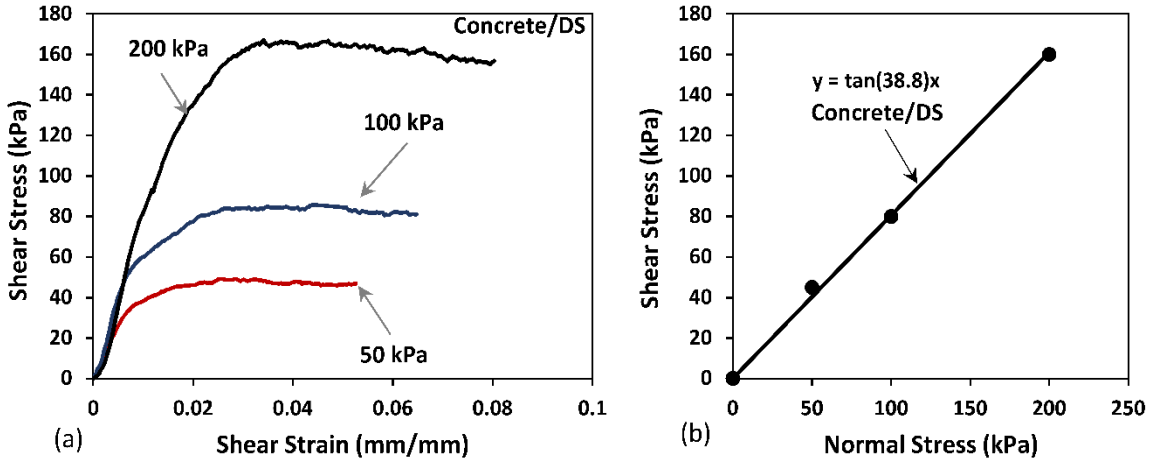

Figure 3. 21 Direct shear tests of concrete with dense sand (DS): (a) shear stress vs. shear strain, and (b) shear stress vs. normal stress

3.3.4 Pile Friction Capacity Implications

To investigate the effect of the interface friction angle of sand coated GS1500, smooth GFRP, steel, and concrete specimens with dense sand, an empirical study was implemented by using the pile friction capacity ($P_{friction}$) formula for driven piles:

$$P_{friction} = Q_s A_s \quad (3.1)$$

where Q_s is the average unit pile-soil shear resistance, and A_s is the pile surface area. These can be expressed as:

$$A_s = \pi D L \quad (3.2)$$

$$Q_s = \sigma_{0avg} K_s \tan\delta \quad (3.3)$$

where D is the pile diameter, L is the pile length, σ_{0avg} is the average effective stress over the pile length taken as $\gamma h/2$, γ is the maximum dry density of the soil used (17.17 KN/m^3), h is the soil depth, K_s is the lateral earth pressure coefficient for driven piles ($1.4\,K_o = 1.4\,(1-\sin\varphi)$), δ is the interface friction angle of the pile material with dense sand, and φ is the internal friction angle of dense sand (44.1°). As shown in Figure 3.22, for L/D = 20

with different pile diameters (D = 0.3, 0.4, 0.5, and 0.6 m), this empirical study found that the pile friction capacity ($P_{friction}$) for a GFRP sand coated pile with a sand coating ratio of 1500 g/m^2 driven in dense sand is greater than the friction capacities of the other pile materials tested (concrete, smooth GFRP, and steel).

In accordance with this empirical study, as shown in Figure 3.22, for pile diameters of 0.3, 0.4, 0.5, and 0.6 m, the friction capacities of concrete piles are 100.0, 237.1, 463.0, and 800.1 KN, respectively. For steel piles, the friction capacities are 67.6, 160.3, 313.1, and 541.1 KN respectively, and for smooth GFRP piles the friction capacities are 79.6, 188.7, 368.6, and 637.0 KN, respectively. For sand coated GFRP piles with a sand coating ratio of 1500 g/m^2, the friction capacities are 111.9, 265.1, 517.8, and 894.8 KN, respectively.

For the newly proposed sand coated GFRP pile with a sand coating ratio of 1500 g/m^2 and L/D = 20, the percentage gains in comparison with concrete, smooth GFRP, and steel piles in dense sand are 11.8%, 40.5%, and 65.4%, respectively. For marine construction, use of the newly proposed GFRP surface coated with 1500 g/m^2 of silica sand is anticipated to increase the GFRP pile friction capacity by 40.5% in comparison with a smooth GFRP pile. The use of concrete and steel piles for marine construction can result in serious interface durability problems due to deterioration. The newly proposed GFRP surface has the potential not only to solve these interface problems but also to increase the pile friction capacity in comparison to concrete and steel piles in dense sand, with percentage gains of 11.8%, and 65.4%, respectively.

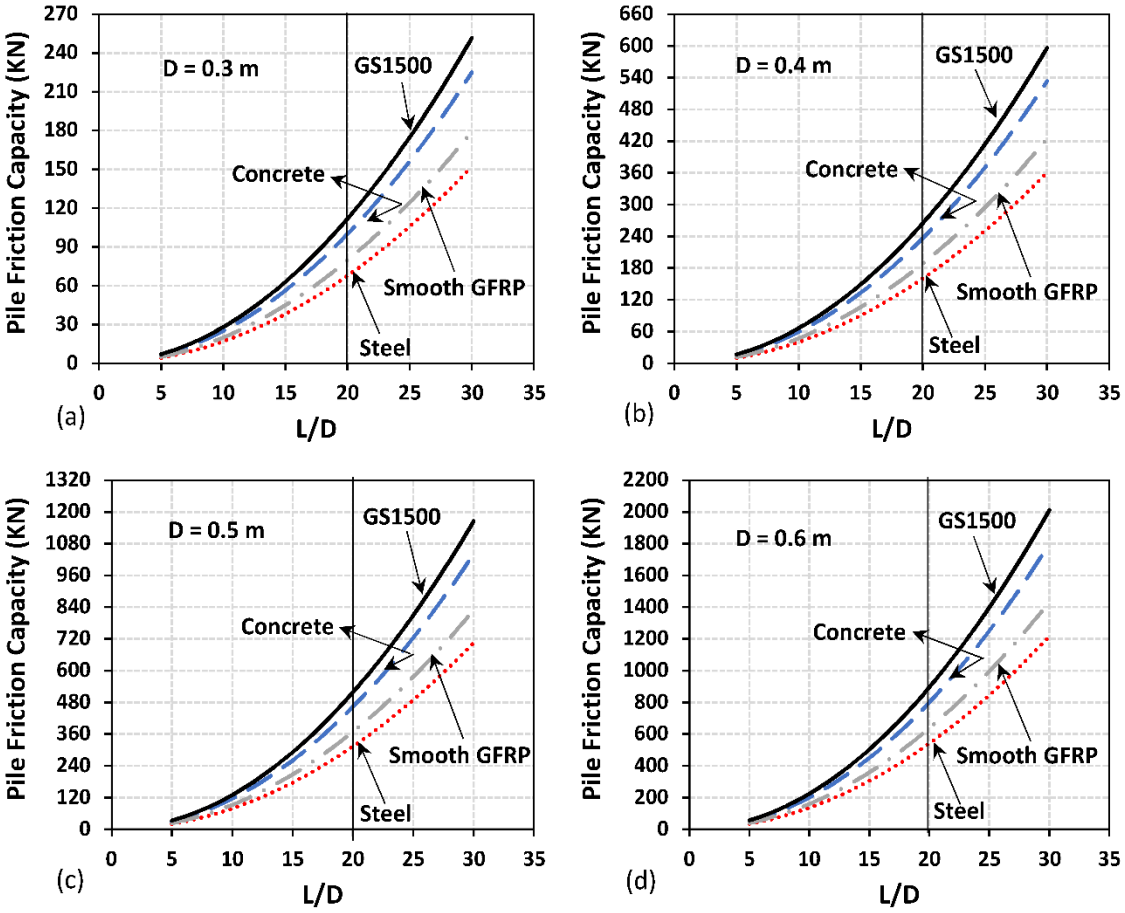

Figure 3. 22 Friction capacities for sand coated GFRP GS1500, smooth GFRP, steel, and concrete driven piles in dense sand vs. pile length/pile diameter ratio for: (a) pile diameter 0.3 m, (b) pile diameter 0.4 m, (c) pile diameter 0.5 m, and (d) pile diameter 0.6 m

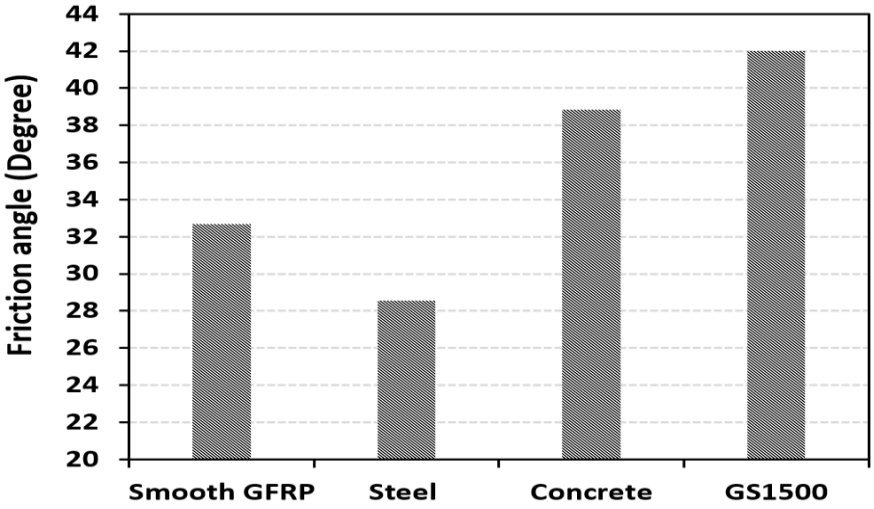

Figure 3. 23 A comparison of interface friction angles for dense sand with smooth GFRP, steel, concrete, and sand coated GFRP GS1500

3.4 CONCLUSIONS

This experimental study was conducted to investigate the properties of the interface between sand coated GFRP sheets and sandy soils. Six different ratios of silica sand to GFRP sheet surface area were studied: 0, 500, 1000, 1500, 2000, and 2500 g/m^2. Different types of soil (sand, silty sand, and sandy lean clay) were placed on top of different sand coated GFRP specimens in a direct shear box, under three different normal pressures: 50, 100, and 200 kPa. The following conclusions can be drawn from the results of this study:

- In comparison to uncoated sheets, the silica sand coating increased the interface friction of GFRP sheets with sandy soils, by enabling soil particles to interlock with the interface by filling voids in the sand coating of the GFRP specimens, thus enhancing the interface behaviour with sandy soils.
- GFRP specimens with a sand coating ratio of 2000 g/m^2 had the greatest interface friction angle (43.3°) with dense silty sand. This value is 16.8% higher than that for GFRP specimens without sand coating, and also exceeds the soil/soil friction angle of 42.7°. For dense sand, GFRP specimens with a sand coating ratio of 1500 g/m^2 had the greatest interface friction angle (42.0°) in this group.
- For sandy lean clay, the optimum sand coating ratio was exhibited by GFRP specimens with a sand coating ratio of 2000 g/m^2. This increased the interface friction angle to 36.8°, with a percentage gain of 131.3% in comparison to GFRP specimens without sand coating. The highest adhesion value (64.0 kPa) was exhibited by GFRP specimens with a sand coating ratio of 1000 g/m^2.
- For dense sand, interface friction angles were compared for steel, concrete, smooth GFRP, and GFRP with a sand coating ratio of 1500 g/m^2. It was found that the sand

coated GFRP had the greatest interface friction angle (42.0°) with dense sand, with percentage gains of 8.1%, 28.5%, and 47.0% in comparison to concrete, smooth GFRP, and steel, respectively.

- A design example of driven pile friction capacity showed that with dense sand a GFRP pile with a sand coating ratio of 1500 g/m^2 had a friction capacity exceeding that of other sand coated GFRP specimens, smooth GFRP, steel, and concrete piles. For a pile length to diameter ratio of 20, the pile friction capacity gains in dense sand for the GFRP pile with a sand coating ratio of 1500 g/m^2 were 11.8%, 40.5%, and 65.4% in comparison to concrete, smooth GFRP, and steel piles, respectively.

ACKNOWLEDGMENTS

The authors wish to express their gratitude to the students Ahmed Mahgoub, Hun Choi, Ali Iranikhah, Mohammad Ashari Ghomi, and Koosha Korramian, and to the technical staff Brian Kennedy and Blair Nickerson at the Department of Civil and Resource Engineering at Dalhousie University, Canada, for their endless help and support.

REFERENCES

Aksoy, H. S., Gör, M., İnal, E. et al. (2016). A new design chart for estimating friction angle between soil and pile materials. *Geomechanics and Engineering*, **10**(3), 315-324.

Almallah, A., Sadeghian, P., El Naggar, H. et al. (2018). *Direct shear tests of sandy soils interfaced with FRP sheets.* Paper presented at CSCE annual conference, Fredericton, Canada.

ASTM C136. (2014). Standard test method for sieve analysis of fine and coarse aggregates.

ASTM D2487. (2011). Standard practice for classification of soils for engineering purposes (unified Soil Classification System).

ASTM D3080. (2011). Standard test method for direct shear test of soils under consolidated drained conditions.

ASTM D698. (2012). Standard test methods for laboratory compaction characteristics of soil using standard effort.

Chu, L. M., & Yin, J. H. (2006). Study on soil-cement grout interface shear strength of soil nailing by direct shear box testing method. *J Geomechanics and Geoengineering*, **1**(4), 259-273.

Frost, J. D., & Han, J. (1999). Behavior of interfaces between fiber-reinforced polymers and sands. *J Geotechnical and Geoenvironmental Eng*, **125**(8), 633-640.

Giraldo, J., & Rayhani, M. T. (2013). Influence of fiber-reinforced polymers on pile-soil interface strength in clays. *Advances in civil engineering materials*, **2**(1), 534-550.

Goh, A. T. C., & Donald, I. B. (1984). *Investigation of soil-concrete interface behaviour by simple shear apparatus*. Paper presented at Transportation Research Board, Washington, USA.

Iskander, M. G., & Hassan, M. (1998). State of the practice review in FRP composite piling. *J Composites for Construction*, **2**(3), 116-120.

Lavanya, I., Prabha, R., Murugan, M. et al. (2014). Behaviour of interfaces between carbon fibre reinforced polymer and gravel soils. *Int J Res Eng Technol*, **3**(11), 156-159.

Lehane, B. M., Jardine, R. J., Bond, A. J., Frank, R. et al. (1993). Mechanisms of shaft friction in sand from instrumented pile tests. *J Geotechnical Eng*, **119**(1), 19-35.

Paikowsky, S. G., Player, C. M., Connors, P. J. et al. (1995). A dual interface apparatus for testing unrestricted friction of soil along solid surfaces. *Geotechnical Testing J*, **18**(2), 168-193.

Pando, M. A., Filz, G. M., Dove, J. E., Hoppe, E. J. et al. (2002). Interface shear tests on FRP composite piles. *Geotechnique*, **4**(1), 52-56.

Pando, M. A. (2003). A laboratory and field study of composite piles for bridge substructures, Dissertation, Virginia Tech.

Potyondy, J. G. (1961). Skin friction between various soils and construction materials. *Geotechnique*, **11**(4), 339-353.

Rouaiguia, A. (2010). Residual shear strength of clay-structure interfaces. Int *J Civil and Environmental Eng*, **10**(3), 6-18.

Sakr, M., El Naggar, M. H. E., Nehdi, M. et al. (2004). Novel toe driving for thin-walled piles and performance of fiberglass-reinforced polymer (FRP) pile segments. *Canadian geotechnical J*, **41**(2), 313-325.

Sakr, M., El Naggar, M. H., Nehdi, M. et al. (2005). Interface characteristics and laboratory constructability tests of novel fiber-reinforced polymer/concrete piles. *J Composites for Construction*, **9**(3), 274-283.

Taha, A. M. (2010). Interface Shear Behavior of Sensitive Marine Clays--Leda Clay. Dissertation, University of Ottawa.

Toufigh, V., Ouria, A., Desai, C. S., Javid, N., Toufigh, V., Saadatmanesh, H. et al. (2015). Interface behavior between carbon-fiber polymer and sand. *J Testing and Evaluation*, **44**(1), 385-390.

Uesugi, M., & Kishida, H. (1986). Influential factors of friction between steel and dry sands. *Soils and foundations*, **26**(2), 33-46.

Uesugi, M. (1987). Friction between dry sand and construction materials. Dissertation, Tokyo Institute of Technology.

Vineetha, V. J., & Ganesan, K. (2014). Interface friction between glass fibre reinforced polymer and gravel soil. *In Advanced Materials Research*, 984, 707-710.

CHAPTER 4 FRICTION BEHAVIOUR OF SAND COATED GFRP PILES IN SAND BOX UNDER AXIAL LOADS

ABSTRACT

In pile construction, conventional pile materials (i.e., concrete, steel, wood) more likely to have durability problems for soil-substructure interaction, especially in-terms of corrosion, and deterioration. These interface problems result in increasing the maintenance cost and reduce the life span of piles. Fiber-reinforced polymers (FRP) has been found to be a potential alternative to eliminate these interface problems, with higher durability, and longer life span compared to the conventional materials. However, more data and records are necessary to adopt this new material in geotechnical practise and pile design. This paper describes the results of an experimental study on the effect of interface on the behaviour of glass FRP (GFRP) piles driven in dense sand under axial loads. The experimental program consists of 5 small scale GFRP piles with different surface roughness. The surfaces of 4 out of 5 GFRP piles were coated with silica sand to enhance the interface behaviour of composite piles. These 5 GFRP piles were compared with a reference control steel pile. The experimental testing was carried out through a steel frame with a hydraulic jack connected underneath a steel top beam. The hydraulic jack applies loads on the head of GFRP piles. The experimental results showed that coating GFRP piles with silica sand enhanced the interface friction of GFRP against sand under axial loads and increased pile ultimate capacity compared to the control GFRP and steel piles.

4.1 INTRODUCTION

In general, pile foundations are used to transfer structural loads to the soil when shallow foundations are not sufficient enough to carry it, or when the suitable soil for construction is deeply located under the ground. Based on its mechanism of transferring the loads from the structure to the soil, there are two types of piles as per AASHTO (2002). The first type is end bearing piles, which transfer the loads from the structure to the soil by its end toe. The second type is friction piles, which transfer the loads from the structure to the soil by its skin friction. Conventional materials (i.e., concrete, steel, wood) have been used in pile manufacturing for a long time. However, these conventional materials are more likely to have interface problems with soil in-terms of durability, corrosion, and deterioration of the material when it's used in harsh environments, or offshore construction.

Since the past few years, there is a trend of using FRP composites in the design of piles to overcome these interface problems (Guades et al. 2010). FRP composites are corrosion resistance, poses higher strength, have lower maintenance cost, and lighter in weight compared to the conventional pile materials. GFRP composites are one of the cost-effective composites. Iskander and Hassan (1998) used GFRP composites for marine fendering and light bearing applications. It has been found that GFRP composites have the advantage of durability against harsh environments. Frost and Han (1999) studied the interface friction behaviour of FRP against sand. The results showed that the interface friction between FRP and sand depends on the surface roughness of FRP, normal stress, and particle angularity of sand. Pando et al. (2000) conducted a full-scale pile load test using FRP tubes filled with concrete and compared it to precast concrete piles. It was found that both pile materials have a similar response in-terms of axial capacity in compression.

Drivability of FRP composites into the soil is one of the concerns to adopt it in pile construction. Ashford and Jakrapiyanun (2001) did a comparison between FRP composite piles with steel and concrete piles in-terms of drivability. The results showed that the impedance of piles composed exclusively of GFRP materials are lower than steel and concrete piles. Sakr et al. (2004) developed a toe driving technique to install empty FRP shells into the soil, and self-consolidating concrete (SCC) was cast into the shells. Results of driving tests and static load tests for FRP-SCC piles were compared to the results of steel closed-end piles. The results showed that the toe driving technique is suitable for installing FRP piles in dense soils. One year later, Sakr et al. (2005) studied the interface characteristics and the constructability tests of FRP piles filled with concrete and compared it to a steel reference pile. The findings indicated that the interface friction angle of FRP pile against dense sand is similar or higher than the reference steel pile.

Guades et al. (2012) evaluated the performance of driving hollow FRP piles. It was found that the factors affecting FRP piles driving are the type of driving hammers used, resistance of soil around, pile impedance, and the strength of pile material. Spiro and Pais (2002) using actual driving tests, found that the post-driving capacity of the FRP pile was 27% higher than prestressed concrete pile. Zyka and Mohajerani (2016) found that FRP piles exhibit similar structural and drivability properties to steel. Abuel-Naga and Shaia (2014) studied the interface friction of FRP tube confined concrete piles during installation process. The results showed that the peak interface shear coefficient between pile material and soil decreases as the normal stress of soil increases. This performance could be explained in terms of the interface dilatancy behaviour and the net effect of the interface shear induced surface roughness change.

Transferring the loads from FRP piles into the soil needs more research and data to have a better understanding of FRP piles' performance under axial loads. Valez and Rayhani (2014) conducted axial and lateral load tests on small scale FRP piles in soft clay. The results showed that FRP piles have suitable characteristics to act as a load bearing member based on axial geotechnical capacity. Valez and Rayhani (2017) performed another investigation on the behavior of small scale FRP piles in soft clay under axial and lateral loads. The results indicated that the lower stiffness of FRP piles leaded to increase pile head displacement under lateral loading, and pile texture and waviness found to be significant on the pile axial capacity.

Direct shear test is one of the effective tests to obtain the interface strength parameters between soil and structure. Vineetha and Ganesan (2014) conducted direct shear tests to investigate the interface friction between GFRP and gravel. They found that the interface friction angle increased when the fiber direction was perpendicular to the shearing load. Lavanya et al. (2014) found that shearing well gravel with carbon FRP (CFRP) resulted in higher interface friction angle compared to poorly graded gravel. Toufigh et al. (2015) found that the surface roughness of FRP material and normal stress level were the controlling parameters for interface friction between FRP and soil. To enhance the interface friction between GFRP and sandy soils, Almallah et al. (2018) conducted several direct shear tests on GFRP specimens with different surface roughness against sandy soils (poorly graded sand, silty sand, and sandy lean clay) and found that the surface roughness of GFRP was the controlling parameter for the interface friction. A mechanism of enhancing the surface roughness of GFRP was introduced in chapter 3 of this study by coating the surface of several GFRP specimens with silica sand with different sand ratios per surface area (0,

500, 1000, 1500, 2000, and 2500 g/m^2). The results showed that coating the surface of GFRP specimens with silica sand using sand coating ratios 1500, and 2000 g/m^2 presented the optimum ratios to increase the interface friction angle against poorly graded sand, silty sand and sandy lean clay respectively.

However, direct shear tests results are not enough alone to understand and confirm the interrace friction behaviour of GFRP piles in sand. In addition to that, GFRP composites have not yet gained wide acceptance in foundation design and geotechnical practise, because of the lack of proper records and design guidelines. Due to these reasons, this study was designed to enhance the interface friction behaviour of GFRP piles driven in dense sand. The surface of GFRP piles was coated with silica sand with different sand coating ratios per surface area to provide a roughened skin for friction piles to improve their frictional load bearing capacity under axial loads.

4.2 Research Significance

Soil-structure interaction for deep foundations have major interface problems (such as corrosion, and deterioration) with conventional pile materials especially in harsh environments and offshore construction. GFRP composites have more durability, corrosion resistance, and less deterioration than the conventional piling materials which can decrease the maintenance cost and extent service life of the system. Researchers are trying to better understand the interface behaviour of GFRP piles with soil to adopt it as potential alternatives to the conventional piles. Enhancing the interface friction between GFRP piles and soil will increase the life span of the substructure and the load capacity of piles as well. The objective of this research is to increase the interface friction resistance of GFRP piles by introducing an effective mechanism by coating the surface of GFRP piles with silica

sand to increase GFRP pile capacities with long life span as deep foundations. This research could be very useful for the construction industry in harsh environments and offshore construction to provide higher capacity for piles with less interface problems.

4.3 Materials and Methods

Four GFRP piles were sand coated with different sand coating ratios per surface area with two control reference piles. These piles were driven in sand and tested under axial loads. The following sections present details of the experimental program.

4.3.1 Test Matrix

A total of 5 GFRP piles with total length (L) 760 mm, and outer diameters (D) ranging from 50 to 61 mm (depends on the sand coating ratio on pile surface) were prepared. Each GFRP pile was fabricated out of four layers of unidirectional fiberglass fabric and epoxy resin. Silica sand was added to the surface of 4 GFRP piles out of 5. The test parameter was the sand coating ratio per surface area of GFRP piles. The sand coating ratios on the surface of the GFRP piles examined in this study were 0, 1000, 1500, 2000 and 2500 g/m^2. To compare the results of GFRP piles, a control steel pile was used. Table 4.1 shows the test pile specimens identified with the specimen identification (ID) as table 4.1 GFRP-X, and Steel. Where GFRP stands for GFRP pile, steel stand for steel pile, and X stands for sand coating ratio per surface area of the pile. For example, GFRP-1500 is a GFRP pile with 1500 g/m^2 of sand coating.

Table 4. 1 Test Matrix for Pile Load Test

Group #	Specimen ID	Sand Coating Ratios (g/m^2)	Pile Outer Diameter D (mm)	L/D	Note
1	GFRP-0	0	54	14.1	GFRP Control
2	GFRP-1000	1000	56	13.6	Sand coated
3	GFRP-1500	1500	59	12.9	Sand coated
4	GFRP-2000	2000	58	13.1	Sand coated
5	GFRP-2500	2500	61	12.5	Sand coated
6	Steel	0	50	15.2	Steel Control

4.3.2 Material Properties

4.3.2.1 GFRP

All piles were prepared with the same unidirectional fiberglass fabric with four layers of GFRP. The weight of the GFRP composite pile without sand coating was 3438.5 g/m^2. Each pile was bonded by an epoxy resin (West System 105), and a hardener (West System 206).

The Fiberglass fabric (dry fiber) has a tensile strength 1500 MPa, areal fabric weight 450 g/m^2, elongation is 2.8%, and E-modulus is 72 GPa as reported by the manufacturer (Haining Anjie Composite Material Co., Zhejiang, China). The elastic modulus and the tensile strength of the GFRP composite were determined as 32 GPa, and 502 MPa respectively, based on tensile tests on GFRP composite specimens.

4.3.2.2 Coating Sand

Sieve analysis test was carried out according to ASTM C136-14 (2014) to determine the properties of Silica sand sparkled on the GFRP composite piles. From the curve of gradation obtained in Figure 4.1(a) the values of D_{10}, D_{30}, D_{50}, and D_{60} were 1.1, 1.4, 1.8, and 1.9 respectively.

The coefficient of gradation (C_c) was found to be 0.9, and uniformity coefficient (C_u) was 1.7. The percentage of the soil retained on sieve No.16 from total Silica sand sample was 96.3% based on sieve analysis test. In general, the used Silica sand was classified as poorly graded sand according to the unified soil classification system (USCS). The Silica Sand used for sparkling the surface of the GFRP piles was only the one retained on sieves #16 and #8.

4.3.2.3 Soil

The soil used for this experimental study was masonry sand. Sieve analysis test according to ASTM C136-14 (2014) was used to classify the engineering properties of the masonry sand. From the curve of gradation obtained in Figure 4.1(a), the values of D_{10}, D_{30}, D_{50}, and D_{60} were 0.2, 0.3, 0.5, and 0.6 respectively. The coefficient of gradation (C_c) was found to be 0.9, and the uniformity coefficient (C_u) was 3.3. The masonry sand was poorly graded sand (SP) according to USCS. Laboratory compaction characteristics of soil using standard effort according to ASTM D698-12 (2012) was carried out to determine the maximum dry density of sand used and the optimum water content as shown in Figure 4.1(b). The maximum dry density of the poorly graded sand was 1746 kg/m^3, and the optimum water content used was 14.5%.

4.3.2.4 Steel

The Steel used in this study has an ultimate tensile strength of 505 MPa, yield tensile strength of 215 MPa, shear modulus of 86 GPa, and modulus of elasticity (E) of 195 GPa based on ASTM A269/A269M.

4.3.2.5 Aluminium

The Aluminium cone used in this study has an ultimate tensile strength of 290 MPa, yield tensile strength of 240 MPa, shear modulus of 25 GPa, and modulus of elasticity (E) of 69 GPa.

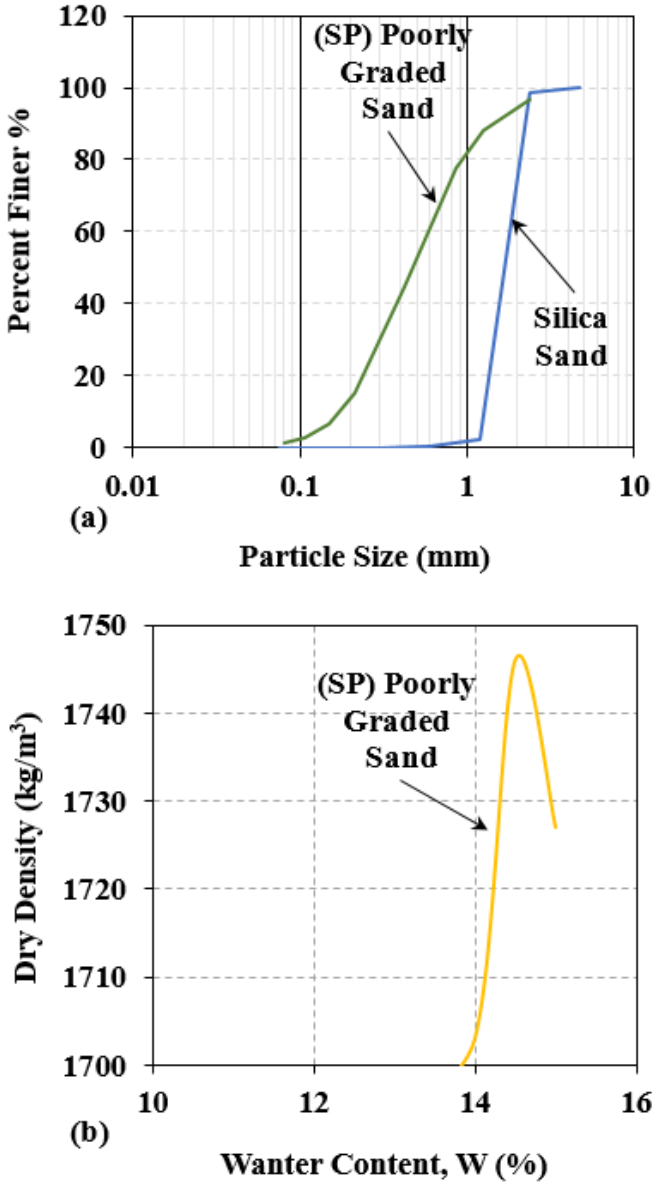

Figure 4. 1 Soil properties: (a) gradation curves; and (b) maximum dry density vs. optimum water content

4.3.3 Specimen Fabrication

A total of 5 GFRP piles with total length (L) 820 mm, and a targeted outer diameter (D) of 54 mm were fabricated. Each pile consists of four layers of glass fabrics bounded together with epoxy resin and hardener. The glass fiber layers of each GFRP composite pile were fabricated with the following fiber directions and order [90/0/0/90]. The 0 degrees layers were axial with no overlap (820 mm x 160 mm) each. The 90 degrees layers were hoop with 50 mm overlap (820 x 210 mm) each.

As shown in Figure 4.2 a plastic pipe with total length of 1840 mm and outer diameter of 45 mm was wrapped with 900 mm length of plastic sheet. The surface of the plastic sheet was brushed gently with epoxy resin plus hardener. The first layer of fiber glass (90 degrees hoop) was wrapped tightly around the plastic pipe. During the process of wrapping, 68.23 g of epoxy resin plus hardener were applied on the glass fiber layer until wrapping is completed. The next three layers of glass fibers were wrapped with the same method and the same amount of epoxy resin plus hardener added in between. After wrapping 4 layers of GFRP is done for each pile [90/0/0/90], wax paper was used around each pile for curing. In the first 30 minutes of the curing process the pile was rotated frequently using the long plastic pipe with two wooden edges at its both ends to ensure that the resin will not be affected by gravity. All specimens were cured for seven days in total from the date of fabrication at room temperature. After curing was done, 50 mm at both ends of each pile were cut by a blade saw to have a pile length in total of 720 mm and outer diameter of 54 mm.

The surface of 4 out of these 5 GFRP piles were sparkled with Silica Sand. Each pile out of these 4 received different sand ratio per surface area of 1000, 1500, 2000, and 2500 g/m^2.

After application of the sand coating, the weight of the composite piles per surface area: GFRP-0, GFRP-1000, GFRP-1500, GFRP-2000, and GFRP-2500 was 3438.5, 4134.4, 4887.6, 5585.2, and 6723.1 g/m^2, respectively. The sand was sparkled uniformly on the surface of the four piles by adding epoxy resin and hardener to surface of these piles. Figure 4.3 Shows the sand coated GFRP piles used in this study. A steel pile was prepared as a second control specimen to be tested similarly to GFRP piles. At the end of each pile, a 40 mm in length of aluminium cone were added to the tip of all 6 piles. Each pile was instrumented with two strain gauges near the pile toe to calculate how much load was mobilized through the bearing tip, and how much load was mobilized along pile shaft.

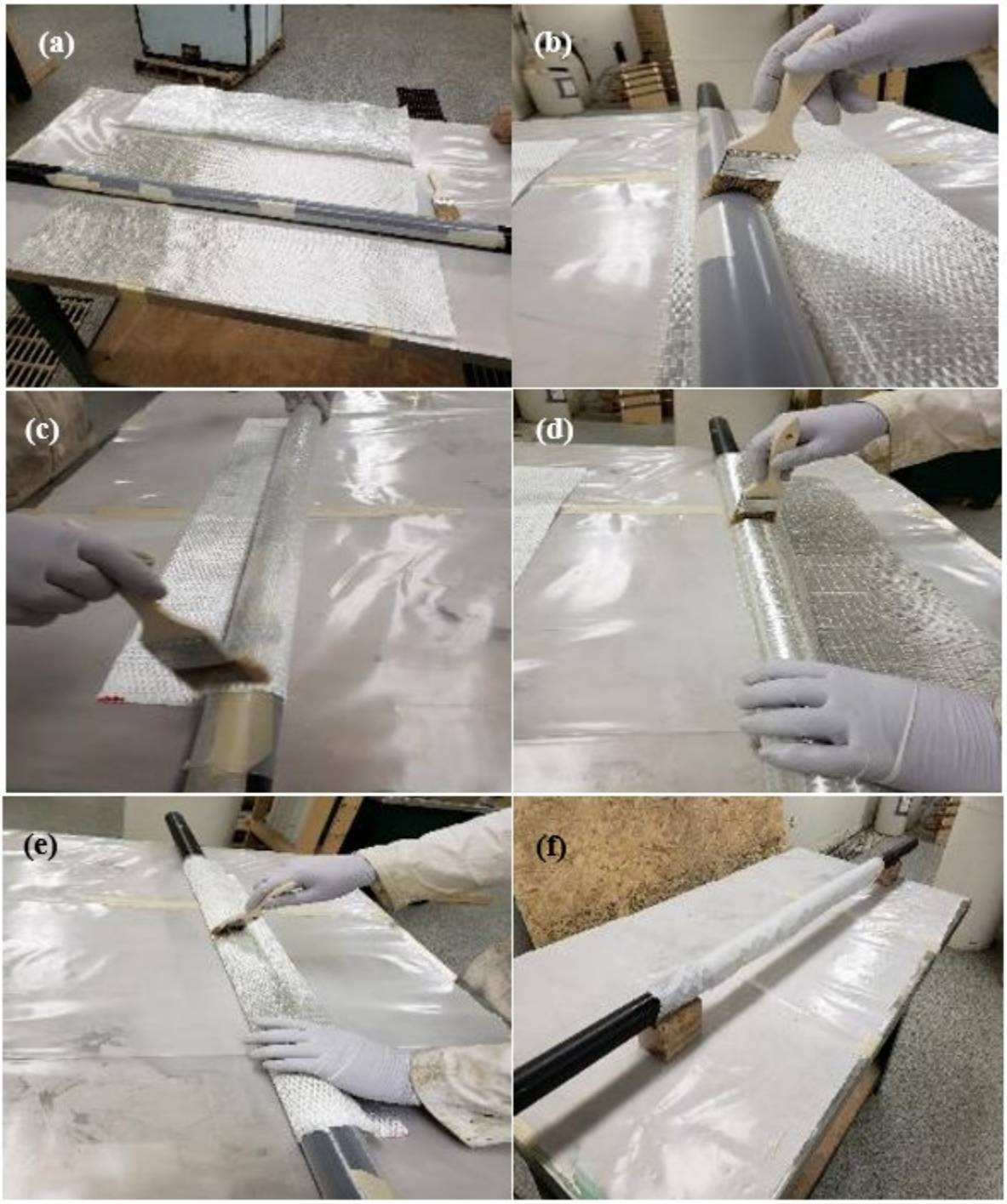

Figure 4. 2 Specimen fabrication of GFRP pile: (a) material used for fabrication; (b) brushing the surface of the plastic pipe gently with epoxy resin and hardener; (c) brushing the fist layer of glass fabric 90 degrees hoop with resin; (d) adding resin to the second and third layers of 0 degree axial of glass fabrics; (e) adding resin to the last layer of glass fabric 90 degrees hoop; and (f) wax paper wrapped around the GFRP pile after completing all pile layers

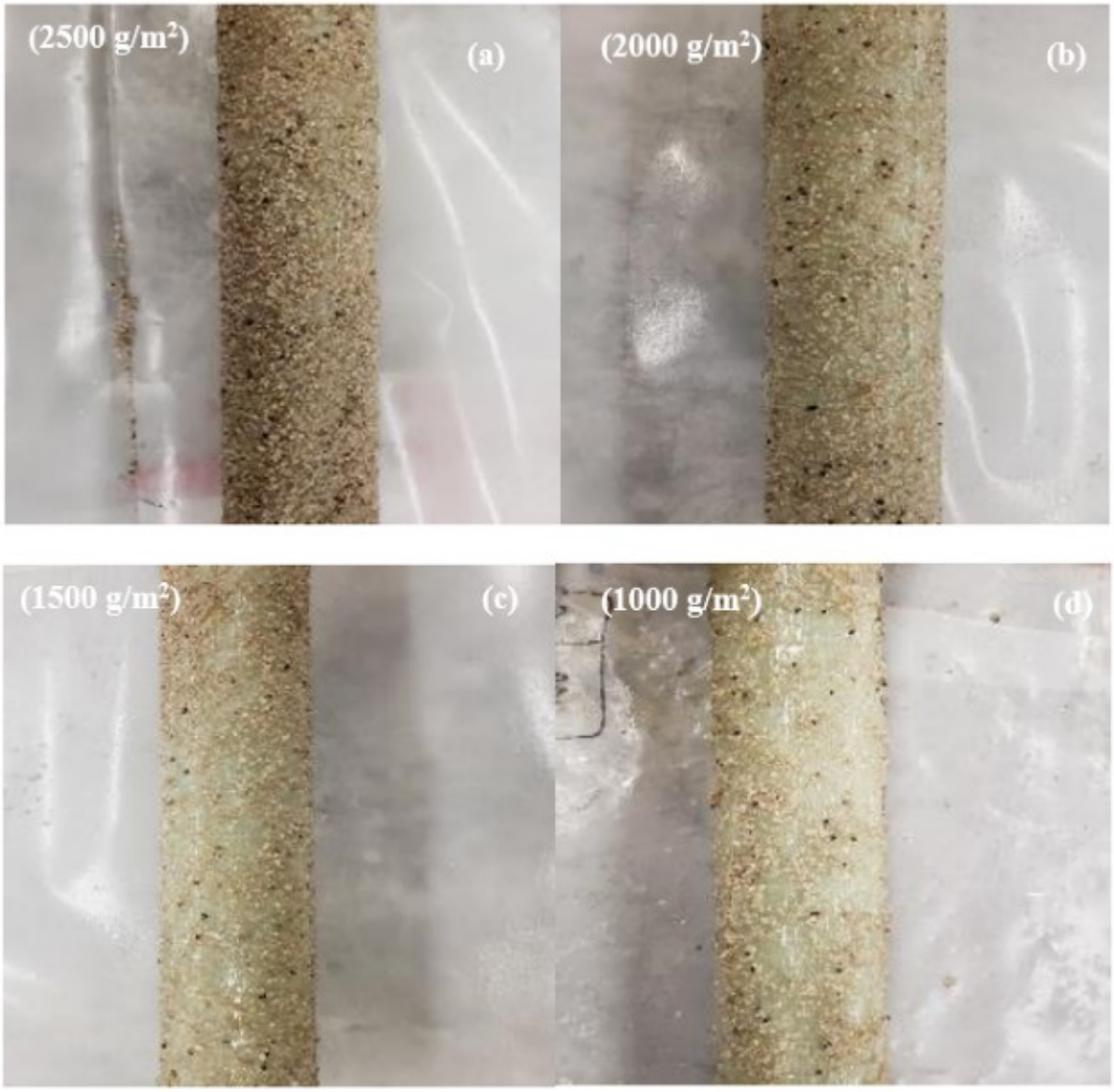

Figure 4. 3 Sand coated GFRP Piles: (a) GFRP-2500, (b) GFRP-2000, (c) GFRP-1500, and (d) GFRP-1000

4.3.4 Test Setup and Instrumentation

A small-scale frame with a soil tank were developed at Dalhousie University as shown in Figure 4.4 and Figure 4.5 to test small scale piles with total length (L) 760 mm, outer diameter (D) ranging from 50 to 61 mm, and L/D ratio ranging from 12.5 to 15.2 as shown in Table 1. Each pile used in this study was tested with a pile head diameter of 150 mm on the top of the pile, and pile toe (cone shape) with 40 mm length and 45° inside slope. The piles were prepared and driven into a soil tank (1200 mm x 910 mm). The soil used was poorly graded sand filling 1000 mm in height of the soil tank. A hydraulic jack with maximum 160 mm stroke was connected to a load cell from its end to measure the amount of loading in Newtons (N). Two string pots were placed on the top of the hydraulic jack with the ability to measure 609.6 mm each of the vertical displacement during driving of piles. Both the load cell and the string pots were connected to the data acquisition system (DAQ) to display and export the results of the test on the digital screen. Four extension pipes made of aluminium were used in driving each pile with outer diameter of 50 mm and lengths of 130, 280, 430, 580 mm. Figures 4.4, 4.5, and 4.6 show the instruments used and the test set up for this study.

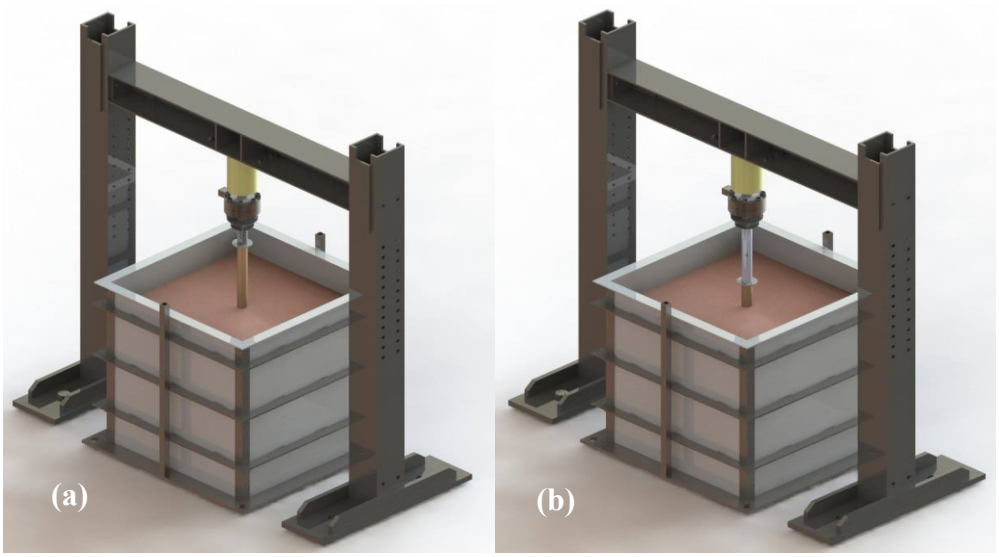

Figure 4. 4 Schematic drawing of test setup and instrumentation: (a) first stage of driving GFRP pile; (b) last stage of driving GFRP pile using steel extension pipe

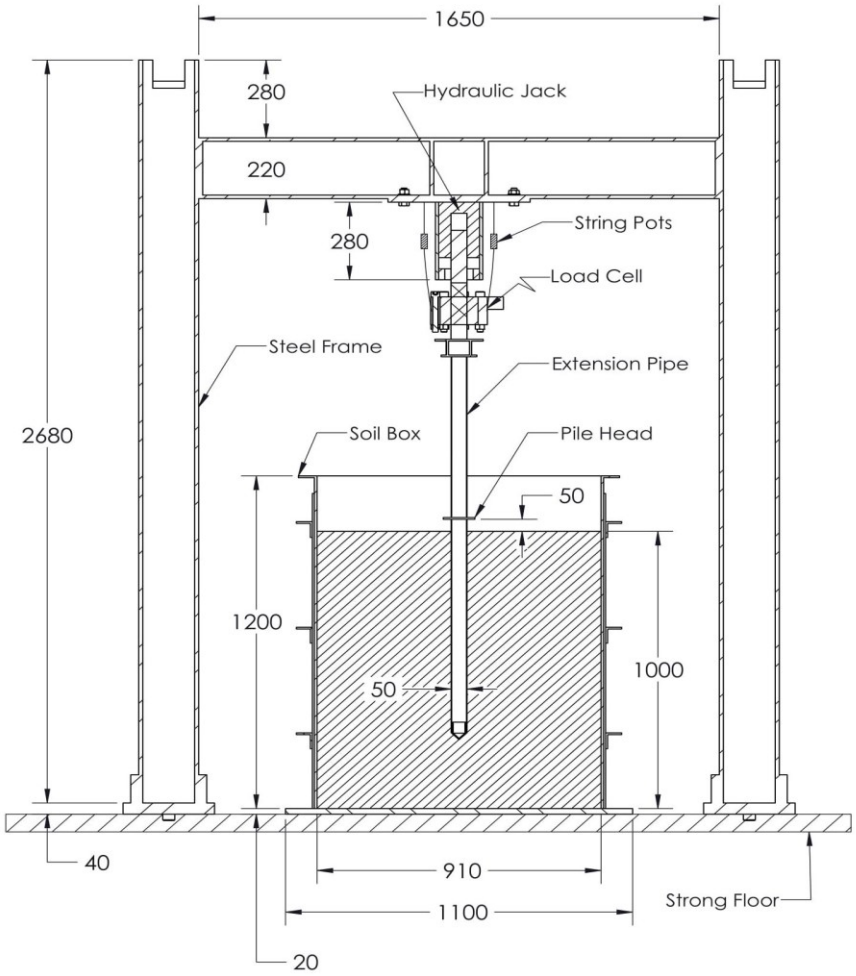

Figure 4. 5 Detailed drawing for pile load test after driving the pile to the desired depth

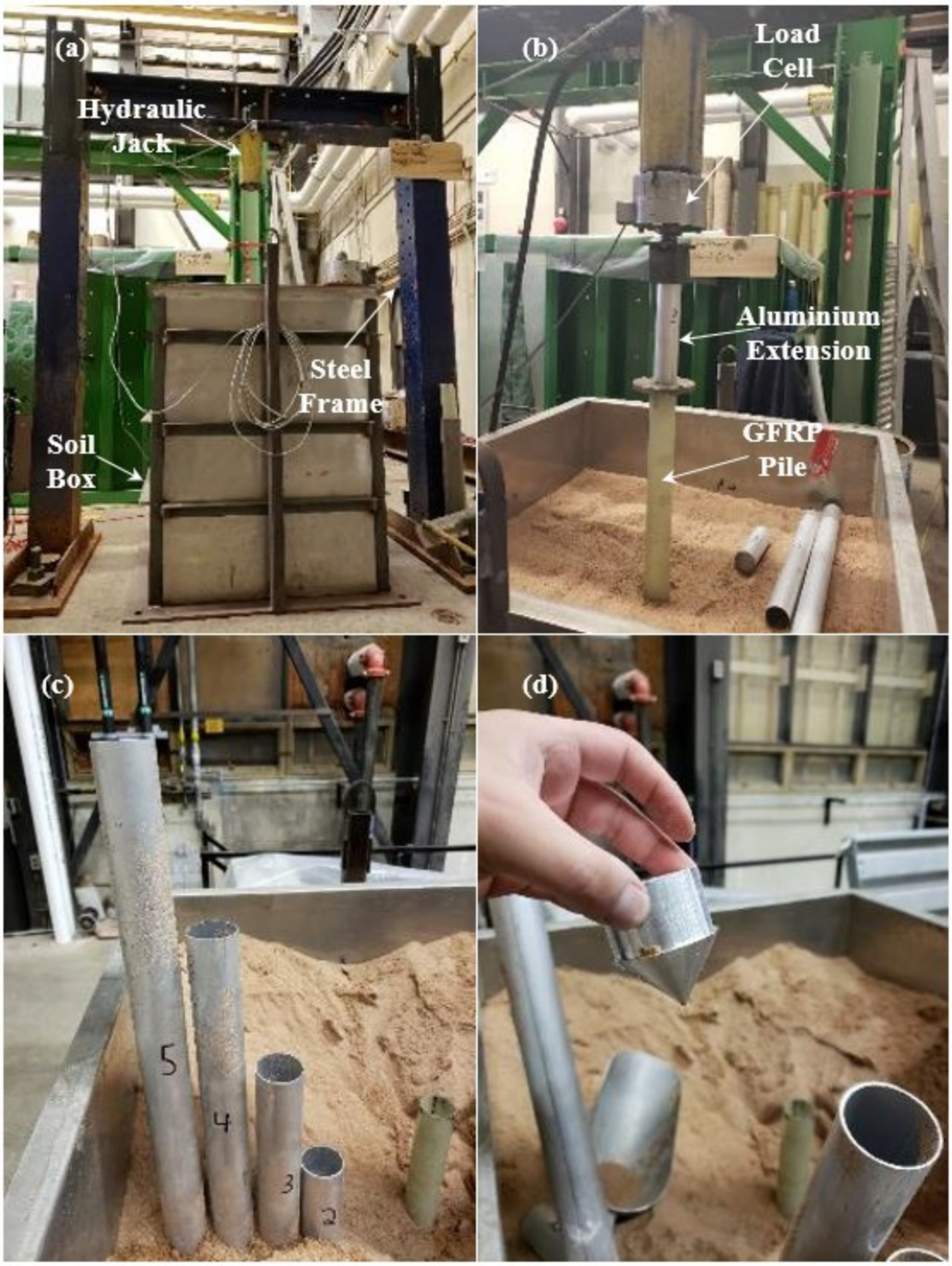

Figure 4. 6 Test set up: (a) blue frame with the soil tank and the hydraulic jack; (b) third stage of driving of GFRP pile using the second aluminium extension pipe; (c) 4 aluminium extension pipes used for driving stages; and (d) pile toe used in cone shape

4.3.5 Test Procedure

Six piles were driven and tested under axial compression load following ASTM D1143 (2007) as shown in Figure 4.4. Each pile was driven into the sand by the hydraulic jack within 5 stages until the distance between the pile head and the surface of the sand in the soil tank becomes 50 mm as shown in Figure 5. Each stage includes driving the pile around 160 mm (the maximum stroke length in the hydraulic jack) downward vertically into the sand except for the last stage which was around 80 mm or more (depends on the initial vertical displacement among driving during the first stage) as shown in Figure 4(a), and 4(b) with a driving rate for all stages 22.7 mm/min.

The first stage of driving was done without extensions starting with the pile toe touching the surface of the sand. The pile was driven around 160 mm into the sand (depends on pile vertical adjustment before driving), then the stroke was back inside the hydraulic jack and a 130 mm aluminum extension was placed between the pile head and the load cell. The pile was driven another 160 mm for the second stage. After the second stage was done, the first extension was removed while the stroke was moving back inside the hydraulic jack. The third stage of driving was performed by placing aluminum extension of 280 in length to drive the pile another 160 mm into the sand. The same procedure was repeated for the fourth stage with 430 mm of aluminum extension pipe. In the last stage, an extension of 580 mm was used, and the pile was driven into the sand 70 mm to leave a distance between the pile head and the surface of sand 50 mm.

During each stage of driving, the loading was measured, and the vertical displacement was correlated with the loads applied to plot the load versus displacement curve for each pile. After driving is completed a static axial compression load test was performed on the pile

head. The pile load test was performed to check the pile head settlement of 10% of pile diameter 50 mm (5 mm settlement) as suggested by De Nicola and Randolph (1999) and the pile ultimate capacity under axial loads. The pile load test was performed to reach 28 mm settlement of pile head then the test was stopped. The pile load test was performed with a loading rate of 0.5 mm/min. After test is done, load vs settlement curve was plotted with the values of pile ultimate load, fiction load, and bearing for each pile for comparison using three different methods of analysis.

4.4 Results and Discussion

4.4.1 Pile Driving Results

All 6 piles used in this study were driven into a dense sand until the distance between the pile head and the soil surface is 50 mm. As shown in figure 4.7 when the pile displacement reaches 680 mm for all piles GFRP-1500 sand coated pile had the highest load needed for diving among all other piles with 13.3 KN. This due to the high interlocking between soil particles and pile surface due to its roughened skin with silica sand coating with sufficient voids needed to enhance the interface mechanism. Sand coated piles GFRP-1000, and GFRP-2000 at 680 mm vertical displacement had almost a similar load needed to drive the pile at that depth with 12.6, and 12.3 KN respectively.

The load needed for driving the sand coated pile GFRP-2500 dropped compared to the other sand coated piles with 11.3 KN needed to embed the pile 680 mm into the soil tank with less interlocking between soil particles and pile surface resulting in less pile skin resistance. Control GFRP and steel piles had almost a close load in-order to drive the pile to the desired level (50 mm distance between pile head and soil surface), noting that the trend at the end

of steel pile driving curve was approaching GFRP pile driving curve as Zyka and Mohajerani (2016) found that FRP and steel piles exhibit similar structural and drivability properties. However, reaching the depth of 680 mm upon driving (before reaching 50 mm distance between pile head and soil surface) steel pile needed 10.2 KN which is 1.1 KN higher than Control GFRP pile (9.1 KN) as Ashford and Jakrapiyanun (2001) found that impedance of piles composed of GFRP is lower than steel.

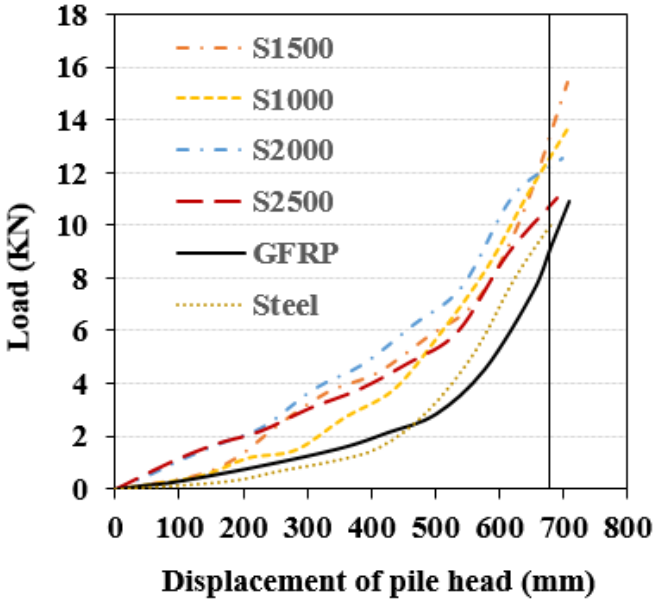

Figure 4. 7 Driving results of all piles

4.4.2 Pile Load Test Results

Pile load test was performed on all 6 piles with applying a static axial load on pile head to find the ultimate capacities of piles (the combination of ultimate bearing and friction capacity as shown in Figure 4.8(a), and 4.8(b). The summary of the results of all pile load tests are presented in Figure 4.9, 4.10(a), and 4.10(b), where (S) stands for sand coating pile. In order to discuss and analyze these experimental results, three methods were used to

find the ultimate load capacity, the ultimate bearing capacity, and the ultimate friction capacity of each pile. These three methods are Brinch and Hansen (1963), modified Chin (1970), and Decourt (1999) The following sections define and explain these three methods with a comparison of all pile load test results for every method.

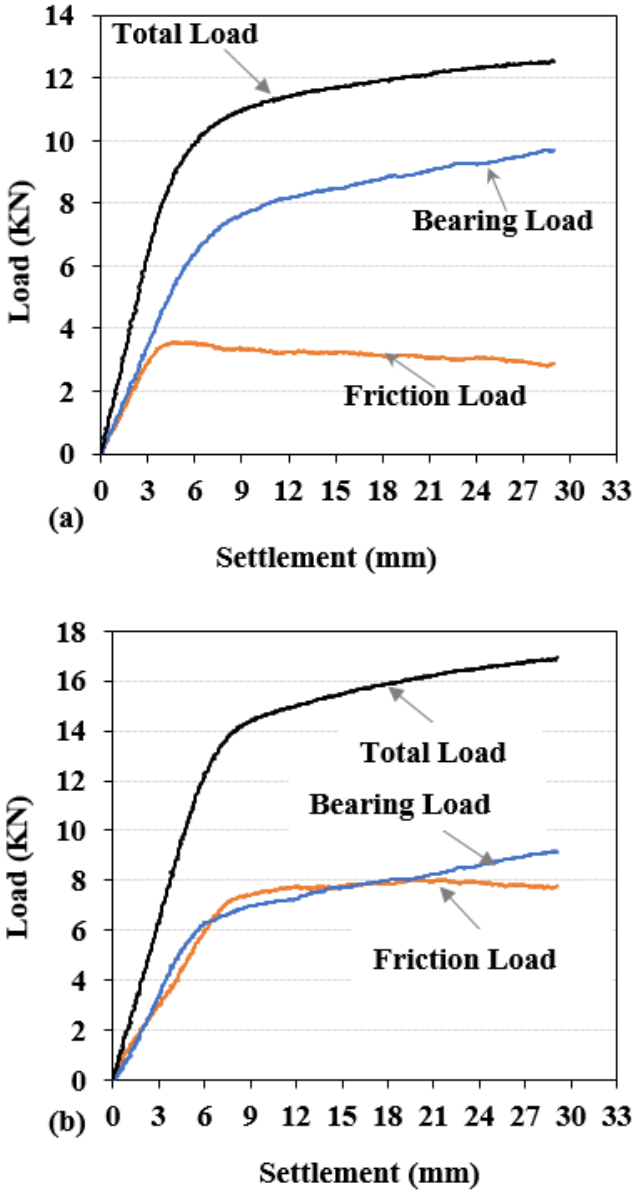

Figure 4. 8 Pile load test results: (a) control pile GFRP-0; and (b) sand coated GFRP-1500 pile (S1500)

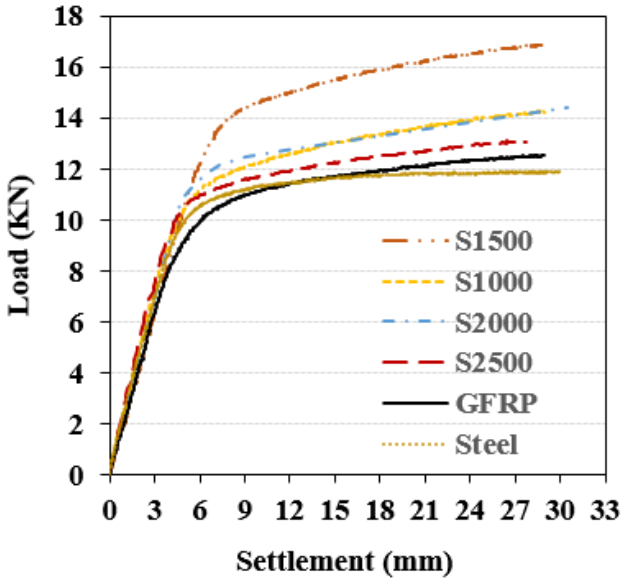

Figure 4. 9 Pile load test results for all piles

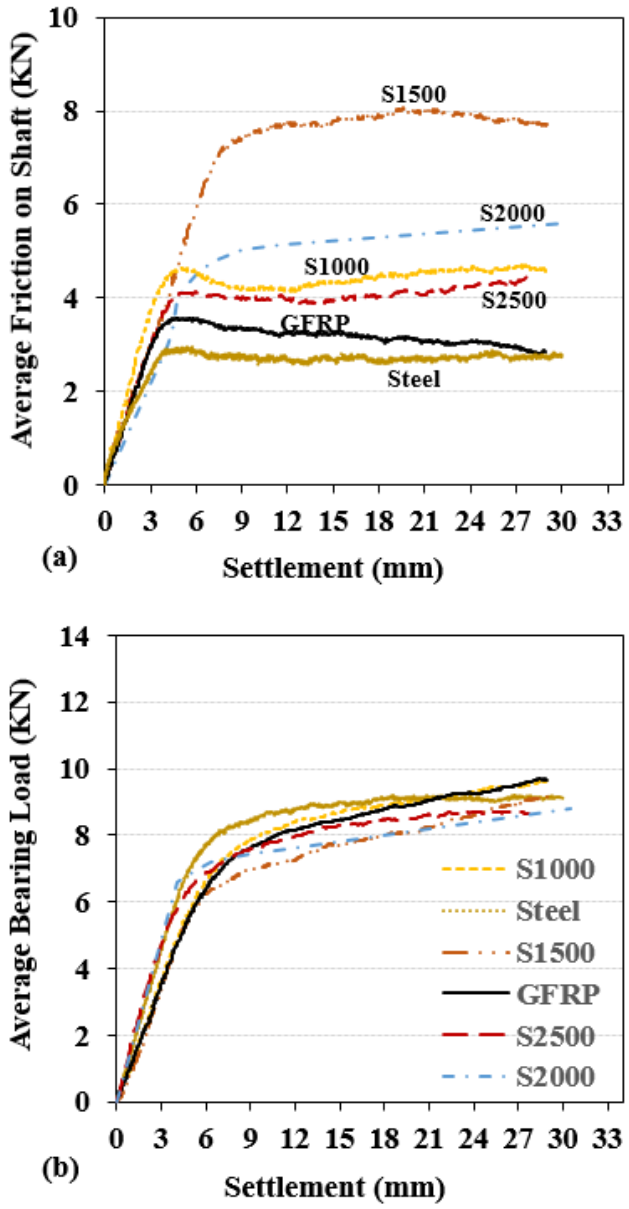

Figure 4. 10 Pile load test results: (a) average friction load along pile shaft for all piles: and (b) average bearing load on pile tip for all piles

4.4.2.1 Brinch and Hansen Method (1963)

This method is used to determine the ultimate capacity of a pile (Q_{ult} in KN) from the total load versus settlement graph (i.e. Figure 4.9) for pile load test by finding a load on the curve

which corresponds to a settlement value 2 times the settlement of $0.9Q_{ult}$. The ultimate bearing capacity and the ultimate friction capacity is taken from the corresponding values of the settlement at Q_{ult}. The values of the ultimate capacities of all pile according to Brinch and Hansen (1963) are presented in the Table 4.2, and Figure 4.11.

Table 4. 2 Pile Ultimate Capacities According to Brinch and Hansen (1963)

Pile type	Ultimate capacity Q_{ult} (KN)	Settlement at Q_{ult} (mm)	Ultimate friction capacity Q_s (KN)	Ultimate bearing capacity Q_b (KN)
GFRP	11.9	16.5	3.2	8.7
S1000	13.4	17.7	4.4	9
S1500	16.7	26.5	7.8	8.9
S2000	14.1	19.7	5.3	8.8
S2500	12.1	12.4	3.9	8.2
Steel	10.7	19.7	2.7	8

Note: S stands for sand coated GFRP pile with the corresponding sand coating ratio

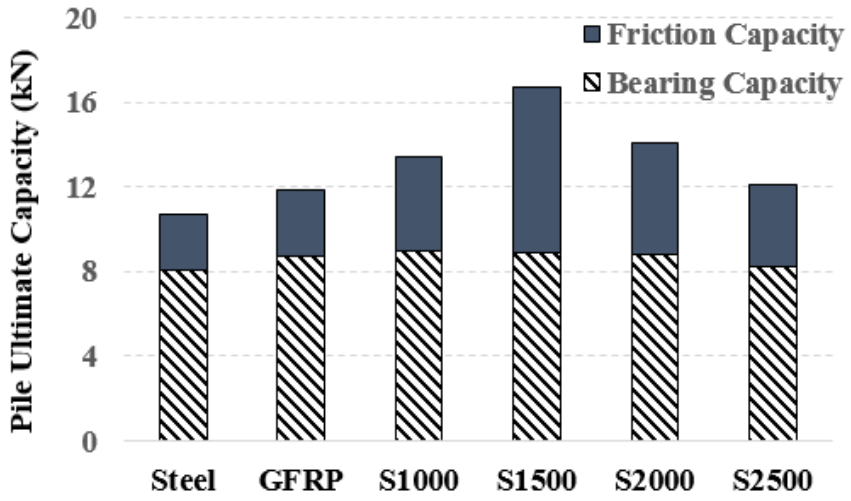

Figure 4. 11 Pile ultimate capacities (Brinch and Hansen method)

As per Brinch and Hansen (1963), the highest ultimate pile capacity among all piles tested was sand coated GFRP pile S1500 (sand coating ratio 1500 g/m^2) with 16.7 KN. This value

is 28.7 % higher than the ultimate capacity of control GFRP, and 36% higher than ultimate capacity of reference steel pile, knowing that the friction component of S1500 pile carried 7.8 KN out of the total ultimate load. The friction component of S1500 was 59% higher than the friction component of GFRP pile with no sand coating, and 65.4% higher than the friction component of control steel pile. Thus, the newly proposed GFRP pile S1500 coated with silica sand with 1500 g/m^2 not only has a longer durability compared to conventional piling material but also has a large ultimate capacity due to its roughened skin and strong interlocking between pile surface and soil particles.

The introduced mechanism of sand coating enhanced the interface friction and the ultimate capacity of GFRP piles as shown in Figure 4.11. especially using the sand coating ratios 1000, 1500, and 2000 g/m^2. Using a sand coating ratio beyond 2000 g/m^2 resulted in a drop in the ultimate capacity of GFRP pile to be close to the capacity of control GFRP pile as the interlocking between pile surface and sand particles became less as the amount voids on pile surface decreased. This decrease was shown in the case of sand coated pile S2500.

4.4.2.2 Modified Chin Method (1970)

In this method, the ultimate capacity of a pile is determined by plotting the curve of settlement/load on y-axis versus the settlement on x-axis. The value of the ultimate capacity is the inverse of the slope of that line multiplied by value of (1.2). The values of the ultimate bearing capacity and the ultimate friction capacity can be identified from the corresponding settlement at the ultimate capacity (Q_{ult}). Table 4.3, and Figure 4.12 summarize the values of ultimate capacities of all piles investigated using the modified Chin method (1970).

Table 4. 3 Pile Ultimate Capacities According to Modified Chin Method (1970)

Pile type	Ultimate capacity Q_{ult} (KN)	Settlement at Q_{ult} (mm)	Ultimate friction capacity Q_s (KN)	Ultimate bearing capacity Q_b (KN)
GFRP	11.9	16.9	3.2	8.7
S1000	13.4	18.2	4.5	8.9
S1500	16.9	29.1	7.8	9.2
S2000	13.2	16.1	5.2	8
S2500	12	12.8	3.9	8.1
Steel	10.9	7.1	2.8	8.1

Note: S stands for sand coated GFRP pile with the corresponding sand coating ratio

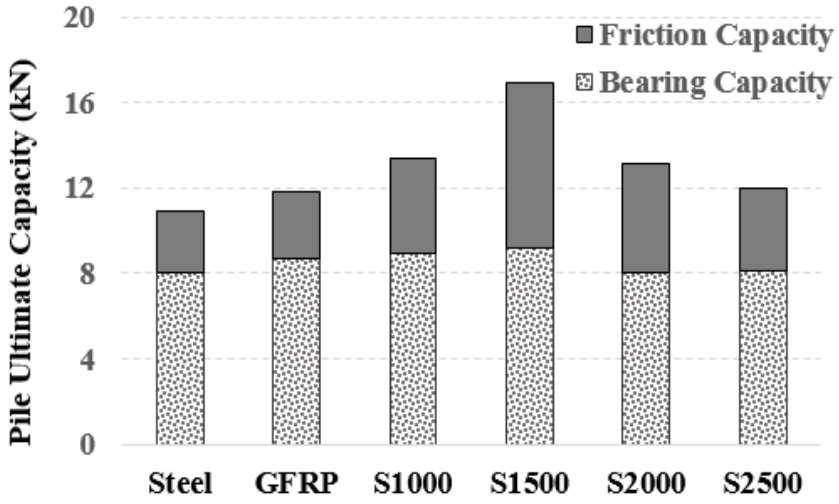

Figure 4. 12 Pile ultimate capacities (modified Chin method)

As per modified Chin method (1970), the ultimate capacity of S1500 pile was the highest among all piles following the same trend of comparison as per Brinch and Hansen Method (1963). The consistent results of both methods used in this study gives a reliable significance on the effect of coating the surface of GFRP piles with silica sand to enhance the interface friction resistance of this composite material to replace the use of conventional piling materials, especially in harsh environments and offshore construction. The friction

component of S1500 pile was 59%, and 64.1% higher the friction components of control GFRP and steel piles respectively.

4.4.2.3 Decourt Method (1999)

The last method used to determine the ultimate capacity of piles in this study was Decourt (1999). In this method each load on pile head was divided on its corresponding settlement and plotted on y-axis versus the applied load on x-axis. The ultimate load was identified by the intersection of the linear regression (last three points) of that curve with the x-axis (applied load). The ultimate bearing load and the ultimate friction load was identified by the corresponding settlement at Q_{ult}. Table 4.4, and Figure 4.13 show the values of ultimate capacities of all piles using Decourt (1999).

Table 4. 4 Pile Ultimate Capacities According to Decourt (1999)

Pile type	Ultimate capacity Q_{ult} (KN)	Settlement at Q_{ult} (mm)	Ultimate friction capacity Q_s (KN)	Ultimate bearing capacity Q_b (KN)
GFRP	12.5	27.2	2.9	9.5
S1000	14.2	28.3	4.6	9.6
S1500	16.8	27.6	7.8	9
S2000	14.4	29.2	5	9.4
S2500	13	25.6	4.3	8.7
Steel	11.8	19.6	2.7	9.1

Note: S stands for sand coated GFRP pile with the corresponding sand coating ratio

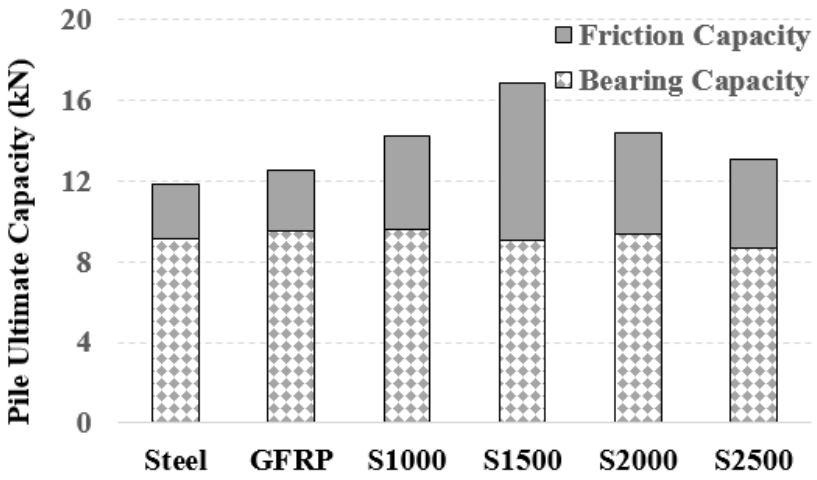

Figure 4. 13 Pile ultimate capacities (Decourt method)

As per Decourt method (1999), S1500 pile presented the optimum ultimate capacity among all other investigated piles, similar to the previous two methods (modified Chin/Brinch and Hansen). The friction component of S1000 pile was the second highest after the friction component of S1500 pile as shown in Table 4.4 due to the large settlement at Q_{ult}. The results of Figure 4.13 confirm the findings of Figures 4.11 and Figure 4.12 in-terms of the effectiveness and significance of the newly proposed sand coated GFRP S1500 pile. These findings can benefit the industry of pile design and manufacturing, especially in marine and offshore construction due to its long durability, overcoming pile-soil interface problems, and its large capacity.

4.4.2.4 Comparison between all methods used in determining pile ultimate capacities

A comparison of pile ultimate capacity for all piles investigated in this study using all three methods was presented in Figure 4.14. Decourt (1999) represented the highest ultimate capacity among all other methods due its large bearing capacity with large settlement at Q_{ult}. Modified Chin (1970) presented similar results in comparison to Brinch and Hansen method (1963) with the same trend, except for sand coated pile S2000, where Bricnh and Hansen method showed higher total ultimate capacity than modified Chin. Sand coated pile S1500 showed the optimum ultimate capacity in all three methods, on the other hand control steel pile presented the lowest ultimate capacity. For Brinch and Hansen, and Decourt methods, the optimum pile ultimate capacities were for sand coated piles S1500, and S2000, while using modified Chin method the optimum pile ultimate capacities were for sand coated piles S1500, and S1000. In all three methods, the pile ultimate capacity dropped after increasing the sand coating ratio up to 2500 g/m^2 as for the case of sand coated pile S2500.

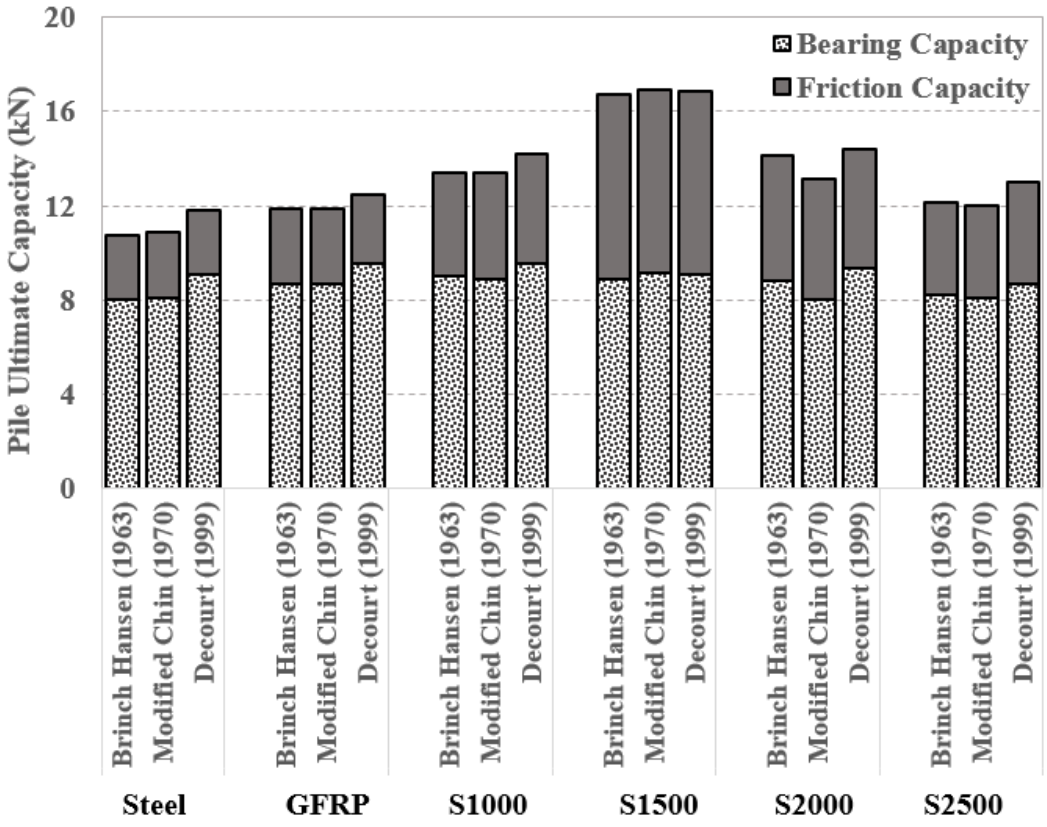

Figure 4. 14 Pile ultimate capacities for all methods used in this study

4.4.3 Comparison between experimental results and calculated results of pile ultimate capacity

The results of this experimental study using all three methods of estimating the pile ultimate capacities were compared with the design theoretical values calculated using the interface friction angles calculated in chapter 3 for sand coated GFRP piles against sand. Table 4.5 presents the calculated design values of ultimate capacity for all piles used in this study. Figure 4.15 shows that the experimental ultimate capacities of all piles are higher than the theoretical calculated capacities. All experimental results fall under a range of -+20% difference with the theoretical results except for sand coated GFRP pile S1500. However, the calculated theoretical pile capacities follow the same trend of comparison with the

experimental capacities as shown in Table 4.5 were S1500 pile presents the optimum ultimate capacity among other piles.

Table 4. 5 Theoretical Pile Ultimate Capacities, Calculated

Pile type	Ultimate capacity Q_{ult} (KN)	Ultimate friction capacity Q_s (KN)	Ultimate bearing capacity Q_b (KN)
GFRP	10.5	3	7.5
S1000	10.9	3.4	7.5
S1500	11.7	4.2	7.5
S2000	10.9	3.4	7.5
S2500	10.7	3.2	7.5
Steel	9.5	1.9	7.5

Note: S stands for sand coated GFRP pile with the corresponding sand coating ratio

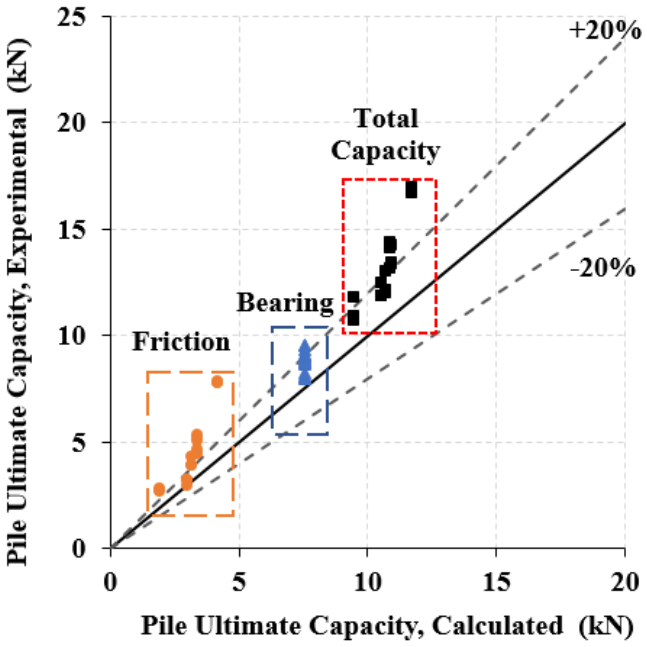

Figure 4. 15 Comparison between experimental and theoretical pile ultimate capacity

4.4.4 Sand Coating Piles' Surface after Testing

To investigate the effect of driving and testing on the sand coated GFRP pile surfaces, and to check the adherent of the sand coating, the weight per surface area was measured before and after testing for each pile. Before testing, the weight per surface for sand coated GFRP piles S1000, S1500, S2000, and S2500 were 4134.4, 4887.6, 5585.2, and 6723.1 g/m^2, respectively. After driving and testing the weight of the composite piles per surface area were 4052.6, 4830.3, 5329.7, and 6623.3 g/m^2, respectively. This comparison shows that the loss of silica sand coating particles coated on the surface of GFRP piles after testing is insignificant. For visual inspection, Figure 4.16 presents a comparison between the surface of two sand coated GFRP piles before and after testing.

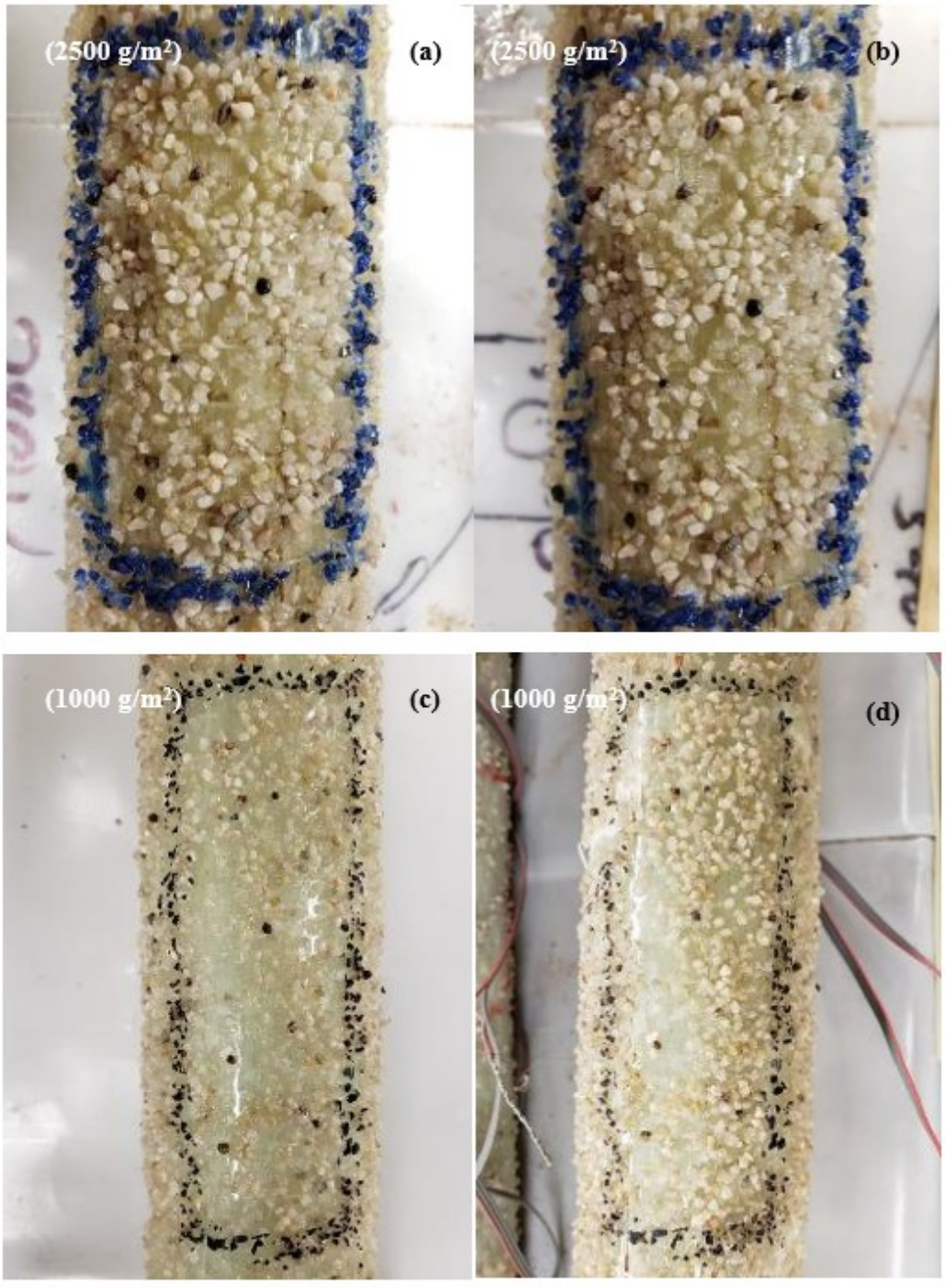

Figure 4. 16 Sand coated GFRP Piles: (a) S2500 pile before testing, (b) S2500 pile after testing, (c) S1000 pile before testing, (d) S1000 pile after testing

4.5 CONCLUSIONS

This experimental study was conducted to enhance the interface friction behaviour of GFRP piles in sand under axial loads to replace the conventional piling materials in pile construction. Four small scale GFRP piles out of five were coated with silica sand with different sand coating ratios per surface area (1000, 1500, 2000, and 2500 g/m^2). All five piles were instrumented and tested in a soil box filled with dense sand under axial loads using a steel frame connected to a hydraulic jack on its top beam. The testing results were compared to the results of a control steel pile. The following conclusions can be drawn from the results of this study:

- Coating the surface of GFRP piles with silica sand enhanced the interface friction behaviour of composite piles against sand under axial loads, as the interlocking between pile surface and sand particles increased with having more interface friction.
- For pile load test, sand coated GFRP pile S1500 with sand coating ratio per surface area 1500 g/m^2 presented the optimum pile ultimate capacity among all other piles tested using three methods of determining the pile ultimate capacity (Brinch and Hanse, modified Chin, and Decourt).
- For all piles investigated in this study, the values of the ultimate bearing capacities near pile tip were so close as all piles have the same pile toe, thus the difference in the total ultimate capacity was due to the variation in the interface friction resistance of each pile.

- Using Brinch and Hansen method, the ultimate capacity of S1500 pile was 28.7, and 36% higher than the ultimate capacities of control GFRP and steel piles, respectively.
- Using modified Chin method, the ultimate capacity of S1500 pile was 29.6, and 35.5% higher than the ultimate capacities of control GFRP and steel piles, respectively.
- Using Decourt method, the ultimate capacity of S1500 pile was 25.6, and 29.8% higher than the ultimate capacities of control GFRP and steel piles, respectively.
- For Brinch and Hansen, and Decourt methods, the optimum pile ultimate capacities were for sand coated piles S1500, and S2000.
- Using modified Chin method, the optimum pile ultimate capacities were for sand coated piles S1500, and S1000.
- Increasing the sand coating ratio over 2000 g/m^2 for GFRP pile surface results in decreasing the pile ultimate capacity as the interlocking between sand particles and pile surface decreases due to the decrease in the number of voids on pile surface having less interface friction.
- For pile driving results, sand coated GFRP pile S1500 required the highest load upon driving to reach the desired embedment depth among all other tested piles.
- The experimental results of this study were higher than the theoretical calculated results falling into -+ 20% difference, except for S1500 pile.
- Insignificant effect occurred after driving and testing sand coated GFRP piles on the sand coating ratios per surface area.

- This newly proposed mechanism of enhancing the interface friction behaviour of GFRP piles through sand coating were found to be effective under axial loads against sand. The results of this study may benefit the industry of pile construction especially in harsh environments and offshore constructions.

ACKNOWLEDGMENTS

The authors express their gratitude to the students (Ahmed Mahgoub, Mostafa Jafarian Abyaneh, Bader Alsaaed, Ali Iranikhah, and Ahmed Moussa) and the technical staff (Jordan Maerz, Jesse Keane, and Brian Kennedy) at the Department of Civil and Resource Engineering at Dalhousie University, Canada, for their endless support and help.

REFERENCES

AASHTO. (2002). Standard specifications for highway bridges. Transportation officials.

Abuel-Naga, H. M., & Shaia, H. A. (2014). Interface friction evolution of FRP tube confined concrete piles during the driving installation process. *Géotechnique Letters*, **4**(1), 52-56.

Almallah, A., Sadeghian, P., El Naggar, H. et al. (2018). *Direct shear tests of sandy soils interfaced with FRP sheets.* Paper presented at CSCE annual conference, Fredericton, Canada.

Ashford, S. A., & Jakrapiyanun, W. (2001). Drivability of glass FRP composite piling. *Journal of Composites for Construction*, **5**(1), 58-60.

ASTM A269/A269M-15a, Standard Specification for Seamless and Welded Austenitic Stainless-Steel Tubing for General Service.

ASTM C136. (2014). Standard test method for sieve analysis of fine and coarse aggregates.

ASTM D1143/D1143M. (2007). Standard Test Methods for Deep Foundations Under Static Axial Compressive Load.

ASTM D2487. (2011). Standard practice for classification of soils for engineering purposes (unified soil classification system).

ASTM D698. (2012). Standard test methods for laboratory compaction characteristics of soil using standard effort.

Chin, F. K. (1970). Estimation of the ultimate load of piles from tests not carried to failure. In *Proc. 2nd Southeast Asian Conference on Soil Engineering,* Singapore.

Frost, J. D., & Han, J. (1999). Behavior of interfaces between fiber-reinforced polymers and sands. *J Geotechnical and Geoenvironmental Eng*, **125**(8), 633-640.

Giraldo, J., & Rayhani, M. T. (2014). Load transfer of hollow fiber-reinforced polymer (FRP) piles in soft clay. *Transportation Geotechnics*, **1**(2), 63-73.

Giraldo, J., & Rayhani, M. T. (2017). Axial and lateral load transfer of fibre-reinforced polymer (FRP) piles in soft clay. *International Journal of Geotechnical Engineering*, **11**(2), 149-155.

Guades, E. J., Aravinthan, T., and Islam, M. M. et al. (2010). *An overview on the application of FRP composites in piling system.* Paper presented at the southern region engineering conference (SREC 2010), Toowoomba, Australia. 65-70.

Guades, E. J., Aravinthan, T., Islam, M. M., & Manalo, A. et al. (2012). A review on the driving performance of FRP composite piles. *Composite Structures*, **94**(6), 1932-1942.

Iskander, M. G., & Hassan, M. (1998). State of the practice review in FRP composite piling. *J Composites for Construction*, **2**(3), 116-120.

Lavanya, I., Prabha, R., Murugan, M. et al. (2014). Behaviour of interfaces between carbon fibre reinforced polymer and gravel soils. *Int J Res Eng Technol*, **3**(11), 156-159.

Nicola, A. D., & Randolph, M. F. (1999). Centrifuge modelling of pipe piles in sand under axial loads. *Géotechnique*, **49**(3), 295-318.

Pando, M., Filz, G., Hoppe, E., Ealy, C., Muchard, M. et al. (2000). *Performance of a composite pile in a full scale Statnamic load testing program*. Presented at 53rd Canadian geotechnical conference. Montreal, Canada, 1, 909-916.

Sakr, M., El Naggar, M. H. E., Nehdi, M. et al. (2004). Novel toe driving for thin-walled piles and performance of fiberglass-reinforced polymer (FRP) pile segments. *Canadian geotechnical J*, **41**(2), 313-325.

Sakr, M., El Naggar, M. H., Nehdi, M. et al. (2005). Interface characteristics and laboratory constructability tests of novel fiber-reinforced polymer/concrete piles. *J Composites for Construction*, **9**(3), 274-283.

Spiro, B. R., & Pais, M.A. (2002). Dynamic pile evaluation and pile load test results – test Piles TP#1, TP#2, and TP#3 at Spit Area, Pembroke Avenue Bridge Replacement, GSI Project, Hampton, VA, 1–2

Toufigh, V., Ouria, A., Desai, C. S., Javid, N., Toufigh, V., Saadatmanesh, H. et al. (2015). Interface behavior between carbon-fiber polymer and sand. *J Testing and Evaluation*, 44(1), 385-390.

Vineetha, V. J., & Ganesan, K. (2014). Interface Friction between Glass Fibre Reinforced Polymer and Gravel Soil. *In Advanced Materials Research*, 984, 707-710.

Zyka, K., & Mohajerani, A. (2016). Composite piles: A review. *Construction and Building Materials*, 107, 394-410.

CHAPTER 5 CONCLUSION AND RECOMMENDATIONS

5.1 CONCLUSION

In this thesis, two phases are presented to study the interface friction behaviour of fiber reinforced polymer piles in sandy soils. In the first phase of this study, six Glass FRP sheets with different surface roughness and silica sand coating ratios were interfaced against different types of sandy soils (poorly graded sand, silty sand, and sandy lean clay) with different soil densities using direct shear box. The results of interface shear tests against dense sand were compared to the results of concrete, steel, and smooth GFRP interface tests against the same sand. In the second phase of this study, pile load tests were performed on five GFRP piles under axial loads in dense sand. Four out of five GFRP piles were coated with silica sand with different sand coating ratios (1000, 1500, 2000, and 2500 g/m^2). The results of the pile load tests were compared with the results of a reference control steel pile. Both phases of this study were aimed to enhance the interface friction behaviour of GFRP piles under axial loads to replace the conventional piling materials (i.e. concrete and steel), especially in marine construction and harsh environments. The major findings are:

- The sand coating mechanism on the surface of GFRP composite material increased its interface friction with sandy soils due to the roughened skin of the composite material, and the high interlocking between the composite surface and soil.

- The optimum sand coating ratio on the surface of GFRP composite obtained from the interface shear test results was 1500 g/m^2 against poorly graded dense sand with interface friction angle (42.0°), which is 7.8% higher than that for GFRP specimen without sand coating against dense sand. While against dense silty sand and sandy

lean clay, the optimum sand coating ratio was 2000 g/m^2 with interface friction angles obtained (43.3°), and (36.8°), respectively, which are 16.8, and 131.3 % higher that for uncoated GFRP specimens against same soils, respectively.

- From the interface shear tests, the optimum sand coating ratio depends on the particle size of the sand interfaced with, as larger particles of dense sand were able to fill the voids of GFRP sand coated surface (1500 g/m^2) and form a strong interface interlocking. While, the smaller particle size of dense silty sand and sandy lean clay were able to fill the voids of GFRP sand coated surface (2000 g/m^2) forming a high interlocking with the composite surface.

- The controlling parameters affecting the interface interaction between GFRP composites and soil were: the density state of soil, particle size of soil, and the surface roughness of the composite material.

- For pile load tests, the optimum sand coating ratio used to enhance the interface friction behaviour of GFRP piles in dense sand under axial loads was 1500 g/m^2 (GFRP S1500 pile), as this pile presented the highest ultimate capacity compared to all other five piles tested in this study.

- Depending on the method used for determining the ultimate capacities of the piles investigated in this study (Brinch and Hanse, Modified Chin, and Decourt), GFRP sand coated pile S1500 had a percentage gain over the ultimate capacities of control GFRP and steel piles ranging from (25.6-29.8%), and (29.8-36%), respectively.

- The mechanism of coating the surface of GFRP piles with silica was found to be effective in enhancing the interface friction of GFRP piles in sand under axial loads due to the roughened skin of the new piling material which increased its friction resistance against sand compared to the uncoated control GFRP pile.
- The newly proposed sand coated GFRP pile with the optimum sand coating ratio 1500 g/m^2 (S1500) may benefit the industry of pile construction, especially in harsh environments as it presents a solution to soil-structure interaction problems occurred with using conventional pilling materials, and due to its large ultimate capacity compared to the control GFRP pile.
- The effect of driving and testing on the surface of GFRP sand coated piles was found to be insignificant due to the strong bond between the composite surface and silica coating sand formed using epoxy resin and hardener.

5.2 RECOMMENDATIONS

For future work, some recommendations and suggestions are made to adopt this new composite piling material in pile foundation industry are presents as follows.

- Pile load test experiments are needed on full scale instrumented GFRP sand coated piles to confirm the results of the small-scale experiments to adopt these new piles in foundation industry.
- Lateral pile load tests are required on both small-scale and large scale GFRP sand coated piles to understand its behaviour as pile foundations under different loading types.

- Cyclic axial load tests are recommended to confirm the behaviour of GFRP sand coated piles under axial loads using a displacement control actuator with incremental loading.
- Filling GFRP sand coated piles with reinforced-concrete and test it under axial and lateral loads in both full scale and large scale to compare the results with hollow GFRP sand coated piles.
- Repeating pile load tests on the hollow GFRP sand coated piles with different number of layers of GFRP fabrics with different degrees and orientations during pile manufacturing and compare the results with the one of this study.
- Small scale field tests ae highly recommended to investigate the effect of soil confining pressure on the interface friction of sand coated GFRP piles with soil.

REFERENCES

AASHTO. (2002). Standard specifications for highway bridges. Transportation officials

Abuel-Naga, H. M., & Shaia, H. A. (2014). Interface friction evolution of FRP tube confined concrete piles during the driving installation process. *Géotechnique Letters*, **4**(1), 52-56.

Aksoy, H. S., Gör, M., İnal, E. et al. (2016). A new design chart for estimating friction angle between soil and pile materials. *Geomechanics and Engineering*, **10**(3), 315-324.

Ashford, S. A., & Jakrapiyanun, W. (2001). Drivability of glass FRP composite piling. *Journal of Composites for Construction*, **5**(1), 58-60.

Allen, E., & Iano, J. (2013). Fundamentals of building construction: materials and methods. John Wiley & Sons.

Almallah, A., Sadeghian, P., El Naggar, H. et al. (2018). *Direct shear tests of sandy soils interfaced with FRP sheets.* Paper presented at CSCE annual conference, Fredericton, Canada.

Anchor Piles, reprinted from MacLean Civil Products, Retrieved on December 10, 2018, from https://www.macleandixie.com/products/item.asp?ITEM_ID=2481, Copyright by Maclean Civil Products.

ASTM A269/A269M-15a, Standard Specification for Seamless and Welded Austenitic Stainless-Steel Tubing for General Service.

ASTM C136. (2014). Standard test method for sieve analysis of fine and coarse aggregates.

ASTM. D1143/D1143M. (2007). Standard Test Methods for Deep Foundations Under Static Axial Compressive Load.

ASTM D2487. (2011). Standard practice for classification of soils for engineering purposes (unified soil classification system).

ASTM D3080. (2011). Standard test method for direct shear test of soils under consolidated drained conditions.

ASTM. D4945. (2012). Standard Test Method for High-Strain Dynamic Testing of Deep Foundations, West Conshohocken, PA, USA.

ASTM D698. (2012). Standard test methods for laboratory compaction characteristics of soil using standard effort.

Atkinson, J. (2007). The mechanics of soils and foundations. CRC Press, Florida, USA.

Aysen, A. (2005). Problem solving in soil mechanics. Taylor & Francis, USA.

Baxter, C. D., Marinucci, A., Bradshaw, A. S., Morgan, R. J. et al. (2005). Field study of composite piles in the marine environment.

Bored Piles, reprinted from Keller Website Worldwide, Retrieved on December 20, 2018, from http://www.kellerholding.com/bored-piles.html/, Copyright by Keller.

CFEM (2006). Canadian Foundation Engineering Manual.

Chellis, R. D. (1961). Pile Foundations, McGraw Hill, New York, USA.

Chin, F. K. (1970). Estimation of the ultimate load of piles from tests not carried to failure. In *Proc. 2nd Southeast Asian Conference on Soil Engineering,* Singapore.

Chu, L. M., & Yin, J. H. (2006). Study on soil-cement grout interface shear strength of soil nailing by direct shear box testing method. *J Geomechanics and Geoengineering*, **1**(4), 259-273.

Coduto, D. P. (2001). Foundation Design Principles and Practices. Upper Saddle River, New Jersey: Prentice-Hall, USA.

Driven Drilled Steel Piles, reprinted from skyline steel website, Retrieved on October 5, 2018, from http://skylinesteel.com/globalnav/applications/bearing-piles, Copyright 2018 by Skyline Steel.

Driven Piles, reprinted from Keller Website Australia, Retrieved on December 19, 2018, from http://www.keller.com.au/solutions/techniques/driven-piles/, Copyright by Keller.

Driven Precast Concrete Piles, reprinted from the constructor website, Retrieved on October 5, 2018, from https://theconstructor.org/geotechnical/driven-precast-concrete-piles/7092/, Copyright 2017 by The Constructor.

Elson, K., Fleming, K., Randolph, M., Weltman, A. et al. (2008). *Piling engineering*. Taylor & Francis.

Fam, A. Z., Pando, M., Filz, G., Rizkalla, S. et al. (2003). Precast piles for Route 40 bridge in Virginia using concrete filled FRP tubes. *PCI journal*, **48**(3), 32-45.

Fam, A. Z., & RizKalla, S. H. (2001). Behavior of Axially Loaded Concrete-Filled Circular Fiber-Reinforced Polymer Tubes. *ACI Structural Journal*, **98**(3), 280-289.

Fam, A. Z., & Rizkalla, S. H. (2002). Flexural Behaviour of Concrete-Filled Fiber-Reinforced Polymer Circular Tubes. *Journal of Composites for Construction*, **6**(2), 123-132.

Fender Piles, reprinted from I am Civil Engineer website, Retrieved December 9, 2018, from https://www.iamcivilengineer.com/what-are-fender-piles/, Copyright by I am Civil Engineer website.

Frost, J. D., & Han, J. (1999). Behavior of interfaces between fiber-reinforced polymers and sands. *J Geotechnical and Geoenvironmental Eng*, **125**(8), 633-640.

Frost, J. D., & Han, J. (1999). Buckling of vertically loaded fiber-reinforced polymer piles. *Journal of reinforced plastics and composites*, **18**(4), 290-318.

Giraldo, J., & Rayhani, M. T. (2013). Influence of fiber-reinforced polymers on pile-soil interface strength in clays. *Advances in civil engineering materials*, **2**(1), 534-550.

Giraldo, J., & Rayhani, M. T. (2014). Load transfer of hollow fiber-reinforced polymer (FRP) piles in soft clay. *Transportation Geotechnics*, **1**(2), 63-73.

Giraldo, J., & Rayhani, M. T. (2017). Axial and lateral load transfer of fibre-reinforced polymer (FRP) piles in soft clay. *International Journal of Geotechnical Engineering*, **11**(2), 149-155.

Goh, A. T. C., & Donald, I. B. (1984). *Investigation of soil-concrete interface behaviour by simple shear apparatus*. Paper presented at Transportation Research Board, Washington, USA.

Guades, E. J., Aravinthan, T., and Islam, M. M. et al. (2010). *An overview on the application of FRP composites in piling system.* Paper presented at the southern region engineering conference (SREC 2010), Toowoomba, Australia, 65-70.

Guades, E. J., Aravinthan, T., and Islam, M. M. et al. (2011). *Driveability of composite piles*. Paper presented at the 1st international postgraduate conference on engineering, designing and developing the built environment for sustainable wellbeing (EDDBE 2011), Queensland University of Technology, Australia, 237-242.

Guades, E., Aravinthan, T., Islam, M., Manalo, A. et al. (2012). A review on the driving performance of FRP composite piles. *Composite Structures*, 94, 932-1942.

Hollaway, L. C. (2010). A review of the present and future utilisation of FRP composites in the civil infrastructure with reference to their important in-service properties. *Construction and Building Materials*, 24, 2419-2445.

Horvath, J. S., Trochalides, T., Burns, A., Merjan, S. et al. (2004). Axial-compressive capacities of a new type of tapered steel pipe pile at the John F. Kennedy International Airport.

Iskander, M. G., & Hassan, M. (1998). State of the practice review in FRP composite piling. *J Composites for Construction*, **2**(3), 116-120.

Iskander, M. G., Hanna, S., Stachula, A. et al. (2001). Driveability of FRP Composite Piling. *Journal of Geotechnical and Geoenvironmental Engineering*, 127, 169-176.

Iskander, M., Mohamed, A., Hassan, M. et al. (2002). Durability of recycled fiber-reinforced polymer piling in aggressive environments. *Transportation research record*, **1808**(1), 153-161.

Iskander, M. G. (2002). Recent Developments in FRP Composite Piling Practice. Paper presented at Transportation Research Board Annual Meeting, Washington, USA, 02-3589.

Kaw, A. K. (2005). Mechanics of composite materials. CRC press, USA.

Lavanya, I., Prabha, R., Murugan, M. et al. (2014). Behaviour of interfaces between carbon fibre reinforced polymer and gravel soils. *Int J Res Eng Technol*, **3**(11), 156-159.

Lehane, B. M., Jardine, R. J., Bond, A. J., Frank, R. et al. (1993). Mechanisms of shaft friction in sand from instrumented pile tests. *J Geotechnical Eng*, **119**(1), 19-35.

Lupini, J. F., Skinner, A. E., Vaughan, P. R. et al. (1981). Drained Residual Strength of Cohesive Soils. *Geotechnique*, **31**(2), 181-213.

Mays, G. C. (Ed.). (2002). Durability of concrete structures: investigation, repair, protection. CRC Press.

Meyerhof, G. (1976). Bearing Capacity and Settlement of Pile Foundations. *Journal of Geotechnical Engineering* - The 11th Terzaghi Lecture, ASCE, 102, 195-228.

Mirmiran, A., Shahawy, M., El Khoury, C., Naguib, W. et al. (2000). Large Beam-Column Tests on Concrete-Filled Composite Tubes. *ACI Structural Journal*, **97**, 268-276.

Mirmiran, A., & Shahawy, M. (2003). Composite pile: A successful drive. *Concrete international*, **25**(3), 89-94.

Nicola, A. D., & Randolph, M. F. (1999). Centrifuge modelling of pipe piles in sand under axial loads. *Géotechnique*, **49**(3), 295-318.

Nishizaki, I., Takeda, N., Ishizuka, Y., Shimomura, T. et al. (2006). A case study of life cycle cost based on a real FRP bridge. In *Third international conference on FRP composites in civil engineering (CICE 2006).* Miami, 99-102.

Novak, M., & F. Grigg, R. (1976). Dynamic experiments with small pile foundations. *Canadian Geotechnical Journal*, **13**(4), 372-385.

O'Rourke, T. D., Drusche, l. S. J., Netravali, A. N. et al. (1990). Shear Strength Characteristics of Sand-Polymer Interfaces. *Journal of Geotechnical Engineering*, **116**(3), 451-469.

Paikowsky, S. G., Player, C. M., Connors, P. J. et al. (1995). A dual interface apparatus for testing unrestricted friction of soil along solid surfaces. *Geotechnical Testing J*, **18**(2), 168-193.

Pando, M., Filz, G., Hoppe, E., Ealy, C., Muchard, M. et al. (2000). Performance of a composite pile in a full scale Statnamic load testing program. In *Proceedings, 53rd Canadian Geotechnical Conference*, **1**, 909-916.

Pando, M. A., Filz, G. M., Dove, J. E., Hoppe, E. J. et al. (2002). Interface shear tests on FRP composite piles. *Geotechnique*, **4**(1), 52-56.

Pando, M. A. (2003). A laboratory and field study of composite piles for bridge substructures, Dissertation, Virginia Tech.

Reddy, E. S., Chapman, D. N., Sastry, V. V. R. N. et al. (2000). Direct shear interface test for shaft capacity of piles in sand. *Geotechnical Testing Journal*, **23**(2), 199-205.

Rouaiguia, A. (2010). Residual shear strength of clay-structure interfaces. Int *J Civil and Environmental Eng*, **10**(3), 6-18.

Potyondy, J. G. (1961). Skin friction between various soils and construction materials. *Geotechnique*, **11**(4), 339-353.

Saafan, M. A. A. (2006). Shear strengthening of reinforced concrete beams using GFRP wraps. *Acta Polytechnica*, **46**(1).

Sadeghian, P., Lai, Y. C., Fam, A. et al. (2010). Testing and modeling of a new moment connection of concrete-filled FRP tubes to footings under monotonic and cyclic loadings. *Journal of Composites for Construction*, **15**(4), 653-662.

Sadeghian, P., & Fam, A. (2010). Closed-form model and parametric study on connection of concrete-filled FRP tubes to concrete footings by direct embedment. *Journal of Engineering Mechanics*, **137**(5), 346-354.

Sakr, M., El Naggar, M. H. E., Nehdi, M. et al. (2004). Novel toe driving for thin-walled piles and performance of fiberglass-reinforced polymer (FRP) pile segments. *Canadian geotechnical J*, **41**(2), 313-325.

Sakr, M., El Naggar, M. H., Nehdi, M. et al. (2005). Interface characteristics and laboratory constructability tests of novel fiber-reinforced polymer/concrete piles. *J Composites for Construction*, **9**(3), 274-283.

Shaia, H. (2013). Behaviour of Fibre Reinforced Polymer Composite Piles: Experimental and Numerical Study, Doctoral dissertation, The University of Manchester, Manchester, UK.

Smith, E. (1960). Pile Driving Analysis by the Wave Equation. *Journal for Soil Mechanics and Foundation Division*, ASCE, **86**, 35-61.

Soltannia, B., & Taheri, F. (2015). Influence of nano-reinforcement on the mechanical behavior of adhesively bonded single-lap joints subjected to static, quasi-static, and impact loading. *Journal of adhesion Science and Technology*, **29**(5), 424-442.

Spiro, B. R., & Pais, M.A. (2002). Dynamic pile evaluation and pile load test results – test Piles TP#1, TP#2, and TP#3 at Spit Area, Pembroke Avenue Bridge Replacement, GSI Project, Hampton, VA, 1–2

Taha, A. M. (2010). Interface Shear Behavior of Sensitive Marine Clays--Leda Clay. Dissertation, University of Ottawa.

Taylor, R. B. (1995). New developments in marine fendering. *Dredging & Port Construction*, **22**(3), 4.

The Difference Between End Bearing Pile and Friction Pile, reprinted from understand construction website, Retrieved on October 1, 2018, from

http://understandconstruction.com/pile-foundations.html, Copyright by understanding construction website.

Timber Piles, reprinted from American pole and timer website, Retrieved October 5, 2018, from https://www.americanpoleandtimber.com/wood-timber-products/dock-pier-materials/, Copyright 2018 by American Pole and Timber.

Timber Piles Strengthened with GFRP, reprinted from five-star products website, Retrieved on October 5, 2018, from https://www.fivestarproducts.com/pileform-f-jacket.html, Copyright 2018 by Five Star Products, Inc.

Toufigh, V., Ouria, A., Desai, C. S., Javid, N., Toufigh, V., Saadatmanesh, H. et al. (2015). Interface behavior between carbon-fiber polymer and sand. *J Testing and Evaluation*, **44**(1), 385-390.

Uesugi, M., & Kishida, H. (1986). Influential factors of friction between steel and dry sands. *Soils and foundations*, **26**(2), 33-46.

Uesugi, M. (1987). Friction between dry sand and construction materials. Dissertation, Tokyo Institute of Technology.

Ulitskii, V. M. (1995). History of Pile Foundation Engineering. *Soil Mechanics and Foundation Engineering*, **32**(3), 110-114.

Velez, J. D. G. (2013). Experimental study of Hollow Fibre Reinforced Polymer Piles in soft clay, Master's Thesis dissertation, Carleton University, Ottawa, Canada.

Vesic, A. (1977). Design of Pile Foundations - Synthesis of Highway Practice No. 42. Presented at Transportation Research Board (TRB), National Cooperative Highway Research Program. Washington, USA.

Vineetha, V. J., & Ganesan, K. (2014). Interface friction between glass fibre reinforced polymer and gravel soil. *In Advanced Materials Research*, 984, 707-710.

Yuan, W., & Mirmiran, A. (2001). Buckling analysis of concrete-filled FRP tubes. *International Journal of structural stability and dynamics*, **1**(3), 367-383.

Zobel, H. et al. (2005). Kompozyty polimerowe w mostownistwie. *Materiały Budowlane*.

Zyka, K., & Mohajerani, A. (2016). Composite piles: A review. *Construction and Building Materials*, 107, 394-410.